Norwegian University
of Life Sciences

Master's Thesis 2023 60 ECTS
Faculty of Chemistry, Biotechnology and Food Science

How enzyme and substrate concentration influence the synergy effect on chitin degradation by *Sm*ChiA and *Sm*AA10A

Ingrid Rokke Elvebakken
Master of Chemistry

Acknowledgments

This thesis presents research performed for the Bioorganic Chemistry Group at the Faculty of Chemistry, Biotechnology and Food Science at the Norwegian University of Life Sciences.

First, I want to thank my main supervisor Professor Morten Sørlie, for the opportunity to perform research for his group. I really appreciate your engagement in science, patience and all the nice conversations. Second, I want to express my gratitude to my co-supervisor Kristine Votvik, for always encouraging and believing in me. In addition, I greatly appreciate the valuable time of Ole Golten, for your great help in the lab, experimental setups and writing. I have learned so much from you. I would also like to thank Dr. Lukas Reider and Dr. Kelsi Hall for helping with cloning and always answering my questions.

A special thanks to all my fellow master students with whom I have shared a great time in the lab over these last years. In particular, thanks to Rannei Skaali and Maja Mollatt who have followed me during this journey and shared the lab bench with me. You have greatly brightened my days. Also, the community with fellow master students Synnøve Elisa Rønnekeiv, Manouck Oussoren, Anine Sætreng and Caroline Østvang Gundersen and the rest in the first-floor corridor. Thanks for great lunch breaks and the special cake on Tuesdays.

Finally, I would like to thank my family for supporting me and trying to understand the content of this thesis. I have felt your encouragement throughout this journey, and I greatly appreciate it. I also have to mention my other family over the past 7-8 years in my Kolbotn IL teammates, for a great community and a break from chemistry. Lastly my partner Elise for always listening and encouraging me, making me laugh and always supporting me.

Ingrid Rokke Elvebakken

Ås, May 2023

Summary

Recalcitrant polysaccharides like cellulose and chitin are profusely produced by organisms in Nature and degrading these for products of value show a large potential in industrial application of a sustainable future of utilizing biomass that previously was considered waste. Chitinolytic enzymes from *S. marcescens* include the key enzymes *Sm*ChiA and *Sm*AA10A (previously known as CBP21). *Sm*ChiA is an exo-acting processive enzyme, which hydrolyze glycosidic bonds from the reduced end of the chitin chain, while the copper-dependent *Sm*AA10A disrupts crystalline chitin by endo-acting oxidative cleavage releasing chain ends for the chitinase. These complimentary actions have been shown to result in synergy effects when these enzymes work together on chitin. This thesis has investigated how the change of enzyme, substrate concentrations, peroxygenase conditions, and pretreatment of the substrate with *Sm*AA10 A influence the chitobiose yield.

The largest synergy effect was obtained at high β-chitin substrate concentrations, relatively low *Sm*ChiA concentration in a 1:10 ratio with *Sm*AA10A and steady low H_2O_2 supply generating peroxygenase conditions. The same chitobiose yield can be obtained by a lower amount of *Sm*ChiA if *Sm*AA10A was present, but *Sm*AA10A gave no synergy effect at lower substrate concentrations. Also at minimal substrate concentrations, *Sm*AA10A negatively influenced chitobiose solubilization by *Sm*ChiA.

The second aim was to clone *Sm*ChiA into the industrial expression system of *P. pastoris*. This resulted in an active enzyme with similar activity compared to *E. coli* produced *Sm*ChiA. This facilitates the cloning of a whole chitinolytic machinery into *P. pastoris* that will secrete properly folded enzymes for easier purification and industrial applications.

Sammendrag

Motstandsdyktige polysakkarider som cellulose og kitin er rikelig produsert av organismer i naturen, og nedbrytning av disse til produkter av verdi holder et stort potensial for bruk i en bærekraftig fremtid som innebærer utnyttelse av biomasse som tidligere var ansett som avfall. Kitin nedbrytende enzymer fra *S. marcescens* inneholder nøkkel-enzymene *Sm*ChiA og *Sm*AA10A (tidligere kjent som CBP21). *Sm*ChiA er et exoaktivt prossessivt enzym som hydrolyserer glykosidbindinger fra den enden av kitin-kjeden, mens kobber-avhengige *Sm*AA10A bryter opp krystallinsk kitin med endoaktiv oksidasjon som frigjør kjede ender til kitinasen. Disse komplementære aktivitetene har vist å gi synergi effekt når disse enzymene jobber sammen på kitin. Denne oppgaven har undersøkt hvordan endring i enzym konsentrasjon, substrat konsentrasjon, peroxygenase betingelser, og forbehandling av substrat med *Sm*AA10A påvirker kitobiose utbytte.

Den største synergi effekten ble oppnådd ved høy β-kitin substratkonsentrasjon, relativt lav *Sm*ChiA konsentrasjon i 1:10 forhold med *Sm*AA10A og stabilt lav H_2O_2 tilførsel som gir peroxygenase betingelser. Det samme kitobiose utbyttet kan bli anskaffet av en lavere mengde *Sm*ChiA hvis var *Sm*AA10A var tilstede, men *Sm*AA10A ga ingen synergi effekt ved lavere substrat konsentrasjoner. I tillegg ved minimal substrat konsentrasjon, påvirket *Sm*AA10A negativt kitobiose oppløsning av *Sm*ChiA.

Det andre målet med oppgaven var å klone *Sm*ChiA inn i det industrielle ekspresjons systemet i *P. Pastoris*. Dette resulterte i aktivt enzym med liknende aktivitet sammenlignet med *E. coli* produsert *Sm*ChiA. Dette legger til rette for kloning av et kitinolytisk maskineri inn i *P. pastoris* som vil sekrere riktig foldet enzymer for enklere rensing og industriell anvendelse.

Table of content

Abbreviations

4-MU	4-methylbelliferone
Å	Ångstrøm
AA	Auxiliary activity
AEC	Anion exchange chromatography
AR	Amplex Red reagent
Ascorbic acid	Ascorbic acid
AU	Absorbance units
bp	Base pair
BSA	Bovine serum albumin
CAZy	Carbohydrate active enzyme database
CAZyme	Carbohydrate active enzyme
CBM	Carbohydrate-binding module
CBP21	Chitin-binding protein 21 from *Serratia marcescens*
CHB	Chitobiase
ChiA	Chitinase A
ChiB	Chitinase B
ChiC	Chitinase C
ChCl	Choline chloride

ChOx	Choline Oxidase
DNA	Deoxyribonucleic acid
dNTP	Deoxyribonucleoside
g	Relative centrifugal force
GH	Glycoside hydrolase
GlcNAc	N-acetyl-D-glucosamine
HIC	Hydrophobic interaction chromatography
HP	High-performance
HRP	Horseradish peroxidase
IEX	Ion exchange chromatography
IPTG	Isopropyl β-D-1-thiogalactopyranoside
kDa	Kilodalton
LB	Lysogeny broth
LC	Liquid chromatography
LP	Low pressure
LPMO	Lytic polysaccharide monooxygenase
MWCO	Molecular weight cut-off
nm	Nanometer
OD	Optical density
ON	Overnight

S.O.C	Super optimal broth
SDS-PAGE	Sodium dodecyl sulphate polyacrylamide gel electrophoresis
SEC	Size exclusion chromatography
UV	Ultraviolet light
WT	Wild type
YNB	Yeast nitrogen base
YPD	Yeast extract peptone dextrose (media)

1 Introduction

During the last decades, the climate crisis has become more alarming due to an increase in emissions, waste, and temperature across the planet. The use of fossil fuels, that is a limited resource, has created a dependency linked to high carbon emissions and plastic waste and inevitably global warming. United Nations (UN) Sustainable Development Goals (SDG) were set in 2015 to gain sustainability of social, economic, and environmental development. Incorporated into several of these tight-knit goals, is the efficiency of how the planet's resources are utilized for energy and consumption, and how the use of them impacts the environment (United Nations, 2015). Specifically goal 7 for “affordable and clean energy”, goal 9 for “industry, innovation and infrastructure”, goal 12 for “responsible consumption and production” and goal 14 “life below water” involves utilizing the resources that are provided by Nature sustainably and can be viewed as tactics to slow down climate change and protect the environment (United Nations, 2015). Utilization of more of earth´s resources in an effective and environmentally friendly way has opened the potential for the degradation of biomass for biofuels and the utilization of products that previously were considered waste.

Biomass made of carbohydrates such as cellulose and chitin are the most abundant biopolymers on earth and species across the globe have developed and adapted specialized enzymatic systems to efficiently utilize these resources. The complexity and specializations that have been created in these enzymes are still hard to understand, but they possess the potential for effective and environmentally friendly degradation into products that can be used, e.g., bioethanol (Inokuma et al., 2013), nanofibers (Chen et al., 2017), antimicrobial food packaging (Lei et al., 2014) and medical applications like wound treatment (Dai et al., 2011), bone regeneration (Kawata et al., 2016) and anticancer effects (Karagozlu & Kim, 2014).

1.1 Chitin

Chitin is a linear polysaccharide, and after cellulose, it is the second most abundant polymer produced in Nature. The monomer of chitin is named N-acetylglucosamine (GlcNAc) with an acetylated amino group at the C2-position, and in polymers they are linked with β-1,4-glycosidic bonds where the GlcNAc units are rotated 180 ° relative to each other (Figure 1.1A) (Roberts, 1992). Chitin is a structural and defense element in the exoskeletons of insects, shells of crustaceans, and in the cell wall of fungi where all of the different organisms have variating amounts of chitin to glycoproteins, calcium carbonate, minerals, and pigments (Chakravarty & Edwards, 2022; Roberts, 1992). For example, in fungi, chitin can be found crosslinked to cellulose, while in the exoskeleton of insects, chitin is found in complexes with proteins (Roberts, 1992). Chitin yield therefore depends a lot on the source, where seafood waste in general is estimated to be 20-30 % chitin, some crustacean orders have 2-12 % chitin whereas *Humarus* lobster shell has 60-75 % chitin(Chakravarty & Edwards, 2022; Younes & Rinaudo, 2015). The structure of chitin chains and cross-linkages results in a high-strength polymer that requires a lot of energy to degrade.

1.1.1 Structure

Chitin chains can be oriented in different networks giving the polymorphs; α-chitin, β-chitin, and γ-chitin. Where α-chitin has chains oriented antiparallelly to each other, β-chitin have chains in a parallel orientation giving a reduced and non-reduced end of the crystal, and γ-chitin is a mix of both orientations (Figure 1.1B). The antiparallel orientation in α-chitin gives a larger network of hydrogen bonding making α-chitin the most stable form of chitin with the shortest distance between the chains, while the parallel-oriented chains in β-chitin yield a more flexible structure compared to α-chitin. The final polymorph, γ-chitin resembles β-chitin in flexibility compared to α-chitin (Hou et al., 2021; Roberts, 1992).

A

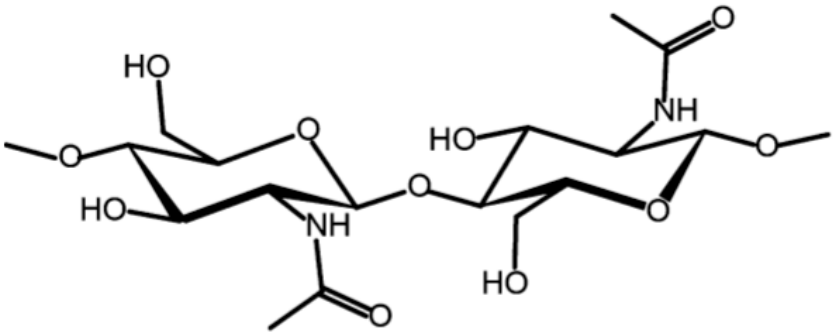

B

Figure 1.1 ***Chemical structure of chitin, (A)*** *with two N-acetyl glucosamine units. Derived from (Vaaje-Kolstad et al., 2013),* ***(B)*** *Display of the arrangement of chains in the polymorphs of chitin. Derived from (Roberts, 1992).*

The structure of the crystal is sheets of polymorphs that give variation between rigid and more amorphous sections, dependent on α- or β-chitin content respectively (Roberts, 1992). A typical source of α-chitin is hard structures like the exoskeleton of shrimp, lobster, and crab, or in cell walls of fungi. While a typical source of β-chitin is more flexible, like squid pen and chaetae of *Aphrodite aculeate* (Roberts, 1992). The third polymorph, γ-chitin is less common in Nature, but have among others been extracted from the cocoon of the *Orgyia dubia* moth (Kaya et al., 2017).

Chitin application and products of value consist of mainly oligosaccharides of chitin or derivates of the deacetylated variant of chitin, called chitosan. Chitosan, a polymer that can be made water soluble polymer that is not as common in Nature, but is produced commercially

by the deacetylation of chitin (with a variating degree of deacetylation)(Roberts, 1992). Extracted chitin and chitosan have a wide variety of applications as they can be turned into polymers that have been used in medicine for wound treatment, tissue engineering, cancer treatment and antibacterial effects (Tharanathan & Kittur, 2003; Younes & Rinaudo, 2015). Bioethanol has been produced from the fermentation of GlcNAc units with species of *Mucor* fungi (Inokuma et al., 2013). Overall chitin products and derivates are viewed as a new type of biomaterial due to its many applications as an accessible resource, with more applications in the future. To achieve this, its necessary to have effective extraction.

1.1.2 Extraction

The industrial extraction of chitin from a natural source includes two main steps; deproteinization and demineralization. Here, the goal is to remove proteins and minerals, as well as additionally the removal of pigment (Roberts, 1992). Demineralization is performed with strong concentrated acids, typically HCl, generating waste and demands large amounts of energy due to high temperatures. Moreover, this can influence the properties of the chitin negatively (Kaur & Dhillon, 2015). Deproteinization involves alkaline treatment, often with NaOH, including high temperatures for an extended time (Roberts, 1992). The consumption of strong acids, bases, heat, and time, while generating waste that needs decontamination increases the need for a less harmful and environmentally friendly method. (Chakravarty & Edwards, 2022; Hou et al., 2021; Roberts, 1992) The biological methods, using enzymes and microorganisms for the extraction of chitin have been researched on a small-scale, with promise, but further research is required to apply this to an industrial scale (Drula et al., 2022; Gooday et al., 1990; Vaaje-Kolstad et al., 2013).

1.2 Carbohydrate active enzymes

Carbohydrate Active enzymes (CAZymes) are enzymes that facilitate the degradation, formation, or modification of glycosidic bonds and are categorized into families in the CAZy database based on their genome sequence, structure, and catalytic mechanism since 1998

(Drula et al., 2022). CAZymes are sorted based on their activity into glycoside hydrolases (GHs), glycosyl transferases (GTs), polysaccharide lysases (PLs), carbohydrate esterases (CEs), and auxiliary activities (Aas), where these enzymes are identified in genomes from mostly bacteria, but also archaea, eukaryotes, and viruses (Drula et al., 2022). The most characterized are the GHs as they have a critical biological function and are the most prominent for polysaccharide degradation (Consortium, 2018). The work performed in this thesis will focus on GHs and AAs, as they are highly relevant for chitin degradation.

1.3 Glycoside hydrolases

GHs are enzymes that hydrolyze the glycosidic bonds in polysaccharides, and come from a variety of species that rely on these enzymes for biological functions ranging from signaling, structure, and energy uptake (Drula et al., 2022). By structure, they are categorized into 3 different topologies called “pocket/crater”, “cleft” and “tunnel”, as seen in Figure 1.2. The “pocket/crater” topology is beneficial for substrates with a lot of free ends as the reducing or non-reducing end fits well in the “pocket”, resulting in exo-activity. In contrast, the “cleft” topology facilitates the binding and cleavage in the middle of the polysaccharide chain, resulting in endo-activity, although often “tunnel” topologies have the ability to enclose the polysaccharide chain resembling the final topology, a “tunnel”, that the substrate can enter and create more enzyme-substrate interactions during hydrolysis and stay bound for consecutive hydrolysis resulting in exo-activity (Davies & Henrissat, 1995).

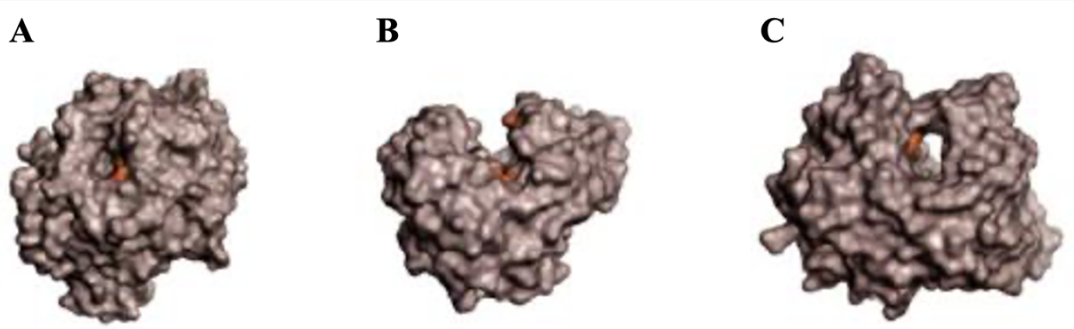

Figure 1.2 ***GH topology****, where (A) is “pocket/crater”, (B) is “cleft” and (C) is “tunnel”. The figure is derived from (Davies & Henrissat, 1995).*

A processive mechanism is when the enzyme cleaves consecutively while remaining associated with the substrate (Horn et al., 2006b). As endo-acting cleave randomly, they need their active site topology to access the flat binding surface of a crystalline substrate, therefore, the relatively open structure often resembles a “cleft” (Figure 1.2B). In contrast to the exo-acting processive enzymes that are associated with great processive cleavage with ”pocket”/ “tunnel” topology (Figure 1.2A/C) (Sørlie et al., 2012).

1.3.1 Mechanism

The general mechanism of GHs cleavage of glycosidic bonds is that an acid catalyzes the cleavage assisted by a nucleophile (water) and a proton donor. As a way of lowering the energy barrier of the hydrolysis, the saccharides are distorted from the stable chair conformation into a transition state boat conformation (Davies & Henrissat, 1995). There are two mechanisms for the hydrolysis of glycosidic bonds by GHs; the retaining and the inverting mechanism, both shown in Figure 1.3.

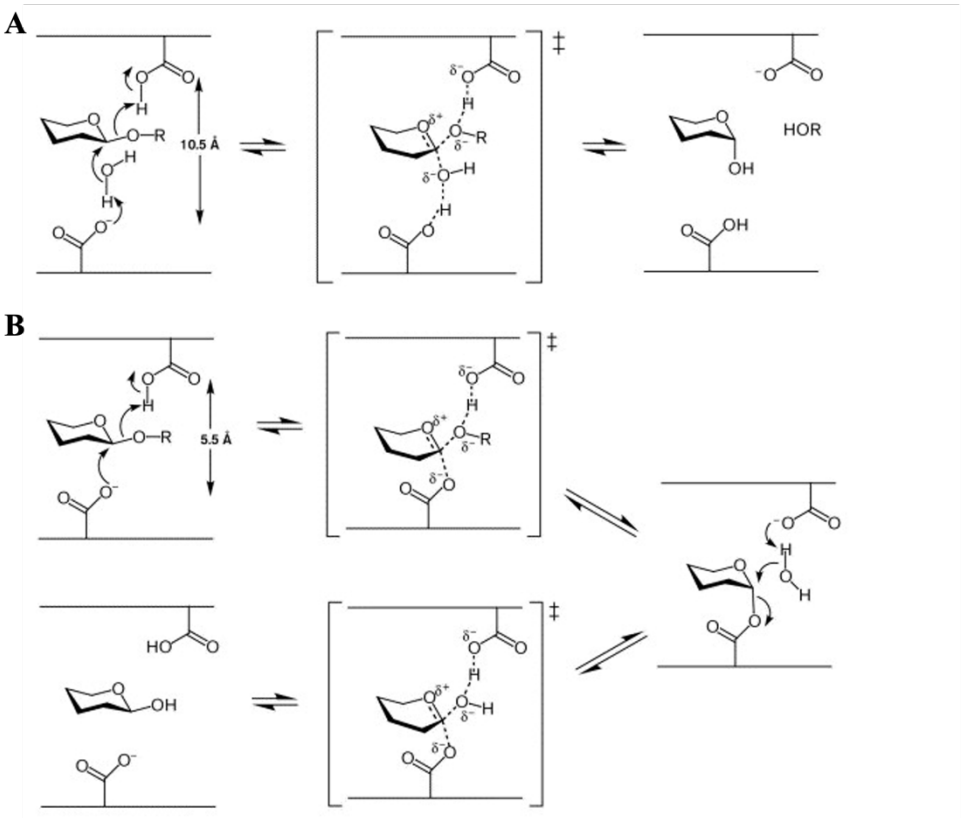

Figure 1.3 ***The two mechanisms of glycoside hydrolases.*** ***(A)*** *the inverting mechanism and* ***(B)*** *the retaining (Davies & Henrissat, 1995; Rye & Withers, 2000)*

Firstly, the inverting mechanism (Figure 1.3A) has two carboxylic acids in the active site with a 10.5 Å distance, where one is the catalytic acid, and one is the catalytic base. The oxygen in the glycosidic bond becomes protonated by the catalytic acid, and the catalytic base activates water that acts as a nucleophile on the anomeric carbon leading to the cleavage of the glycosidic bond (Davies & Henrissat, 1995; Koshland Jr, 1953; Rye & Withers, 2000).

Secondly, for the retaining mechanism (Figure 1.3B), the two carboxylic acids in the active site are 5.5 Å apart, and similarly one acts as the catalytic acid and the other the catalytic base. Firstly, the acid protonates the oxygen in the glycosidic bond and the base acts as a nucleophile on the anomeric carbon, forming a covalently linked intermediate. Secondly, a water molecule becomes deprotonated by the catalytic acid from the last step, that now acts as a base. The water performs a second nucleophilic attack on the anomeric carbon resulting in the cleavage of the glycosidic bond and disruption of the covalently linked intermediate (Davies & Henrissat, 1995; Koshland Jr, 1953; Rye & Withers, 2000).

1.4 Chitinases

Within the GH group, a subgroup of GHs are chitinases that hydrolyze the glycosidic bond in chitin and are found mostly in families GH18 (retaining mechanism, Figure 1.3B) and GH19 (inverting mechanism, Figure 1.3A) in the CAZy database (Henrissat, 1991; Koshland Jr, 1953). Chitinases can be exo-acting, where they cleave glycosidic bonds from an end of the chitin chain, where they are specialized to target the reducing or non-reducing end of the chitin chain. In comparison, endo-acting chitinases cleave glycosidic bonds at random along the chitin chain, often in more amorphous regions. In addition, like GHs chitinases often possess processive cleavage, where the chitinase cleaves glycosidic bonds constitutively without dissociating from the substrate (Beckham et al., 2014).

The processive chitinases all have in common that their active sites are encapsulated in aromatic residues (mostly tryptophan) that facilitate hydrophobic interactions with the carbohydrate substrate, giving a stronger enzyme-substrate complex resulting in processive mechanisms. The stacking of the sugars also forms a large surface for hydrophobic interactions, that are non-specific and of less strength than hydrogen bonding, making the energy barrier for sliding the substrate lower (Parsiegla et al., 2008; Quiocho, 1989; Vyas, 1991). In the chitin chain, every other GlcNAc unit has the same orientation, giving productive binding for hydrolysis occurring for every second sugar unit, resulting in chitobiose product. The strength in the hydrophobic interactions influences intrinsic enzyme speed, resulting in a boost in degradation when the aromatic residues are mutated, but often yielding less degree of processivity (Zakariassen et al., 2009).

1.5 Auxiliary activity

Early research on the degradation of recalcitrant polysaccharides developed the idea that unknown enzymes break down large polysaccharides making chains accessible to the GHs (Reese et al., 1950). AAs were previously categorized in the families CBM33 and GH61, and the redox enzymes called lytic polysaccharide monooxygenases (LPMO) were discovered (Vaaje-Kolstad et al., 2010). In the CAZy database, there are seven curator-approved AA families (AA9-11, 13.17), where all are redox active enzymes classified as LPMOs (Drula et

al., 2022). The separation from CAZy database families of CBM33 and GH61 was mainly due to the metal-ion cofactor important to the activity of the LPMOs, changing CBM33 and GH61 to AA10s and AA9s, later resulting in the addition of more families (Drula et al., 2022).

1.6 Lytic polysaccharide monooxygenases

LPMOs are endo-acting redox enzymes that disrupt the carbohydrate crystal by oxidation of the glycosidic bond in either the C1 or C4 positions (Vaaje-Kolstad et al., 2010; Vaaje-Kolstad et al., 2017). LPMOs have been found to be active towards cellulose and chitin (Forsberg et al., 2014), hemicellulose (Agger et al., 2014), xylan (Frommhagen et al., 2015), soluble substrates (Isaksen et al., 2014) and more, and LPMOs are found in AA families from mostly fungal (AA9, AA11, AA13, AA14, and AA16) and bacterial species (AA10) with some exceptions (Drula et al., 2022). The mainly studied LPMOs are in families AA9 and AA10 (Drula et al., 2022), where AA10 will be the focus of this thesis.

1.6.1 Structure

The LPMOs activity towards a crystalline surface is facilitated by the flat binding site structure and an overall triangular shape (Eijsink et al., 2019; Vaaje-Kolstad et al., 2017). The first crystal structure of an AA10 LPMO by Vaaje-Kolstad et al. (2005), prior to knowing the function of the enzyme in 2010 (Vaaje-Kolstad et al., 2010). Upon reviewing over 20 unique crystals, all LPMOs have in common a core structure comprised of a conserved histidine brace coordinating a copper ion, in addition to two β-sheets in a β-sandwich made by a total of seven to eight β-strands, that resembles immunoglobin or fibronectin-like core structures. The variation in the structure comes from the loops and helixes connecting the β-strands (Vaaje-Kolstad et al., 2017). Due to variations between one module and multinodular, with or without CBMs, the LPMOs can vary greatly in size.

The active site of LPMOs is characterizable by their conserved conformation with a histidine brace coordinating a copper ion, where without the copper ion the LPMO is not active. Still, copper has a high affinity that will ensure copper binding in the active site, if the metal ion is present (Quinlan et al., 2011).

1.6.2 Mechanism

After the discovery of LPMOs in 2010 by Vaaje-Kolstad and co-workers (Vaaje-Kolstad et al., 2010) LPMOs have gained interest due to their relevance in biomass degradation, both in the laboratory and in the cellulose-degrading industry (Johansen, 2016). However, the reaction mechanism still remains enigmatic. LPMOs were first thought to utilize molecular oxygen as the co-substrate (Vaaje-Kolstad et al., 2010), but recent evidence indicates that hydrogen peroxide is the relevant co-substrate (Bissaro et al., 2017; Kuusk et al., 2018; Rieder et al., 2021c; Wang et al., 2018).

Independent of co-substrate, an LPMO reaction is initiated by the reduction of the Cu(II) ion in the active site to Cu(I) by an external reducing agent. Small organic molecules such as ascorbic acid, gallic acid, or cysteine are often used to donate this electron (Vaaje-Kolstad et al., 2010). Monooxygenase conditions require two electrons per catalytic cycle, and therefore a high amount of reductant, while peroxygenase conditions only require a priming reduction of the copper ion to gain activity (Bissaro et al., 2017; Kuusk et al., 2018).

The originally suggested mechanism utilizing molecular oxygen for oxidation gave rise to the LPMO name, explained by $R\text{-}H + O_2 + 2e^- + 2H^+ \rightarrow R\text{-}OH + H_2O$, thereby monooxygenase (Horn et al., 2012). This theory has been shown to be questionable because of the reaction mechanism demanding two electrons, the first to reduce the copper and the second electron that has to gain access to the active site at a later stage, when it is shielded due to the formation of the enzyme-substrate complex, and therefore sterically challenging (Bissaro et al., 2017).

Evidence supporting the peroxygenase reaction, $R\text{-}H + H_2O_2 \rightarrow R\text{-}OH + H_2O$, that only includes one electron involved in a “priming” reduction of the copper-ion to LPMO-Cu(I) that

gains catalytic activity for multiple cycles. This reaction have an increased reaction speed by orders of magnitude compared to O_2 reactions and thus is the relevant co-substrate (Bissaro et al., 2017; Kuusk et al., 2018; Rieder et al., 2021b; Wang et al., 2018). Experiments conducted by Bissaro et al. (2017) with a low amount of reductant (for only priming purposes) show that the consumption of H_2O_2 by the LPMO correlates with the measured oxidized product. Isotope-labeled, $H_2{}^{18}O_2$ experiments showed that the oxygen that was added to the substrate in the oxidation comes from H_2O_2 over O_2, even at low H_2O_2 concentrations (Bissaro et al., 2017). Recent studies supporting H_2O_2 as the true co-substrate have investigated that intrinsic enzymatic activity of the LPMO happens either by the formation of H_2O_2 *in situ* from molecular oxygen by the LPMO, or external addition of H_2O_2 (Bissaro et al., 2017; Kuusk et al., 2018; Wang et al., 2020). The true mechanism of the catalytic action involving H_2O_2 is still not fully characterized, but discussions include the formation of a Cu(II)-O• (oxyl) directed by hydrogen bonds, and the copper(II)-oxyl will hydrolyze the substrate resulting in the cleavage of the glycosidic bond (Bissaro et al., 2017; Wang et al., 2018).

An enzyme's ability to produce *in situ* H_2O_2 can be referred to as oxidase activity. Dependent on the nature of an LPMO, reactions condition including what substrate, reductant, and free copper concentration, LPMOs possess different abilities in producing *in-situ* H_2O_2 by reduction of O_2 (Bissaro et al., 2017; Golten et al., 2023; Rieder et al., 2021b; Stepnov et al., 2021; Stepnov et al., 2022). The initial LPMO experiments investigating the O_2 mechanism, are most likely slow due to the rate-limiting reduction of O_2 to H_2O_2 by the LPMO (difference between different LPMOs, reductant, and substrate), rather than oxygen being the true co-substrate (Bissaro et al., 2020).

1.6.3 LPMO stability

Since peroxygenase reaction has high catalytic activity, it is of great interest to use externally added H_2O_2. Still, high initial amounts of H_2O_2 often lead to the inactivation of the LPMO (Bissaro et al., 2017; Kuusk et al., 2019). A high level of H_2O_2 can be accumulated without the external addition of H_2O_2, either by reduced LPMOs reducing O_2 to form H_2O_2, typically

in the absence of substrate, or by the oxidation of reductant, induced by free copper concentration (Stepnov et al., 2021).

Different experimental measures will minimize the accumulation of H_2O_2 while still benefitting from the high reaction rate by peroxygenase condition. They include high substrate concentration, low amounts of unbound copper ions, low controlled supply of external H_2O_2, and the use of additional enzymes for *in-situ* production of H_2O_2 (Bissaro et al., 2017; Forsberg et al., 2019; Kuusk et al., 2019; Stepnov et al., 2021). Independent of mono or peroxygenase conditions, a high substrate concentration will ensure binding sites for the LPMO. This way the LPMO will use the oxidative species that are forming in a constructive matter on the substrate (Bissaro et al., 2017; Kuusk et al., 2018; Loose et al., 2018). The presence of free copper ions in reaction setups including reductant also imposes a risk due to the reduction Cu(II) to Cu(I) will reduce O_2 and give H_2O_2 that will accumulate, increasing the importance of removing excess copper after copper-saturation of the LPMO to avoid unproductive reduction of free copper (Stepnov et al., 2021). Next, a high external initial H_2O_2 dose will lead to a high rate of initial oxidative damage to the LPMO, therefore it's suggested to gradually supply the reaction with an H_2O_2 concentration that does not surpass the amount the LPMO can utilize for oxidative cleavage (Bissaro et al., 2017; Kuusk et al., 2018; Kuusk et al., 2019). Also, choice of reductant, buffer and pH will influence the accumulation of H_2O_2 and LPMO activity and should be considered dependent on LPMO when selecting reaction parameters (Golten et al., 2023).

1.6.3.1 External H_2O_2 production by *Arthrobacter globiformis* choline oxidase

In this thesis, the use of a choline oxidase (ChOx) from *Arthrobacter globiformis* to produce a controlled production of H_2O_2 at a low rate over the course of the experiments was implemented (Figure 1.4) (Gadda, 2003), to avoid the addition of a high amount H_2O_2 at the initial phase of the reaction, risking inactivation. Bissaro et al. (2017) used a glucose oxidase for a controlled *in situ* production of H_2O_2 in an LPMO reaction and achieved similar results

as for the external supply of H_2O_2.

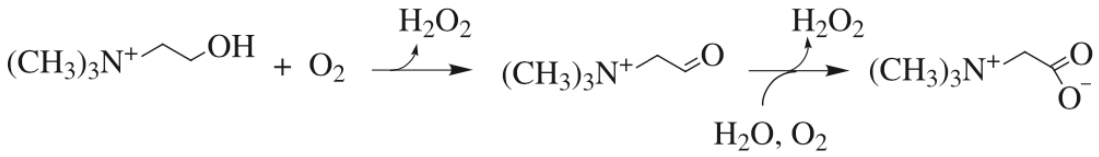

Figure 1.4 ***AgChOx reaction scheme when oxidizing choline****. Derived from (Gadda, 2003).*

The *Ag*ChOx will oxidize choline in a two-step oxidation to glycine-betaine with the intermediate of betadine-aldehyde, and the reaction produces two H_2O_2 molecules per cycle, as shown in Figure 1.4 (Gadda, 2003).

1.7 *Serratia marcescens* chitinolytic machinery

The gram-negative bacteria *Serratia marcescens* encodes the genes for a synergistic machinery of enzymes for chitin degradation. *S. marcescens* in the presence of chitin expresses several GHs and an LPMO, where the GHs were named Chitinase A (ChiA), Chitinase B(ChiB), Chitinase C (ChiC), Chitinase D (ChiD) and Chitobiose (CHB) and the LPMO *Sm*AA10A (previously known as CBP21) (Vaaje-Kolstad et al., 2013). Already in 1969, a study proved *S. marcescens* to be the most effective chitin degrader among 100 microorganisms (Monreal & Reese, 1969). The early studies separated and isolated the 5 different chitinolytic enzymes, cloned, categorized, and investigated the basic enzyme mechanism on chitin (Fuchs et al., 1986; Henrissat, 1991; Jones et al., 1986; Sundheim et al., 1988). Then, Brurberg et al. investigated how to improve the procedures for purification and conducting enzymatic assays to assess the efficiency of the GH degradation of chitin (Brurberg et al., 1994; Brurberg et al., 1995; Brurberg et al., 1996).

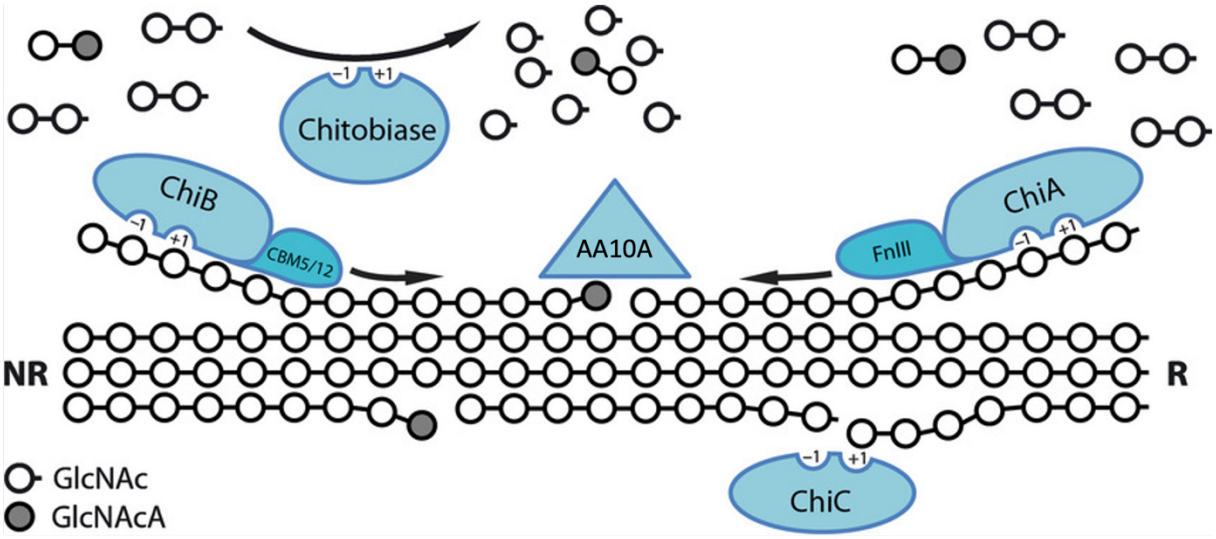

Figure 1.5 ***Schematic display of the chitinolytic machinery of S. marcescens on chitin****. Chitin is displayed in chains organized as β-chitin marked with reduced ® and non-reduced (NR) ends where GlcNAc units (white circles) and where GlcNAc is oxidized to aldonic acids, GlcNAcA (filled circles). The exo-acting ChiB (works from NR end) and SmChiA (works from R end) produce chitobiose recessively, ChiC endo-acts on the chitin chain producing random breakage of the glycosidic bonds in amorph areas, while AA10A acts on crystalline regions oxidizing glycosidic bonds. Chitobiase (CHB) produces monomers from soluble oligomers. The figure was derived, with minor adjustments from Vaaje-Kolstad et al. (2013)*

The *S. marcescens* chitin degrading system utilizes several enzymes in synergy, that can be defined as the sum of two or a group working together is greater than the individual sums combined (Wood & Garcia-Campayo, 1990). Figure 1.5 display a schematic overview of the chitinolytic enzymes in *S. marcescens* and describes how different acting enzymes in synergy break down β-chitin (Vaaje-Kolstad et al., 2013). The first two GH18 processive exo-acting chitinases, *Sm*ChiA and *Sm*ChiB, act from the reduced and non-reduced end of the chitin chain, respectively. Both enzymes have their own unique CBMs named, FnIII, and CBM5/12, respectively. The third GH18, *Sm*ChiC is an endo-acting chitinase that usually binds and cleaves glycosidic bonds to amorphous parts of the crystalline chitin, resulting in chitin chain breaks releasing chain ends for *Sm*ChiA and *Sm*ChiB to cleave further by acting exo-processive. Due to the highly crystalline nature of the polysaccharide, as proposed by Reese et al. (1950) and demonstrated by Vaaje-Kolstad et al. (2010), *S. marcescens* contain an LPMO *Sm*AA10A, that performs oxidative catalysis of the C1-H bond resulting in the break of the scissile glycosidic bond of highly crystalline chitin regions. Lastly, chitinolytic organisms usually require an easily accessible substrate to grow efficiently, and therefore often need

GlcNAc monomers to utilize for energy or carbon sources. This highlights the importance of the GH20 chitobiose, that catalyzes the degradation of chitobiose to mainly GlcNAc (Toratani et al., 2008).

Interestingly, Mekasha et al. suggested an optimized cocktail with all *S. marcescens* chitin-degrading enzymes to produce GlcNAc monomers. It was observed a 70-75 % yield with an enzyme cocktail containing approximately 40 % *Sm*ChiA, 30 % *SmChiB*, 20 % *Sm*ChiC and 2 % *Sm*AA10A, indicating the importance of the presence of *Sm*ChiA compared to the relatively low amount of *Sm*AA10A for optimal chitin degradation (Mekasha et al., 2017).

1.7.1 *Sm*ChiA

The most efficient *S. marcescens* chitinase in degrading chitin alone is the GH18 *Sm*ChiA (Hamre et al., 2014; Vaaje-Kolstad et al., 2013), which is a 58.5 kDa enzyme with a "cleft" topology (1.3 and Figure 1.2B) and contains 540 residues. The enzyme was first cloned by Sundheim et al. (1988), and crystal structures from Papanikolau et al. (2001) showed the deep "cleft" topology (Figure 1.6), that almost resembles a "tunnel" (1.3 and Figure 1.2C). Moreover, the cleft is encapsulated by aromatic residues on both sides of the catalytic acid associated with carbohydrate binding and sliding of the substrate after hydrolysis for exo-acting processive GHs (see 1.3). The deep "cleft" topology is due to the insertion of 70-90 amino acids in the active site, also seen in several other chitinases (Horn et al., 2006b). In addition to the aromatic residues near the active site, the FnIII N-terminal module also has aromatic residues exposed, promoting substrate binding and has been shown to increase *Sm*ChiA catalysis (Uchiyama et al., 2001). The "cleft" topology is normally associated with endo-acting GHs, so interestingly *Sm*ChiA also has displayed endo-activity on chitin (Brurberg et al., 1996; Horn et al., 2006b; Horn et al., 2009) as well as a preferably processive exo-acting mode of action.

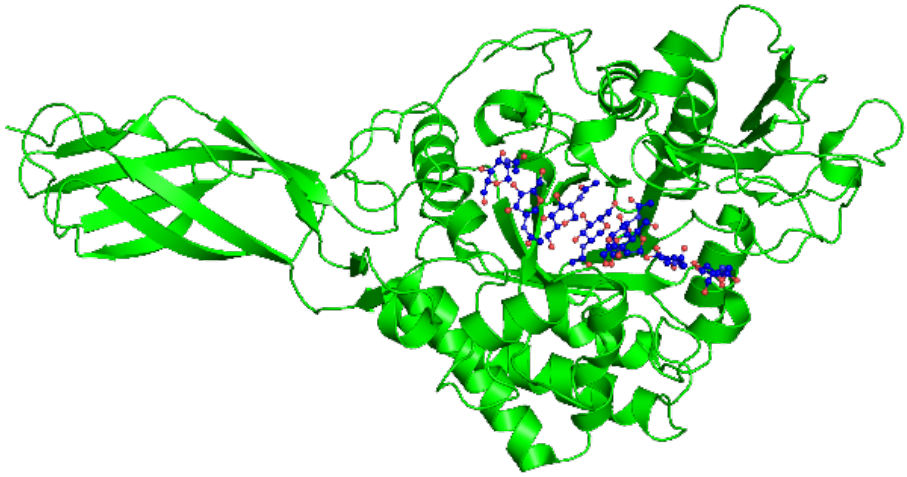

Figure 1.6 ***Crystal structure of SmChiA with substrate****. Inactive mutant by mutating the glutamate in the active site to glutamine, E315Q) with a* $(GlcNAc)_8$*. The enzyme is colored green and the chitooligomer has blue carbons and red oxygens. The substrate binds in the subsites (PDB: 1EHN) (Papanikolau et al., 2001).*

Compared to the other chitinases from *S. marcescens*, *Sm*ChiA has the highest initial degree of processive action (Hamre et al., 2014). The degree of processivity is often linked to stacking interactions in the active site with the carbohydrate substrates by aromatic residues (Horn et al., 2006a; Zakariassen et al., 2009). When mutated, the degree of processivity of the enzyme decreases and the binding free energy with the substrate becomes less (Hamre et al., 2015b; Hamre et al., 2019; Horn et al., 2006a; Horn et al., 2006b; Uchiyama et al., 2001; Zakariassen et al., 2009). The strong interactions between the GH and the carbohydrate polymer are linked to the GH being stuck to the carbohydrate polymer, that is also the case for *Sm*ChiA (Hamre et al., 2015b; Hamre et al., 2019; Igarashi et al., 2011). In addition, it has been reported that as the substrate becomes more recalcitrant, the degree of processivity decreases, as shown for *Sm*ChiA (Hamre et al., 2014).

In enzymatic assays, *Sm*ChiA is viewed as a stable enzyme with a broad pH and temperature activity range, with the optimal condition at a pH of 6.1 and temperatures between 50 and 60 °C (Brurberg et al., 1996). Product inhibition have been viewed on the mM scale for chitobiose (Brurberg et al., 1996; Kuusk et al., 2015). As it being the single most efficient chitin degrading chitinase of *S. marcescens*, *Sm*ChiA is a natural choice for the investigation of the interaction between a GH and an LPMO, *Sm*AA10A.

1.7.2 *Sm*AA10A

The crystalline disruptive enzyme of *Sm*AA10A that oxidatively cleaves glycosidic bonds was discovered by Vaaje-Kolstad et al. (2010), originally named Chitin Binding Protein 21 (CBP21), now named *Sm*AA10A, it contains 170 residues and a molecular weight of 19 kDa. The catalytic activity on chitin results in the oxidation of the C1-H bond followed by the cleavage of the glycosidic bond, generating a non-reduced end and an aldonic acid for the reduced end (Vaaje-Kolstad et al., 2010). Substrate binding is facilitated by hydrogen bonds (Loose et al., 2018), as well as several hydrophobic residues, that when the binding residues are mutated *Sm*AA10A loses some of its ability to bind to the crystalline chitin (Agger et al., 2014; Vaaje-Kolstad et al., 2010).

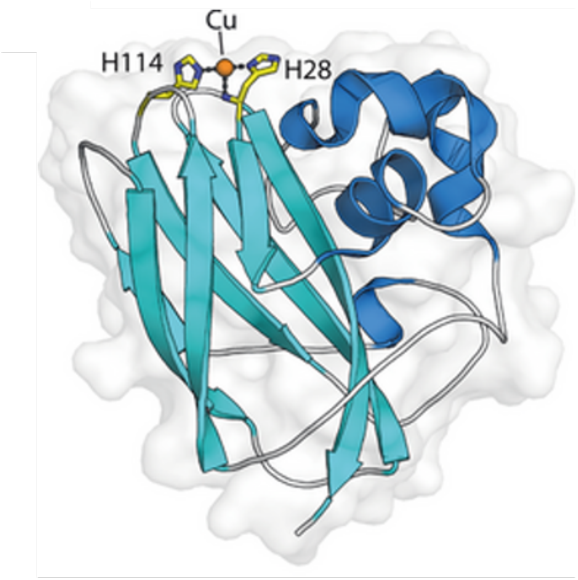

Figure 1.7 ***Structure of SmAA10A,*** *where the two histidine residues coordinating the copper ion (orange) is displayed in yellow. The figure is derived from (Vaaje-Kolstad et al., 2013).*

*Sm*AA10A has been reported to be more active on β-chitin crystalline substrate than α-chitin (Vaaje-Kolstad et al., 2010). It is suggested that the rate-limiting step of *Sm*AA10A catalytic action in the presence of an external reductant and O_2, also called monooxygenase conditions, is *Sm*AA10A´s ability to form H_2O_2 from molecular oxygen, therefore explaining why the rate of reactions with O_2 is slow (Bissaro et al., 2017). Under externally added H_2O_2 reaction conditions, also known as peroxygenase conditions, *Sm*AA10A displayed a k_{cat} (measured reaction rate) by orders of magnitude higher compared to under O_2 reaction conditions

(Kuusk et al., 2018; Vaaje-Kolstad et al., 2010), though Kuusk et al. (2018) reported optimal H_2O_2 concentrations at μM levels, and that often normal reaction conditions used (100 μM range) will lead to inactivation.

1.8 Aim of the thesis

Carbohydrate-active enzymes in biomass degradation hold large potentials to utilize polysaccharides produced in nature that previously have been considered waste as a source to yield products of value. These resources, such as chitin, cellulose, and more, can contribute to the environmental and sustainable future of biofuel and medical advances. Investment in this technology to create products of value at a low use of energy will contribute to the reduction of climate change and be a significant contribution to reaching the SDGs set by the UN.

The soil bacterium *S. marcescens* contains a chitinolytic machinery consisting of three GH18, one GH20, and an AA10. The complementary abilities and synergetic action of these enzymes in chitin degradation are of high interest to explore. In this regard, it is highly interesting to explore how the most efficient catalyst of chitin hydrolysis, *Sm*ChiA interplay with the newly discovered *Sm*AA10A that act on the crystalline parts of chitin creating new chain-ends for *Sm*ChiA to act upon. *Sm*AA10A and *Sm*ChiA have previously shown to have synergistic effects on the degradation of β-chitin. The aim of this thesis is to investigate how this synergistic effect can be boosted by analyzing chitobiose yield *Sm*ChiA in the presence of *Sm*AA10A. The experimental setups included varying the enzyme concentrations, when *Sm*AA10A was added, substrate concentrations, and the amount and delivery of H_2O_2 in the presence of *Sm*AA10A.

In addition, *Sm*ChiA was cloned into the industrial expression system of *P. pastoris*, as the beginning of a long-term goal of creating a complete chitinolytic cocktail easily expressed and secreted in relative pure yields enabling easy down-stream purification and utilization in biomass conversion to products of value.

2 Materials

2.1 Equipment

Table 2.1 ***Utilized laboratory instruments with application and supplier.***

Instrument	Application	Supplier
BioLogic LP system	LPLC	BioRad
Cary 8454 UV/Vis	Absorbance	Agilent Technologies
Dionex ™ Ultimate™ 3000 RSLC system	HPLC	ThermoFisher Scientific
GelDoc ™ Go System	Gel imaging	Bio-Rad
Nanodrop One	Absorbance	ThermoFisher Scientific
Nanophotometer ®	Absorbance	ThermoFisher Scientific
NGC Chromatography system	IEX, SEC, HIC	BioRad
Varioskan LUX Multimode microplate reader	Amplex Red assay	ThermoFisher Scientific

Table 2.2 ***Table of laboratory equipment.***

Equipment	Specifications	Supplier
Autoclave tape	12 mm	Merck
Automatic pipettes	Finnpipette ™ F2 pipetting system Single channel	Merck

	Multichannel	
Block heater		ThermoFisher Scientific
Centrifuges	Sorvall Lynx 6000 4530 R centrifuge Minispin centrifuge	ThermoFisher Scientific Eppendorf Eppendorf
Centrifuge rotors	F-35-6-30 rotor FA-45-30-11 F9-6 × 1000 LEX Fixed Angle Rotor Fiberlite ™ F21-8 × 50y Fixed Angle Rotor Fiberlite ™	Eppendorf Eppendorf ThermoFisher Scientific ThermoFisher Scientific
Centrifuge tubes	1 L bottle 50 mL tube	ThermoFisher Scientific
Centrifuge filters	Amicon ® Ultra-15, 15 ml 10 kDa cutoff 30 kDa cutoff	Merck Millipore
Column	1.5 x10 cm (18 mL volume) column	Bio-Rad
Concentrator	Vivaflow 200 tangential crossflow concentrator 10 000 da cutoff Amicon ® Ultra-15 Centrifugal filter units 10 kDa cutoff 30 kDa cutoff 50 kDa cutoff	Merck Millipore

Cryogenic tubes	2 mL	Sarstedt
Cuvettes	Plastic Semi-Micro cuvettes 12.5 × 12.5 × 45 mm Quartz Hellma ™ Suprasil ™ Quartz 104B Semi- Micro Cell cuvettes Electroporation: Gene Pulser / MicroPulser	Merck ThermoFisher Scientific Bio-Rad
Disposable pipettes	1 mL & 3 mL - plastic	VWR
Electroporation system	Gene pulser II Pulscontroller plus	Bio-Rad
Electrophoresis system	Mini-PROTEAN Tetra system Mini-Sub GT cell (9.2x25.5x5.6 cm) PowerPac ™ basic power supply Blue tray UV/stain free tray Agarose gel casting tray	Bio-Rad
Electrophoresis gel	Mini-PROTEAN TGX Stain-Free Precast Gel 10 well 15 well	Bio-Rad
Filter	Steriltop: 0.45 µm	Merck

	Syringe filter 0.45 µm 0.20 µm	Sarstedt
Filter plate	96-well	Sarstedt
Freezer and fridge	4 °C -20 °C -80 °C	Bosch SANYO
Glassware	Baffled shake flasks Beakers Blue-cap bottles Erlenmeyer beaker Graduated cylinders Volumetric flask Test tubes Cell spreader	Schott-Duran VWR
HPLC vials and caps	Micro vials 200 µL - plastic Red caps	ThermoFisher Scientific
Ice Maker	KF 145	PORKKA
Incubators	Static: Thermaks static incubator T100 Thermal cycler Shaking: Multitron Standard Thermomixer C	 Termaks Bio-Rad Infors Eppendorf

Inoculation loops	Disposable plastic: 1 µL	Merck
Magnets		IKA
Magnetic stirrer	Fisherbrand ™	ThermoFisher scientific
Microtiter microplate	96-well 96-well filter plate	ThermoFisher Scientific
Milli-Q	Milli-Q® Direct water purification system	Merck
Parafilm	5 cm	VWR
Petri dishes	9 cm	Heger
pH meter	pH110M	VWR
Pipette tips	Next generation tip refill (size range 2 µL - 5 mL)	VWR
Pumps	Peristaltic Masterflex ™ pump drive Vacuum pump (With multiscreen HTS vacuum manifold)	Merck Millipore (Merck)
Scales		VWR
Spatulas		
Sterile bench	Av-100	TelStar
Syringes	1 mL – 50 mL	Merck
Tubes	PCR tubes – 200 µL 1.5 mL / 2.0mL	Axygen

	15 mL 50 mL	Greiner Bio-One
Vortex	MS 3 basic	IKA
Water bath	30-45 °C	Julabo

Table 2.3 ***Columns with specification, application, and supplier.***

Column	Specification / application	supplier
Chitin resin	/ Chitin affinity chromatography	NEB
HiLoad 16/160 Superdex 75 pg	120 mL / SEC	Merck
HiTrap Phenyl HP	5 mL / HIC	Cytiva
HiTrap Q FF	5 mL / IEX	Cytiva
Rezex RFQ-Fast Acid	H^+ (8 %) 7.8 x 100 mm column / HPLC	Phenomenex

Table 2.4 ***Kits with suppliers.***

Kit	Supplier
DNA clean and concentrator ™ - 5	Zymo Research
E.Z.N.A ® Plasmid DNA mini kit I	Omega Biotek

2.2 Chemicals and reagents

Table 2.5 ***List of chemicals.***

Chemical	Detail	Supplier
4-methylumbelliferone (4-MU)	4-MU sodium salt: MW = 198.20	Merck
4-methylumbelliferone di-N-acetyl glucosamine (4-MU(GlcNAc)$_2$)		Merck
Agar powder	$(C_{12}H_{18}O_9)_n$	Merck
Ammonium sulphate	$(NH_4)_2SO_4$	Merck
Ampicillin disodium	$C_{16}H_{18}N_3NaO_4S$	Invitrogen
Amplex red	$C_{14}H_{11}NO_4$	Invitrogen
Antifoaming agent	Antifoam 204	Merck
Bis-tris	$C_8H_{19}NO_5$	Merck
Chemically competent *E. coli*	One Shot ® TOP10 BL21(DE3)	Life technologies
Chloroform	$CHCl_3$	VWR
Choline chloride	$(CH_3)_3N(Cl)CH_2CH_2OH$	Merck
Citric acid	$C_6H_6O_7$	Merck
Copper sulfate	$CuSO_4$	Merck
Dextrose	$C_6H_{12}O_6$	Merck

Di-N-acetyl glucosamine $(GlcNAc)_2$	$C_{16}H_{28}N_2O_{11}$	Megazyme
Disodium hydrogen phosphate	Na_2HPO_4	Merck
Electrocompetent *P. pastoris* BSYBG11	Yeast strain	Bisy Gmbh
Ethanol	C_2H_5OH	VWR
Ethylenediaminetetraaceticacid (EDTA)	C10H16N2O8	Merck
Gycerol	$C_3H_8O_3$	VWR
Hydrogen chloride	HCl	Merck
Hydrogen peroxide	H_2O_2	VWR
L-ascorbic acid	$C_6H_6O_6$	Merck
Methanol	CH_3OH	Honeywell
N-acetyl glucosamine (GlcNAc)	$C_8H_{15}NO_6$	Megazyme
NuPAGE® LDS Sample Buffer	4 x	Invitrogen
NuPAGE® Sample reducing agent	10 x	Invitrogen
Sucrose	$C_{12}H_{22}O_{11}$	Merck
S.O.C media	Super optimal broth	Invitrogen
Sodium chloride	NaCl	VWR
Sodium carbonate	Na_2CO_3	VWR
Sodium dihydrogen phosphate	NaH_2PO_4	Merck
Sodium hydroxide	NaOH	VWR

Sulfuric acid	H_2SO_4 (analyze grade)	Merck
SYBR safe DNA gel stain	[10 000x] in DMSO	ThermoFisher scientific
Squid pen β – Chitin	Milled to 75-200 µm	France chitin
Tris	$C_4H_{11}NO_3$	Merck
Tris, acetate, EDTA (TAE) buffer	10 x	Bio-Rad
Tris/glycine/SDS buffer	1 x	
Tryptone	C_3H_5NO	VWR
Ultrapure ™ agarose	$(C_{12}H_{18}O_9)n$	Invitrogen
Yeast extract	$C_{19}H_{14}O_2$	Invitrogen

2.3 Buffers and media

Table 2.6 ***Self prepared media****. Per 1 L if not stated otherwise. All filtrations were performed using a 0.20 µm or 0.45 µm filter.*

Media	**Preparation per L**
Lysogeny broth (LB)	5 g Yeast extract 10 g Tryptone 10 g Sodium Chloride If agar: 15 g agar If low salt: 0.5 g/L

	Dissolve all reagents in ddH_2O to desired volume. Autoclave at 121 °C for 15 min.
Terrific broth (TB)	12 g Tryptone 24 g Yeast extract 4 mL 85 % (v/v) glycerol Dissolved in ddH_2O and volume adjusted to 900 mL before autoclavation at 121 °C for 15 min. Phosphate solution (0.5 liter): 11.57 g potassium dihydrogen phosphate 62.7 g dipotassium hydrogen phosphate Dissolve all reagents in ddH_2O and volume adjust to 0.5 L. Autoclaved at 121 °C for 15 min. Prior to usage mix 1/10 total volume of phosphate solution with 9/10 of the rest.
Yeast extract-peptone-dextrose media (YPD)	10 g Tryptone 20 g Yeast extract 20 g dextrose If agar: add 15 g agar Dissolve all reagents in ddH_2O and volume adjust. Autoclave at 121 °C for 15 min.

Table 2.7 ***Self-prepared buffers and solutions.*** *All filtrations were performed using a 0.20 µm or 0.45 µm filter and volume adjustments were performed using ddH_2O.*

Buffers and solutions	**Preparation per L**

Bis-Tris/HCl (500 mM) pH range: 5.8-7.2	104.62 g Bis-Tris Dissolved in ddH_2O and pH adjusted with HCl prior to volume adjustment.
Tris-HCl (1 M) pH range: 7.5-9.0	121.14 g tris Dissolved in ddH_2O, pH adjusted with HCl and volume adjusted with ddH_2O. For 50 mM Tris-HCl + 200 mM NaCl: 11.688 g NaCl Dissolved into ddH_2O with 50 mL 1 M Tris-HCl with desired pH, pH adjusted with HCl and volume adjusted with ddH_2O.
Sodium phosphate (500 mM) pH range: 5.8-8.0	A stock of 500 mM was prepared individually of sodium dihydrogen phosphate and disodium hydrogen phosphate: 59.99 g NaH_2PO_4 70.98 g Na_2HPO4 The salt was dissolved in 1 L MQ individually. For specific pH the content of each stock was adjusted for the final buffer, assuming 25 °C. Example, 1 L 500 mM sodium phosphate buffer pH 7: 615 mL Na_2HPO4 500 mM stock 385 mL NaH_2PO_4 500 mM stock
Citrate phosphate buffer	0.1 M citric acid 19.21 g citric acid Dissolved in ddH_2O

	100 mL buffer was prepared by mixing 17.9 mL citric acid and 12.8 mL 500 mM disodium hydrogen phosphate stock (see sodium phosphate buffer) in 69.3 mL MQ.
Spheroplast buffer	146.13 mg EDTA Dissolved in ddH_2O pH adjusted to pH and volume adjusted before filtration to prepare 0.5 mM EDTA pH 8.0 100 mL Spheroplast buffer: 3.423 g sucrose Dissolved in 10 mL 1 M Tris-HCl pH 8.0 and 100 µL 0.5 mM EDTA pH 8.0. Volume adjusted with ddH_2O to 100 mL and store at 4 °C.
Chitin affinity buffer A (CA buffer A)	1 M ammonium sulphate + 50 mM Tris-HCl pH 8.0 132.14 g ammonium sulphate 50 mL 1 M Tris-HCl pH 8.0 Dissolved ammonium sulphate in MQ, added Tris-HCl and pH adjusted. Volume adjusted before filtered.
Chitin affinity elution buffer (CA elution buffer)	20 mM Acetic acid 1149 µL 99.8 % acetic acid Added to ddH_2O and volume adjusted prior to filtering
Anion exchange buffer A (IEX buffer A)	20 mM Tris-HCl pH 8.0 20 mL Tris-HCl 1 M stock Volume adjusted and filtered.
Anion exchange buffer B (IEX buffer B)	20 mM Tris-HCl pH 8.0 + 1 M NaCl 20 mL Tris-HCl 1 M stock

	58.44 g Sodium chloride Dissolved sodium chloride in ddH_2O, added Tris-HCl from stock and pH adjusted. Volume adjusted and filtered.
Hydrophobic interaction chromatography buffer A (HIC buffer A)	50 mM Bis-Tris HCl pH 6.5 + 2 M ammonium sulphate 100 mL 500 mM Bis-Tris HCl stock 264 g ammonium sulphate Dissolved ammonium sulphate in ddH_2O, added Bis-Tris HCl, pH adjusted prior to volume adjustment, then filtered.
Hydrophobic interaction chromatography buffer B (HIC buffer B)	50 mM Bis-Tris HCl pH 6.5 100 mL 500 mM Bis-Tris HCl stock Bis-Tris stock added to ddH_2O and pH adjusted before volume adjusted, and filtered.
Size exclusion buffer (SEC buffer)	20 mM Bis-Tris pH 6.5 + 150 mM NaCl 40 mL 500 mM Bis-Tris HCl stock 8.766 g sodium chloride Dissolved the salt in ddH_2O, added the Bis-Tris and pH adjusted. Volume adjusted and filtered.
Storing buffer *Sm*AA10A	Storing buffer for *Sm*AA10A is 50 mM sodium phosphate pH 7.0 100 mL 500 mM sodium phosphate stock pH 7.0 Added to 900 mL ddH_2O.
5 mM sulfuric acid	5 mM sulfuric acid (2 L) 556 µL sulfuric acid Added to ddH_2O and volume adjusted to 2 L

2.4 Proteins and standards

Table 2.8 ***List of proteins and standards***

Protein	Details	Supplier
*Ag*ChOx	Choline oxidase	Provided by Ole Golten
Benchmark ™ protein ladder	Protein standard for SDS-page	Life technologies
Bovine serum albumin (BSA)	Protein alternative for no activity	Invitrogen
Generuler	DNA standard	Invitrogen
SapI		New England BioLabs
*Sm*AA10A	LPMO	Self-produced
*Sm*ChiA	Chitinase	Self-produced
SmCHB	Chitobiase	Provided by Ole Golten
SwaI restriciton enzyme	Linearization of pBSY	New England BioLabs

2.5 Primers

Table 2.9 ***List of primers with sequence.***

Primer	Sequence 5´-3´	T_m (°C)
Ost1-FWD	TTCTTTTGTTACTTACATTTTACCGTTCCG	65
AOXT-REV	AAAATGAAGCCTGCATCTCTCAGGCAAATG	71

2.6 Software

Table 2.10 ***List of software's.***

Software	Used for
Chromeleon 7 – ThermoFisher Scientific	HPLC analysis
ChromLab - Bio-Rad	HIC / SEC / IEX
Microsoft excel	Data analysis
Microsoft Powerpoint	Illustration and presentation preparation tool
ProtParam - Expasy	Determine
PyMOL – Warren Lyford DeLano	Protein visualization tool
SkanIt 6.0.1 – ThermoFisher Scientific	Amplex red assay
SnapGene - Dotmatics	DNA alignment tool

3 Methods

3.1 Cloning *Sm*ChiA into *Pichia pastoris*

The yeast expression system of *P. pastoris* is one of the most used industrial species for recombinant proteins and heterologous expression. Some of the advantages are folding in the endoplasmic reticulum, to ensure appropriate folding and its ability to secrete proteins without interfering proteins giving for easy purification (Karbalaei et al., 2020). In addition, the use of yeast expression systems have proved valuable for bacterial enzymes as a bacterial β-mannanase (degrades mannans in hemicellulose) has successfully been cloned into *P. pastoris* (Vu et al., 2012). It is already an expression system utilized for protein production, e.g., vaccines (Balamurugan et al., 2007), insulin (Baeshen et al., 2016), and fungal LPMOs (Kittl et al., 2012).

The gene for the bacterial enzyme Chitinase A from *Serratia marcescens* (*Sm*ChiA) was cloned into the yeast *Pichia pastoris (P. pastoris)* for potential future industrial use. The gene and plasmid were optimized for expression in yeast supplied by Dr. Lukas Reider, and the primers were supplied by Dr. Kelsi Hall. Cloning of *Sm*ChiA into *P. pastoris* was performed by cloning the gene into the plasmid pBSYP$_{gcw14}$Z- OST1 after the stuffer fragment was removed (Figure 3.1). Then the plasmid was transformed into the *E. coli* One Shot ® Top10 strain to produce a high plasmid copy number for sequence verification and transformation into *P. pastoris*. A protein precipitation test was conducted to select transformations that gave a high protein yield, due to the effect of insertion location in the *P. pastoris* genome, transformants will have different expressions resulting in different protein yields.

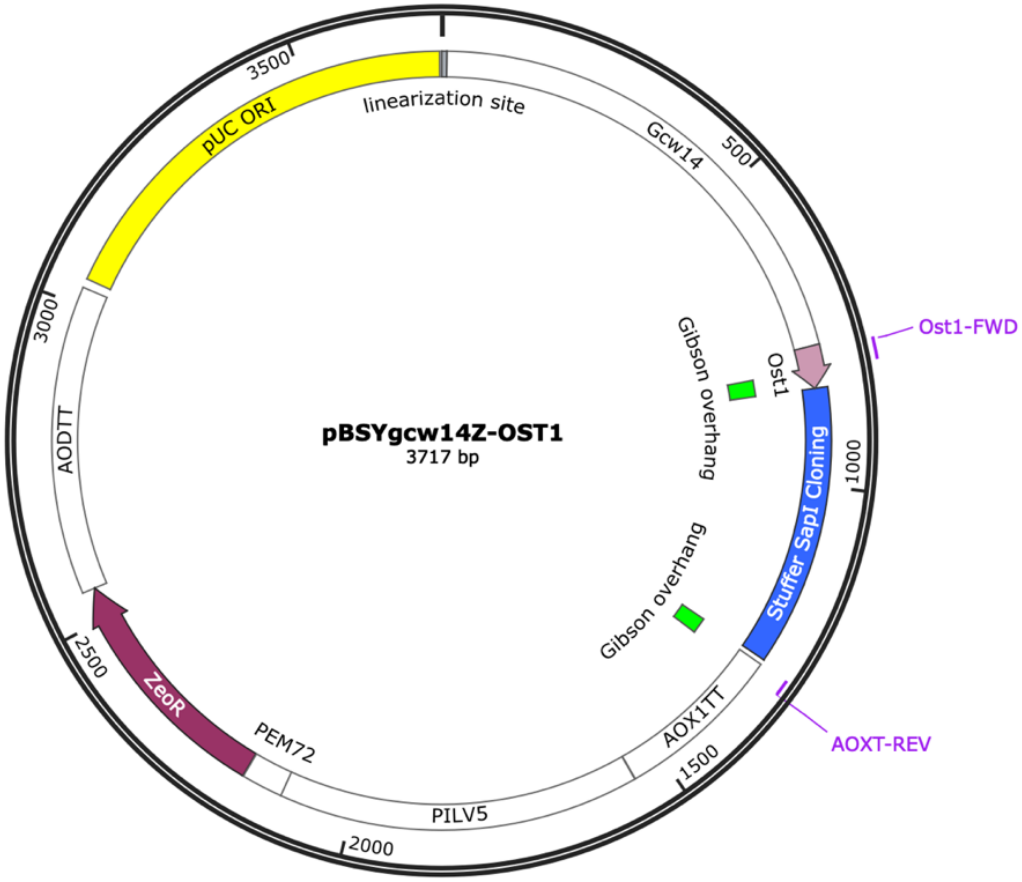

Figure 3.1 ***The pBSYgcw14-Z-Ost1 plasmid.*** *Marked with the features; linearization site, Gcw10 (promotor), Ost1 as signal peptide for secretion into the extracellular matrix, the stuffer SapI cloning fragment, AOX1TT (terminator), ZeoR (zeocin resistance gene), AODTT (terminator) and pUC ORI (origin of replication). The primers (marked in purple) Ost1-FWD binds near the signal peptide and the AOXT-REV binds in the terminator after the stuffer.*

Figure 3.1 shows the plasmid pBSYP$_{gcw14}$Z- OST1, with the main component as the Ost1 signal peptide for secretion into the extracellular matrix, stuffer fragment that can be removed with SapI restriction enzyme, zeocin resistance gene (ZeoR) and the linearization site. After the stuffer was removed, the insertion of the *chiA* gene were performed with Gibson cloning. The Gibson overhangs (marked with green boxes) will create asymmetric overhangs that ensure that the gene is inserted the correct way. After cloning and cultivation in *E. coli* One Shot ® Top 10, the plasmid was cleaned, linearized by SwaI before transformation into *P. pastoris* by electroporation.

3.1.1 Cloning of *Sm*ChiA into pBSYP$_{gcw14}$Z- OST1

Materials:

- *Sm*ChiA gene
- pBSY$_{gcw14}$Z- OST1
- SapI restriction enzyme
- 10X NEBuffer
- Gibson Assembly ® Master Mix (2x)
- T100 ™ Thermal Cycler
- NanoDrop One

Method:

The stuffer fragment was removed from the pBSYP$_{gcw14}$Z- OST1 plasmid by incubating 1 µg of plasmid with 1 µL SapI restriction enzyme in 5 µL NEBuffer for 15 minutes at 37 °C in a T100 ™ Thermal Cycler. The restriction enzyme was inactivated by increasing the temperature to 65 °C for 20 minutes. The *chiA* gene was cloned into the plasmid by Gibson cloning (New England Biolabs), with a total reaction volume of 10 µL consisting of the gene, plasmid and Gibson Assembly ® Master Mix, shown in Table 3.1. The mix was prepared on ice before incubated at 50 °C for 60 minutes in T100 ™ Thermal Cycler, before samples were put back on ice.

Table 3.1. Gibson Assembly reactions for insertion of SmChiA into the plasmid pBSY$_{gcw14}$Z- OST1

Reagent	**Amount**
Gibson Assembly Master Mix	2 µL
Plasmid: pBSYP$_{gcw14}$Z- OST1	100 ng
Insert: *Sm*ChiA	50 ng
ddH_2O	up to 10 µl

3.1.2 Transformation of pBSYPgcw14Z- OST1 *Sm*ChiA into chemically competent *E. coli* One Shot ® Top10

Materials:

- Gibson cloning sample of pBSYP$_{gcw14}$Z- OST1_*Sm*ChiA
- One Shot ® Top10 chemically competent *E. coli* cells
- Zeocin
- Sterile glycerol
- S.O.C media
- Low salt LB-agar plates with 25 µg/mL zeocin
- Thermomixer C incubator
- Sterile bench
- 70 % ethanol
- Eppendorf 5430/5340R centrifuge
- Termaks static incubator

Method:

The Gibson cloning sample (3.1.2) was transformed into One Shot ® Top10 chemically competent *E. coli* cells by incubating 2 µL sample with 50 µL cells on ice for 20 min, and then heat shocking the mixture for 30 seconds at 42 ℃. After the heat shock, the cells rested for 2 minutes on ice before adding 250 µL prewarmed S.O.C media (37 ℃) followed by a 1-2 hour incubation at 37 ℃ and 225-350 rpm agitation. After incubation, three volumes of cells (20, 100 and 140 µL) were plated separately on LB-zeocin (25 µg/mL) agar plates to ensure a successful selection and transformation. The agar plates were incubated at 37 ℃ overnight in a Termaks static incubator. Single colonies on the plates were picked for further screening.

3.1.3 Colony DNA screen by Polymerase Chain Reaction

Transformants of pBSYP$_{gcw14}$Z- OST1_*Sm*ChiA One Shot ® Top10 *E. coli* (3.1.2) were screened using colony polymerase chain reaction (colony PCR), for colony confirmation for

correctly sized DNA. Colony PCR will amplify the DNA sequence between primers Ost1-FWD and AOXT-REV (Figure 3.1) corresponding to the inserted *Sm*ChiA gene if the transformation was successful.

Materials:

- DNA Template (colonies from plate in 3.4.2)
- RedTaq Mastermix (2x)
- Forward primer (OST1-FWD)
- Reverse primer (AOXT-REV)
- ddH_2O
- T100 ™ Thermal Cycler

Method:

Isolated colonies were screened by colony PCR as displayed in Table 3.2. A mix of RedTaq Mastermix (Sigma-Aldrich), primers and ddH_2O was prepared in separate 0.2 mL tubes, one for each colony to be screened. Colonies were picked with a sterile toothpick and gently stirred into the mix along with a tube without a colony as the negative control.

Table 3.2. Content for colony PCR reactions.

Component	Final concentration	x 1 reaction (25 µL)
RedTaq Master mix (2x)	1 x	12.5 µL
Forward primer	10 pmol/µL	2.5 µL
Reverse primer	10 pmol/µL	2.5 µL
ddH_2O		7.5/6.5 µL
DNA template (colony)		tip of pipette/1 µL

Colony PCR amplification of the gene was performed in a T100 ™ Thermal Cycler as shown in Table 3.3 before the PCR samples are analyzed by DNA agarose gel electrophoresis.

Table 3.3. PCR program for colony PCR with primers OST1-FWD and AOXT-REV. The annealing temperature is based on the melting temperature of the primers. The extension time was based on the length of the gene.

Step	Temperature (°C)	Time	Cycles
Initial denaturation	95	5 min	
Denaturation	95	30 sec	25 x
Annealing	62	40 sec	
Extension	72	110 sec	
Final extension	72	5 min	

3.1.4 DNA agarose gel electrophoresis

DNA agarose gel electrophoresis was used to verify successful transformation by analyzing the colony PCR samples for DNA fragment sizes corresponding to the *Sm*ChiA gene. The method separates DNA fragments by length as the negatively charged DNA will travel towards a positive electrode under a current. Separation is dependent on fragment size as short fragments will travel faster and longer in the gel, while longer fragments will be more retained. To visualize the travel, a dye mix was added to the samples and a DNA standard of different sizes for comparison.

Materials:

- Ultrapure Agarose ™
- Tris Acetate-EDTA 10x buffer
- SYBR ™ safe DNA gel stain
- PowerPac ™ Basic power supply
- Gel box

- Colony PCR product (5.1.3)
- Gel Loading Dye, Purple (6x)
- GeneRuler 1 kb DNA ladder
- GelDoc ™ Go Imaging system (Bio-Rad)
- Blue Tray (for GelDoc ™ Go, Bio-Rad)
- Microwave

Method:

An agarose gel was made by melting 0.4 g agarose in 40 mL 1x Tris Acetate-EDTA buffer (TAE buffer) in a microwave. When cooled to touching temperature, 4 µL SYBR ™ safe DNA gel stain was added to the solution before it was poured into a level casting tray with combs corresponding to the desired number of wells. When the gel was set (approximately 20 min), the comb was removed, and the gel was placed in a gel box that was filled with TAE buffer. The samples (PCR product) were added to the gel as 10 µL in separate wells as well aswell as 5 µL GeneRuler 1 kb DNA ladder. A current of 120 V was applied using a PowerPac ™ Basic power supply and after 20 minutes the gel was imaged in the GelDoc ™ Go Imaging system using the Blue Tray and analyzed for DNA fragments corresponding to the size of the *Sm*ChiA gene.

3.1.5 Small-scale cultivation for glycerol stock preparation and plasmid production

Confirmed colony PCR samples were grown on a small-scale for glycerol stock preparation and plasmid production. Plasmid was isolated for sequence verification and transformation into *P. pastoris*.

Materials:

- Colonies from plates
- LB-media with 25 µg/ml zeocin
- Multitron Standard shaking incubator
- Sterile bench

- 80 % sterile glycerol
- Cryotubes
- Eppendorf 5430/5340R centrifuge
- E.Z.N.A ® Plasmid DNA Mini Kit 1
- Heat block
- Minispin centrifuge
- NanoDrop One
- Primers: Forward primer (OST1-FWD), Reverse primer (AOXT-REV)

Method:

Verified colonies by PCR screen were inoculated by taking a small tip of a toothpick and gently stirring it into 5 mL LB-zeocin media in a 50 mL tube. The culture was grown overnight at 37 °C and 200 rpm in a shaking incubator. Glycerol stocks of the cultures were prepared by mixing culture and 80 % sterile glycerol 1:1 in cryotubes for storing at -80 °C.

The rest of the culture was centrifuged at 5000 g for 1 min in an Eppendorf 5430/5340R centrifuge. The supernatant was gently removed and the plasmid from the highly dense cell culture was isolated using the E.Z.N.A ® Plasmid DNA Mini Kit 1, before plasmid concentrations were estimated by Nanodrop One at 260 nm. Sequencing samples were prepared by mixing 6 uL of 100 ng/µL plasmid with 6 µL of 5 pmol/µL primer and sending to Eurofins Genomics. Both forward and reverse primer was necessary for each sample to get full coverage of the *chiA* gene.

3.1.6 Transformation of electrocompetent *P. pastoris* cells

Electrocompetent cells of the eukaryotic yeast *P. pastoris* will take up the linear plasmid by electroporation and insert it randomly into its own genome. Prior to electroporation, the plasmid was linearized by SwaI restriction enzyme that will only cut the plasmid at the linearization site seen in Figure 3.1. Electroporation is performed by applying short electrical pulses to the cells that will create temporary pores in the cell membrane for DNA to pass through.

Material:

- Purified plasmid form 3.1.5
- SwaI restriction enzyme
- 10x NEBuffer
- T100 ™ Thermal Cycler
- DNA Clean & Concentrator ™ - 5 kit
- NanoDrop One
- Electrocompetent *P. pastoris* cells BSYBG11
- Electroporation cuvette 2 mm
- Gene Pulser II
- Thermomixer C
- YPD-agar plates with 100 µg/mL Zeocin
- Termaks static incubator
- Primers (Ost1-FWD and AOXT-REV)

Method:

The purified plasmid was linearized by mixing 3 µg plasmid with 3 µL SwaI restriction enzyme, 15 µL of 10x NEBuffer and ddH2O to a total of 150 uL, while on ice. The linearization was performed by incubation at 25 °C for 1.5 hours in a T100 ™ Thermal Cycler, before the enzyme was inactivated at 65 °C for 20 minutes. Linearized plasmid was cleaned by the "DNA Clean & Concentrator ™ - 5" kit, and the DNA was eluted by adding 10 µL pre-heated ddH2O (Zymo research). The concentration of the DNA was estimated by NanoDrop One by A-280.

The electroporation mixture consists of 1000 ng of linearized plasmid added to 50 µL electrocompetent *P. pastoris* BSYBG11 cells, and was gently mixed in a 2 mm electroporation cuvette on ice. The mixture was electroporated by applying a 2 kV pulse to the cells by a Gene Pulser II. Directly after, the cells recovered in 500 µL 1 M sorbitol and 500 µL sterile YPD media for 2-4 hours at 30 °C agitated at 600 rpm in a Thermomixer C. After incubation three different volumes of the cells (50, 100 and 200 µL) were plated on

separate YPD-agar plated with 100 µg/mL zeocin and incubated at 30 °C for 2 days in a Termaks static incubator.

Colony PCR of transformants was performed, as in 3.1.3, to screen the colonies for the *Sm*ChiA gene. Same temperature program as previously colony PCR that is shown in Table 3.3. The PCR samples were analyzed on a DNA agarose gel electrophoresis as in 3.1.4 and analyzed for the presence of 1600 bp size gene fragment.

3.1.7 Small-scale culture of *P. pastoris* for glycerol stock and protein expression test

Due to expression differences based on locus and the copy number effect of the gene insert into *P. pastoris*, different transformants will give different protein yields (Rieder et al., 2021a). Therefore, expression of *Sm*ChiA in the transformants were examined by a protein precipitation test of a small-scale culture where glycerol stocks were prepared of cultures with good yield. Protein expression can be examined by performing a Methanol/Chloroform protein precipitation test on the supernatant of the culture as the Ost1 signal peptide will secrete *Sm*ChiA to the extracellular matrix. The method will separate the protein from the salt and media of the culture, and by SDS-page (3.1.8) thw proteins can be visualized, and size evaluated.

Material:

- YPD-zeocin agar plates with *P. pastoris* transformants 3.1.6
- YPD liquid media
- Zeocin
- Multitron Standard shaking incubator
- 80 % sterile glycerol
- Tabletop centrifuge
- Eppendorf Centrifuge 5430/5430R
- Table top vortex

Method:

Colonies from 3.1.6 were separately inoculated in 5 mL liquid YPD with 100 µg/mL zeocin. The cultures and negative control of *P. pastoris* BSYBG11 strain were grown at 30°C for approximately 48 hours in a Multitron Standard shaking incubator at 200 rpm before they were subjected to the protein precipitation test.

The methanol/chloroform protein precipitation test was performed on a culture by transferring 500 µL into a 1.5 mL tube and centrifuging it for 1 minute at 14 000 g to obtain the supernatant. A new tube of 1.5 mL was added 100 µL of the supernatant, that was treated with 400 µL methanol, 100 µL chloroform and 300 ddH_2O, with thoroughly mixing by vortex between each addition. Then the sample was centrifuged at 14 000 g for 2 minutes in a Eppendorf Centrifuge 5430/5439R, resulting in protein precipitated between the top aqueous and bottom organic layer. The top layer was gently removed by pipetting before the addition of 400 µL methanol. Next, the solution was vortexed before being subjected to a 3 min spin at 14 000 g, before the organic layer was gently removed by pipetting from the pellet, and residue methanol was evaporated. Lastly, the pellet was resuspended in 10 µL ddH_2O.

The protein content of the samples and negative control was analyzed by SDS-page electrophoresis (next section, 3.1.8), and glycerol stocks from cultures with a high yield were prepared by mixing 700 µL culture with 700 µL 80 % sterile glycerol and stored at -80 °C.

3.1.8 Sodium dodecyl sulfate polyacrylamide gel electrophoresis (SDS-page)

The protein content of a solution can be visualized by sodium dodecyl sulfate polyacrylamide gel electrophoresis (SDS-page). Therefore, it can be used to see the proteins in a precipitation test or protein samples. SDS-page separates the proteins by size as there is a constant ratio between size and charge when the proteins are denatured by heat and treated with sodium dodecyl sulfate (Reynolds & Tanford, 1970). The treatment gives the protein a negative charge that under a current will travel at different rates based on size, thus separation. When compared to a protein standard, different sizes of protein in a sample can be evaluated.

Materials:

- Sample (containing protein)

- LDS-loading buffer: ½ 4x LDS loading dye + 1/5 10 x Reducing agent + 3/10 ddH_2O
- SDS-page buffer: Tris/glycine/SDS buffer
- Ladder: Unstained protein standard
- Mini-PROTEAN Tetra system
- Mini-PROTEAN TGX Stain-Free Precast Gel
- PowerPac basic power supply
- GelDoc ™ Go Imaging system
- T100 Thermal Cycler
- UV/stain-free tray

Method:

Samples were mixed 1:1 with LDS-loading buffer and heated at 95°C in a T100 Thermal cycler for 5 min to denature and charge the protein. A volume of 10-20 µL sample and 3 µL Unstained protein ladder was gently pipetted to individual wells of a Mini-PROTEAN TGX Stain-Free Precast Gel that was submerged in SDS-page buffer in a Mini-PROTEAN Tetra system. A 180 V current was applied for 37 by the PowerPac basic supply, before the gel was visualized in the GelDoc ™ Go Imaging system using the UV/stain-free tray.

3.2 Cell cultivation for protein synthesis

Because proteins are complex molecules, protein synthesis by cells were used for the enzymes *Sm*AA10A and *Sm*ChiA. The genes of the desired enzymes are cloned into a model plasmid for transformation into a specialized protein expression strain, here *E. coli* and *P. pastoris*.

3.2.1 Cell cultivation of *Sm*ChiA by *P. pastoris*

The *P. pastoris* transformant of pBSYP$_{gcw14}$Z- OST1_*Sm*ChiA (3.1) was used for protein expression and production as it will produce the enzyme that can be easily accessed from the supernatant of the culture. For industrial purposes, the secretion into the extracellular matrix gives the advantage of easier protein purification.

Materials:

- Glycerol stock of *P. pastoris* with pBSYP$_{acw14}$Z- OST1_*Sm*ChiA
- YPD-agar plates with 100 µg/mL zeocin
- Termaks static incubator
- Baffled shake flasks
- YPD liquid media
- Multitron Standard shaking incubator
- Sorvall Lynx 6000 centrifuge
- Steritop 0.45 µm filter
- Vivaflow 200 TFF cassette, 10 000 MWCO
- Masterflex Peristaltic Load pump size 16

Method:

A glycerol stock from a high yielding transformant in the protein expression test (3.1.7) visualized by SDS-page (3.1.8) was plated on a prewarmed YPD-zeocin (100 µg/mL) agar plate. The plate was incubated at 30 ℃ in a Thermaks static incubator for 36-48 hours. A 1 µL inoculation loop was used to inoculate approximately 1 cm cell mass into 500 mL YPD media in a 2 L baffled flask (no antibiotic). The flask opening was covered with a breathable filter to ensure good airflow as the culture was incubated in a Multitron Standard shaking incubator at 30 ℃ for 60 hours.

The signal peptide for S*m*ChiA in pBSYP$_{acw14}$Z- OST1_*Sm*ChiA in *P. pastoris* is the OST-1 that will ensure secretion into the extracellular matrix of the culture. Culture supernatant was separated from cells in a 500 mL culture by centrifugation in a Sorvall Lynx 6000 centrifuge at 8000 g, 4 ℃ for 15 minutes. The supernatant was gently decanted and filtered with Steritop 0.45 µm filters. Subsequently, the filtered supernatant was concentrated to a volume of approximately 50-100 mL using a Vivaflow 200 TFF cassette at 10 000 MWCO coupled with a Masterflex peristaltic pump. The obtained concentrated supernatant was stored in the fridge upon further protein purification.

3.2.2 Protein production of *Sm*ChiA by *E. coli* BL21 (DE3)

For protein synthesis of *Sm*ChiA by the expression strain *E. coli* BL21 (DE3), an in-house glycerol stock was used as it have previously been cloned. The plasmid pET28b_*Sm*ChiA has the T7/lac promoter, that is inducible by addition of IPTG preferably at the exponential growth phase at OD_{600} at ~0,6. After induction, the cells will prioritize protein synthesis over the cell cycle.

Materials:

- Kanamycin
- Glycerol stock: *E. coli* BL21(DE3) pET28b_*Sm*ChiA
- Multitron standard shaking incubator
- Antifoaming agent
- Blue-cap bottle 1L
- Sparger connected to blue cap
- Aeration system with sparger lids
- AV-100 laminar air flow cabinet (Telstar)
- Water bath – first 37 °C then reduced to 30 °C
- 1 mM IPTG
- Thermo Scientific™ Sorvall™ LYNX 6000 centrifuge

Method:

A 50 mL preculture made up of LB-media, with 30 µg/mL kanamycin, was inoculated by a 1 µL inoculation loop from the glycerol stock, to grow overnight at 37 ℃ and 200 rpm. The following morning, 500 mL of pre-warmed TB-media containing kanamycin and anti-foaming agent, was inoculated by the entire preculture. The culture was grown at 37 ℃ and 200 rpm until the OD_{600} was approximately 0.6-0.8, then the culture was induced with 1mM IPTG. After induction, the temperature was reduced to 30 ℃ and grew overnight for approximately another 16-20 hours.

The culture was transferred into a 1 L centrifuge tube and centrifuged at 4000g for 12 minutes at 4 ℃ in a Sorvall™ LYNX 6000 centrifuge to form a pellet. The supernatant containing the

extracellular fraction was decanted and the pellet was kept at fridge temperature until further purification.

3.2.3 Protein production of *Sm*AA10A in *E. coli* BL21 (DE3)

The LPMO *Sm*AA10A (previously known as CBP21) was purified as previously described by Vaaje-Kolstad et al. (2005). An in-house glycerol stock of *E. coli* BL21 (DE3) containing the plasmid pRSETb_*Sm*AA10A with ampicillin resistance was used for cultivation.

Materials:

- Glycerol stock: *E. coli* BL21(DE3) star cells containing pRSETb_*Sm*AA10A and
- LB media
- Ampicillin
- Baffled shake flask 2 L
- Inoculation loop
- Sterile bench
- Multitron standard shaking incubator
- Thermo Scientific™ Sorvall™ LYNX 6000 centrifuge

Method:

Cells from *E. coli* BL21(DE3) containing pRSETb_*Sm*AA10A glycerol stock were inoculated in a baffled flask with 1 L LB media with 50 µg/mL ampicillin with an 10 µL inoculation loop in a sterile bench to avoid contamination. The flask was incubated at 37 ℃ and agitated at 200 rpm with aluminum foil covering the opening for approximately 16 hours.

The culture was centrifuged at 4000g for 12 minutes at 4 ℃ in a Sorvall™ LYNX 6000 centrifuge to form a pellet, and the supernatant was decanted as the cell pellet was kept in the fridge upon further purification.

3.2.4 Isolation of periplasmic extract with cold osmotic shock protocol

This method is the first purification step applicable for the proteins secreted to the periplasm that are cultivated in *E. coli* BL21(DE3), both *Sm*ChiA (3.2.2) and *Sm*AA10A (3.2.3). The signal peptide translocate the protein to the periplasmic space, therefore, the correctly produced and folded protein needs to be extracted from the periplasm.

Materials:

- Cell pellet (3.2.2 and 3.2.3)
- Cold spheroplast buffer
- Cold 5 mM $MgSO_4$
- Thermo Scientific™ Sorvall™ LYNX 6000 centrifuge
- 0,2 µm syringe filter

Method:

The cell pellet was resuspended gently in 50 mL cold spheroplast buffer (Table 2.7) and rested on ice for 5-10 min while stirring it at regular intervals to avoid sedimentation. The suspension was centrifuged for 20 minutes at 8000 g and 4 °C in a Sorvall™ LYNX 6000 centrifuge, before the supernatant was decanted (the sucrose fraction) and the cell pellet was equilibrated to room temperature. The cell pellet was resuspended in 20 mL cold 5 mM magnesium sulfate while on ice and stirred for 10 minutes before it was centrifuged at 15 000 g for 12 minutes at 4 °C to obtain the periplasmic extract (PPE) as the supernatant. The PPE was filtered with a 0.2 µm syringe filter and stored at 4 °C until further purification.

Successful isolation of the correct fraction and that it contains the desired protein was verified by visualizing dilutes of PPE, sucrose fraction, cell pellet and media for protein content and size by SDS-page (3.1.8).

3.3 Chromatographic purification of protein

A variety of chromatographic methods can be utilized for protein purification based on the properties of the protein and how to remove unwanted proteins. The principle of chromatography is that different substances in a mix can be separated by their interaction with two phases. A stationary phase that the proteins will interact with as they travel with a mobile phase. The interaction will make the proteins elute at different times, giving the retention time that is often specific making it a method to separate and keep different fractions of a protein solution.

3.3.1 Anion exchange chromatography

Ion exchange chromatography is a method applied to separate molecules with charge in a liquid mobile phase with a stationary phase made up of an oppositely charged resin. Anion exchange chromatography (IEX) has a cation (positive charge) resin making negative compounds have a higher affinity based on net charge. The strength of the bond between the protein and the stationary phase will vary with pH. The isoelectric point (pI) of the protein (the point where the protein has a net change of zero) is used for deciding the pH of the mobile phase. If the pH of the mobile phase is higher than the pI, then the protein will have a net negative charge (Miller, 2005). A mobile phase gradient that changes the pH is used to elute proteins based on affinity to the column.

Materials:

- PPE with *Sm*ChiA (3.2.2 and 3.2.4)
- IEX buffer A: 20 mM Tris-HCl pH 8.0
- IEX buffer B: 20 mM Tris-HCl pH 8.0 + 1 M NaCl
- Column: HiTrap Q FF 5mL (Cytiva)
- Instrument: Bio-Rad NGC Chromatography system
- System: ChromLab Method Editor
- BioFrac fraction collector (Bio-Rad)
- 20 % ethanol

- Amicon Ultra-15 centrifugal filter units n30 kDa cutoff
- Storage buffer *Sm*ChiA: 20 mM Tris-HCl pH 7.5 + 150 mM NaCl
- Eppendorf Centrifuge 5430/5430R
- NanoDrop One

Method:

The PPE-filtrate was buffer adjusted by adding Tris-HCl pH 8.0 to a final concentration of 20 mM while it reached room temperature. With a flow of 2 mL/min the HiTrap Q FF 5mL (Cytiva) IEX column was adjusted to IEX buffer A before the sample was applied at 1 mL/min flow. The column was washed with IEX buffer A until UV A-280 stabilized, then the elution of protein was assisted by an applied gradient of 0 to 5 % IEX buffer B across 5 minutes followed by a gradient from 5-50 % IEX buffer B across 30 minutes. Fractions of 3-5 mL were collected and analyzed on SDS-page for protein content (3.1.8), and fractions with protein content corresponding to *Sm*ChiA was concentrated and buffer exchanged to *Sm*ChiA storing buffer using Amicon Ultra-15 centrifugal filter units with a 30 kDa cutoff for at least 3 cycles. The protein concentration was estimated using NanoDrop One in at least 3 technical replicates and purity was estimated using an SDS-page of dilutions.

3.3.2 Hydrophobic interaction chromatography (HIC)

Hydrophobic interaction chromatography (HIC) is a liquid chromatography method for separating compounds in a mixture based on hydrophobicity (Miller, 2005). The stationary phase consists of hydrophobic resin where hydrophobic proteins will have a longer retention time than hydrophilic proteins. The use of salts in the mobile phase will strengthen the interaction between the proteins and the stationary phase, and by applying a gradient in the mobile phase to reduce salt content, it will decrease the strength of the interaction between the column and proteins, eluting proteins of different hydrophobicity at different times.

Materials:

- Sample (concentrated supernatant 3.2.1)
- HIC buffer A: 50 mM Bis-Tris pH 6.5 + 2 M ammonium sulfate

- HIC buffer B: 50 mM Bis-Tris pH 6.5
- Ammonium sulfate (salt)
- Column: 2x HiTrap Phenyl HP 5 mL (Cytiva)
- Instrument: Bio-Rad NGC Chromatography system
- System: ChromLab Method Editor
- BioFrac fraction collector (Bio-Rad)
- Amicon Ultra-15 centrifugal filter units 10 kDa cutoff

Method:

A sample of 50 – 100 mL concentrated supernatant of *Sm*ChiA produced in *P. pastoris* (3.3.1) was adjusted to HIC buffer A to assure proper binding to the column. HIC purification was performed using the BioRad NGC chromatography system with the ChromLab software connected to a BioFrac fraction collector. Two 5 ml HiTrap Phenyl HP columns were attached to the system and washed with ddH_2O before being adjusted to the HIC buffer A by 3 column volumes. The sample was loaded on the column at a 2.0 mL/min flow rate. Removal of non-specific proteins was performed by washing with HIC buffer A for approximately 6 column volumes at a flow rate of 3 mL/min. By applying a gradient from 100 % HIC buffer A to 100 % HIC buffer B over 40 mL at a flow rate of 2 mL/min, the protein was eluted. The elution was monitored by a UV-detector at 280 nm. Fractions were collected using the BioFrac fraction collector and analyzed for protein content on SDS-page (3.1.3), and fractions with protein corresponding to the size of *Sm*ChiA were concentrated by Amicon Ultra-15 centrifugal filters 30 kDa cutoff to approximately 1 mL.

3.3.3 Size exclusion chromatography

To remove unspecific proteins from the solution, size exclusion chromatography (SEC) can be utilized to separate the proteins by size. The stationary phase is an inert material with pores that will retain small proteins as they will pass through some or all of the pores giving a longer retention time, while large proteins will not travel through the pores, giving the shortest retention time (Miller, 2005).

Material:

- Protein sample (3.3.2)
- SEC buffer: 20 mM Bis-Tris pH 6.5 + 150 mM NaCl
- Amicon Ultra-15 centrifugal filter units 10 kDa cutoff
- Column: HiLoad 16/160 Superdex 75 ng 120 mL
- Instrument: Bio-Rad NGC Chromatography system
- System: ChromLab Method Editor
- BioFrac fraction collector (Bio-Rad)
- Eppendorf Centrifuge 5430/5430R
- Storage buffer *Sm*ChiA: 20 mM Tris-HCl pH 7.5 + 150 mM NaCl

Method:

A HiLoad 16/160 Superdex 75 pg 120 mL column was attached to the Bio-Rad NGC Chromatography system and at a rate of 1 mL/min, the column was thoroughly rinsed with ddH_2O , before it was equilibrated with SEC buffer. Protein sample was applied, and isocratic elution was detected by an UV-detector A-280. Fractions were collected with the BioFrac fraction collector and analyzed on SDS-page (3.1.8). Based on the SDS-page, fractions with desired protein content were concentrated using Amicon Ultra-15 filter unit of 30 kDa cutoff. After buffer exchange to storage buffer, *Sm*ChiA protein concentration was estimated in triplicate using NanoDrop One A-280.

3.3.4 Chitin affinity chromatography

The chitin active LPMO, *Sm*AA10A, was separated from the PPE (3.2.4) by chitin affinity (CA) chromatography as the protein will bind to a stationary phase consisting of a chitin resin. After the elution of all irrelevant proteins and salts, the mobile phase was changed to elute the *Sm*AA10A and collecting fraction for SDS-page visualization for protein content. *Sm*AA10A has been previously purified by chitin affinity chromatography in Vaaje-Kolstad et al. (2005) as a one-step purification method for efficiency.

Materials:

- PPE with *Sm*AA10A (3.2.3 and 3.2.4)
- CA buffer A: 1 M $(NH_4)_2SO4$ + 50 mM Tris-HCl pH 8.0 (Table 2.7)
- CA elution buffer: 20 mM acetic acid
- Instrument: Bio-rad BioLogic LP
- Software: LP Data View
- Column: packed Chitin Resin (NEB) in a 1.5 x10 cm (18 mL volume) column
- Filtered 20 % ethanol
- Amicon Ultra-15 centrifugal filters 10 kDa cutoff
- Eppendorf Centrifuge 5430/5430R

Method:

Firstly, the chitin resin column was flushed with two column volumes of ddH_2O, and then equilibrated with the CA buffer A. The PPE with *Sm*AA10A was equilibrated to the 1 M $(NH_4)_2SO_4$ and 50 mM Tris-HCl pH 8.0, then the UV monitoring at 280 nm was zeroed before applying the sample with a 1.5 mL/min flow rate. When the UV-signal was stabilized at approximately zero, the mobile phase was changed to the elution buffer. Elution of the protein was monitored by UV and 3-4 mL fractions were collected manually and analyzed on SDS-page for protein content (3.1.8). Fractions containing protein of the desired size were concentrated using Amicon Ultra-15 centrifugal filters 10 kDa cutoff, and protein concentration was estimated by measuring triplicates of the protein solution by NanoDrop One at A-280.

3.3.5 Copper saturation of LPMO

The LPMO *Sm*AA10A is a mono-copper-dependent enzyme, therefore, for the enzyme to gain proper function and enzymatic activity it was incubated with a copper solution. The protein-copper solution must be thoroughly washed to remove excess copper that interferes with the LPMO activity, and that was done by thoroughly washing with buffer in filter units.

Materials:

- *Sm*AA10A fractions isolated by chitin affinity (3.3.4)

- Storage buffer for *Sm*AA10A: 50 mM Sodium phosphate buffer pH 7.0
- Amicon Ultra-15 centrifugal filter units 10 kDa cutoff
- 50 mM Copper sulfate
- Eppendorf Centrifuge 5430/5430R

Method:

A 3-fold molar excess of copper was added to the protein solution and incubated on ice for 30 min to ensure copper-LPMO binding. After it was concentrated and diluted for at least 5 cycles in Amicon Ultra-15 centrifugal filter units with the storage buffer, each time the concentrated solution was diluted 1:15. After washing, the protein concentration was estimated using NanoDrop One A-280 in three technical replicates using *Sm*AA10A storing buffer as the blank.

3.4 Oxidase activity of *Ag*ChOx

Peroxygenase conditions for *Sm*AA10A were performed by the addition of *Ag*ChOx for *in situ* production of H_2O_2. To estimate the oxidative activity of *Ag*ChOx, some adjustments were made to the Amplex Red assay (Kittl et al., 2012). As H_2O_2 was produced by *Ag*ChOx, horse radish peroxidase (HRP) utilizes H_2O_2 to catalyze the Amplex red reagent to resorufin. The production of resorufin is stoichiometrically equal to the production of H_2O_2, and was measured spectrophotometrically, assuming Amplex Red reagent and HRP is not limiting factors (Zhou et al., 1997). This reaction was monitored over time in a plate reader to estimate H_2O_2 production per minute.

Materials:

- 500 mM Sodium phosphate buffer pH 7.0
- 2000 nM stock of *Ag*ChOx
- 10 mM Choline Chloride (ChCl)
- Amplex red Reagent (AR)
- 50 U/ml Horseradish peroxidase (HRP)

- 10 mM H_2O_2
- 96-well Microtiter plate
- Varioskan LUX
- Software: ScanIT 6.0.1

Method:

Amplex Red assay of *Ag*ChOx with the substrate choline chloride (ChCl). The protocol described by Kittl et al. (2012) was adjusted to fit the Choline Oxidase. The activity was measured in three biological replicates, each having three technical replicates. The 100 µL sample included *Ag*ChOx of varying concentration from 0-800 nM, 100 µM AR, 5 U/mL HRP in 50 mM Sodium phosphate buffer pH 7.0. The reactions were initiated by adding 1 mM ChCl as a substrate to drive the *Ag*ChOx enzyme reaction. The plate reader, Varioscan LUX, monitored the resorufin production every 8 seconds at UV A-540 for a minimum of 20 minutes to record the formation of resorufin in the linear range of the reaction.

A standard curve of known H_2O_2 (concentrations of 0-40 µM) was performed in three technical replicates for each biological replicate of *Ag*ChOx. It included ChCl, HRP and AR in sodium phosphate buffer pH. 7.0 at the same concentrations as described earlier and was initiated by the addition of H_2O_2. The background absorbance shown in the 0 µM H_2O_2 samples, was subtracted from the results both for the standard and the Amplex Red assay

3.5 Relative enzyme activity on 4-methylbelliferone

Enzymatic activity for *Sm*ChiA was measured by testing the enzymes on a synthetic substrate that contains a fluorescent group, 4-methylbelliferone (4-MU) attached to chitobiose. Its already shown that *Sm*ChiA is active towards the substrate 4-MU-$(GlcNAc)_2$ (complex undetectable by fluorescent), that corresponds to the substrate $(GlcNAc)_3$ (Brurberg et al., 1996). When *Sm*ChiA cleaves the bond between 4-MU and $(GlcNAc)_2$ it releases the fluorescent group that was detected by a fluorometer and was viewed as a direct measurement of enzymatic activity (Brurberg et al., 1996).

Material:

- Enzyme stocks 1.9 nM (*Sm*ChiA produced both in *P. pastoris* and *E. coli*)
- 500 µM 4-MU-$(GlcNAc)_2$
- 1 µM 4-MU
- 200 mM Citrate phosphate buffer pH 6.0
- BSA 10 mg/mL
- 0.2 M Sodium carbonate
- Water bath at 37 ℃
- Fluorometer

Method:

Samples were prepared in triplicates to a final concentration of 69 µM 4-MU-$(GlcNAc)_2$, 0.1 mg/mL BSA in 0.2 M citrate phosphate buffer pH 6.0. This mix was preheated in a 37 ℃ water bath for 2 minutes before the reaction was initiated with 0.19 nM *Sm*ChiA. Negative controls (without enzyme) and samples were incubated for exactly 10 minutes before the reactions were stopped by adding 0.19 M sodium carbonate. Prior to measuring the samples, the fluorometer was calibrated by setting 100 µL 1 µM 4-MU to a desired value of 500 FLOU (units) and the blank was 0,19 M sodium carbonate.

3.6 Enzymatic activity on β-chitin

As chitin is the second most abundant polysaccharide substrate in nature, it is a resource with high potential if there is an efficient degradation to a product of value. The enzymes *Sm*ChiA and *Sm*AA10A have known activity towards β-chitin, and the efficiency of this degradation over time and cooperation between the enzymes was investigated further in this thesis by adjusting concentrations and conditions.

Reactions were performed for the enzymes (*Sm*AA10A and *Sm*ChiA) individually and together in time-course experiments, divided into reactions with one of the enzymes, where β-chitin was pretreated with *Sm*AA10A for 24 hours prior to addition of *Sm*ChiA and when *Sm*AA10A and *Sm*ChiA was added consecutively, and included the addition of *Ag*ChOx as an

H_2O_2 source. Of note, as long *Sm*ChiA was present in the reaction, the specified time of the reaction was from when the chitinase was added.

Material:

- 20 mg/mL β-chitin
- Enzymes:
    - *Sm*ChiA
    - *Sm*AA10A
    - *Sm*CHB
    - *Ag*ChOx
    - BSA
- 10 mM ascorbic acid
- H_2O_2
- 500 mM Sodium phosphate buffer pH 7.0
- 10 mM ChCl
- Thermomixer C
- 100 mM sulfuric acid
- 96-well filter plate
- 96-well microtiter plate
- Multiscreen ® HTS vacuum manifold (Merck)
- Multitron standard shaking incubator

Method:

Every reaction was performed in triplicate and had a mix of 50 mM sodium phosphate buffer pH 7.0, ddH_2O and β-chitin (10, 2.5 and 0.45 mg/mL) preheated in a Thermomixer C at 37 ℃ at 850 rpm in 2 mL reaction tubes. For all reactions including *Sm*AA10A (1 µM or 0.1 µM), the LPMO was preincubated for approximately 30 minutes to assure binding to the substrate, as non-bound LPMO has a higher risk of inactivation, before the reaction was initiated with ascorbic acid (1 or 0,1 mM) and/or H_2O_2. (50, 150 or 300 µM). For reactions only containing *Sm*AA10A, reactions were initiated by the addition of ascorbic acid, but for reactions including *Sm*ChiA (1 µM, 100, 50 or 10 nM), the reaction time was determined from when

the chitinase was added. If *Ag*ChOx (100, 200, 400 or 800 nM) was present, it was added directly after *Sm*ChiA, and the reaction also included 1 mM ChCl.

Reactions investigating the different effects of both *Sm*AA10A and *Sm*ChiA was performed by either incubating the reaction mix with *Sm*AA10A for 24 hours prior to adding *Sm*ChiA or or adding both at the same time.

The maximum duration of the reactions was a total time for 72 hours, and that included 72 hours "synergy" or 24 hours "pretreatment" plus 48 hours with *Sm*ChiA.

Reactions were terminated by either 50 mM H_2SO_4 (SmChiA alone and pretreatment/ synergy experiments) added to reaction aliquots and filtering the mixture through 96-well filter plates, or only filtering (SmAA10A alone) before samples were treated with 1 µM *Sm*CHB overnight to ensure that the oxidized chitooligosaccharides can be measured as oxidized chitobiose. All samples were stored at -20 °C.

3.7 Analysis of chitin oligosaccharides by HPLC

High-performance liquid chromatography (HPLC) is an analytic liquid chromatography method. The system has a higher speed, resolution, sensitivity and accuracy than regular liquid chromatography (Miller, 2005). This also means that the sample needs to be small to ensure these advantages. A Rezex RFQ- fast acid H^+ column was used to separate the analytes by isocratic elution based on retention, where its able to separate the oxidized and native sugars and the large sugars elute first and the small last.

Materials:

- Standard dependent on sample:
- A2 standard (Chitobiose)
- A2-ox standard (Chitobionic acid) (provided by Rannei Skaali)
- A1 standard (GlcNAc)
- System: Dionex UltiMate 3000
- Column: Rezex RFQ- Fast acid H^+ (8%) 7.8 x 100 mm

- 5 mM sulfuric acid
- Software: Chromeleon 7
- Samples (3.6)

Method:

Mono and/or disaccharides of chitin were analyzed using the Rezex RFQ- Fast acid H^+ (8%) 7.8 x 100 mm column attached to the Dionex UltiMate 3000 system. The system applied 5 mM sulfuric acid at 1 mL/min at 85 °C. Isocratic elution of samples was detected by UV at 194 nm. Dependent on sample, standards curves were prepared by analyzing standards of 25-3000 µM A2, A1 and/or A2ox prepared in house. Chromatograms of samples were compared with standards and integrated for peak area.

4 Results

4.1 Protein production and isolation

4.1.1 Purification of *Sm*ChiA from *E. coli* BL21 (DE3)

An in-house glycerol stock of *Sm*ChiA pRSETb in *E. coli* BL21 (DE3) was cultivated as stated in 3.2.2, before the PPE was isolated using the cold osmotic shock protocol (3.2.4) where the different fractions from the protocol were analyzed for protein content on SDS-page (3.1.8 presented in Figure 4.1B). The isolated PPE was purified by IEX with a HiTrap Q FF 5 mL column (3.3.1) separating the proteins based on a net charge using under conditions (20 mM Tris-HCl pH 8.0) where *Sm*ChiA was calculated to have a charge using the ProtParam tool (Expasy). Purification was performed by applying a gradient with IEX buffer B (20 mM Tris-HCl pH 8.0 + 1 M NaCl) as shown by the chromatogram in Figure 4.1A, and collected fractions were analyzed for protein content by SDS-page (3.1.8) shown in Figure 4.1C.

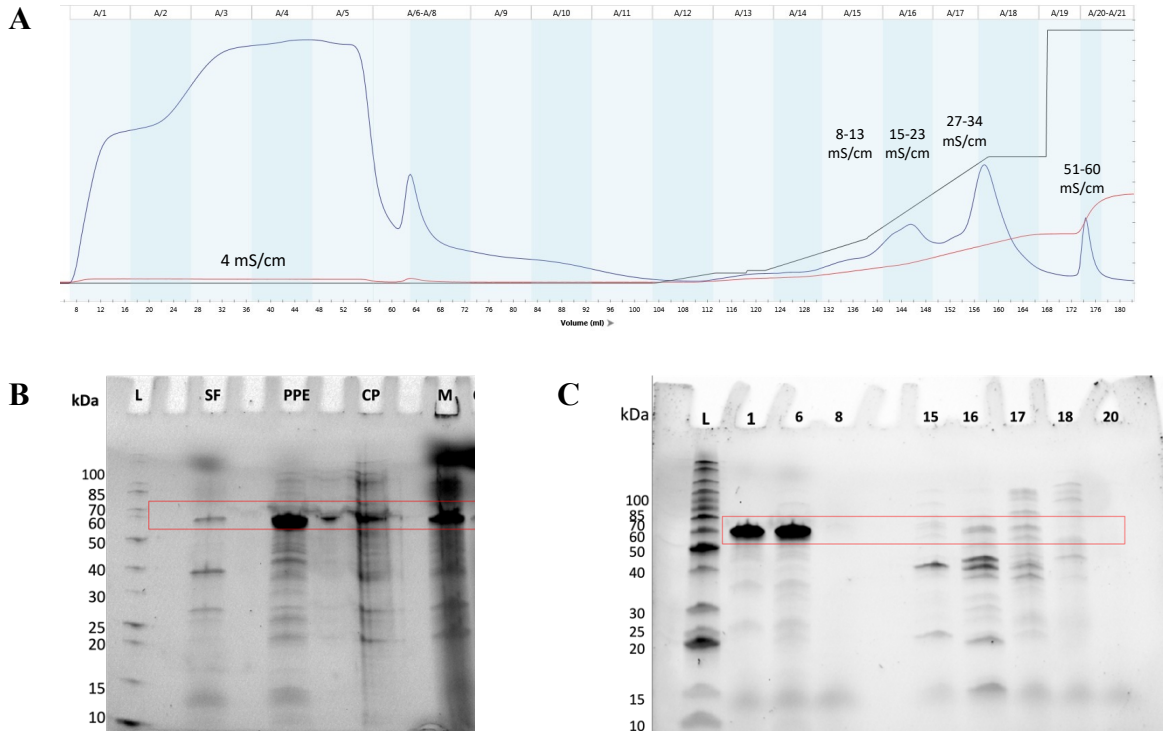

Figure 4.1 ***Anion exchange chromatography of pET28b_SmChiA.*** ***(A)*** *IEX chromatogram of PPE from E. coli BL21(DE3) pET28b_SmChiA. Y-axis shows the UV-absorbation in mAU, x-axis is the volume in mL, the blue trace is UV-absorbation, and the black trace % of IEX buffer B (20 mM Tris-HCl pH 8.0 + 1 M NaCl). Conductivity was marked at different stages of the elution.* ***(B)*** *Protein content during periplasmic extraction of the sucrose fraction (SF), periplasmic extract (PPE), cell-pellet (CP), and media (M).* ***(C)*** *Fractions from IEX analyzed on SDS-page. Both (B) and (C) have the same protein ladder (L) and marked the protein bands with the size of 60-70 kDa.*

The SDS-page gel of the different fractions of the cold osmotic shock protocol (Figure 4.1B) showed that the PPE contained bands with the appropriate size of *Sm*ChiA (approximately 60 kDa), with only small bands of the same protein for the other cold osmotic shock fractions (SF, CP, and M in Figure 4.1B) indicating a successful isolation of the periplasmic extract. IEX purification of the *Sm*ChiA PPE presented the chromatogram in Figure 4.1A, with the blue line showing the UV A-280 trace, indicates that separation of protein fraction was achieved as seen by distinct peaks in the UV trace. The collected fractions of the elution were visualized by SDS-page (Figure 4.1C) where fractions 1-6 were concentrated to 1 mL before the protein concentration was estimated in triplicate on Nanodrop One to be 111 µM and a yield of 6.8 mg.

4.1.2 Purification of *Sm*AA10A from *E. coli*

The LPMO *Sm*AA10A was produced from an in-house glycerol stock of *E. coli* BL21 (DE3) pRSETb_*Sm*AA10A by inoculating 500 mL LB media with a glycerol stab before growing for approximately 16 hours at 37 °C with 200 rpm shaking (3.2.3). The PPE was extracted with the cold osmotic shock protocol as described in 3.2.4, and *Sm*AA10A was purified from the PPE by a one-step purification method using affinity chromatography with a chitin resin (NEB) as column material, as described in 3.3.4. The PPE was adjusted to the mobile phase CA buffer A (1 M $(NH_4)_2SO4$ + 50 mM Tris-HCl pH 8.0) before application to the chitin resin (NEB) and *Sm*AA10A was eluted with the CA elution buffer (20 mM acetic acid), as the protein content was monitored by UV A-280 Figure 4.2A. Collected fractions were analyzed on SDS-page (3.1.8) as shown in Figure 4.2B.

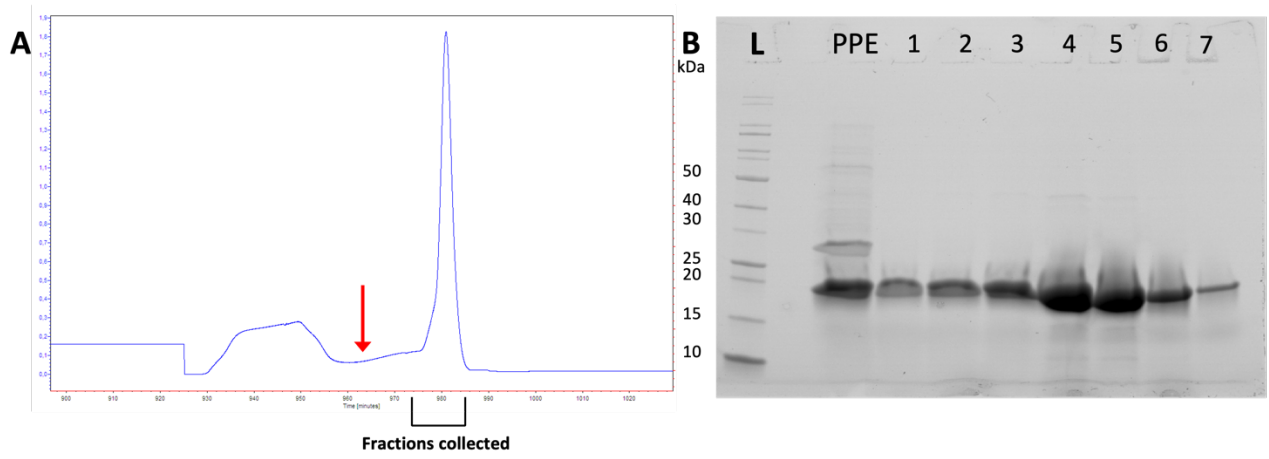

Figure 4.2 ***Chitin affinity purification of SmAA10A. (A)*** *Chromatogram of purification of SmAA10A by chitin affinity derived from LP data view (Bio-Rad). The blue trace is the UV-absorbation, x-axis shows UV-absorption A-280 and y-axis is time in minutes. The red arrow is where the buffer was changed from CA buffer A (1 M $(NH_4)_2SO_4$ + 50 mM Tris-HCl pH 8.0) to CA elution buffer (20 mM acetic acid).* ***(B)*** *SDS-page gel of periplasmic extract (PPE) and fractions from chitin affinity. The protein ladder (L) marked with sizes from 50-10 kDa.*

The chromatogram of the PPE containing *Sm*AA10A shows a clear increase of UV A-280 absorbation peak after the change to CA elution buffer (Figure 4.2A, red arrow indicating buffer change to elution buffer), and the peak fractions were collected that were analyzed on SDS-page in Figure 4.2B together with the PPE. All fractions, from 1-7 including the PPE, contained a protein corresponding to just under 20 kDa size (*Sm*AA10A is 19 kDa). In the

PPE a band between 25 and 30 kDa also appears that is not present in the fraction collected by chitin affinity chromatography, indicating that the purification was successful. Fractions 1-7 in Figure 4.2B were concentrated to approximately 1 mL by Amicon Ultra-15 centrifugal filter units and protein concentration was estimated in triplicate by Nanodrop One A-280.

The protein solution was copper saturated as stated in 3.3.5 by incubation with a 1:3 molar ratio of protein to copper sulfate on ice for 30 minutes before the solution was thoroughly washed (by repeatedly concentrating and diluting) with 50 mM sodium phosphate pH 7.0 using an Amicon Ultra-15 centrifugal filter unit to remove excess copper that could interfere with enzymatic assays later. The estimated concentration after copper saturation was 951 µM and corresponding to a 15 mg yield of copper saturated *Sm*AA10A.

4.2 Enzymatic assays

4.2.1 Oxidative activity of *Ag*ChOx

The hydrogen peroxide production of *Ag*ChOx was estimated by the Amplex ™ Red assay, as there is a direct correlation between the amount of hydrogen peroxide and measured resorufin absorption. The production rate was measured by mixing different concentrations of *Ag*ChOx (0 to 800 nM), 1 mM choline chloride, 100 µM Amplex™ Red reagent, 5 U/mL HRP in 50 mM sodium phosphate pH 7.0. The absorbance measurements were converted to a concentration using a hydrogen peroxide standard curve from 0 to 40 µM (data in appendix Figure 8.1A). Only measurements from the linear production rate were used (50-200 sec), as 800 nM *Ag*ChOx only is linear in this interval (shown in appendix Figure 8.1B).

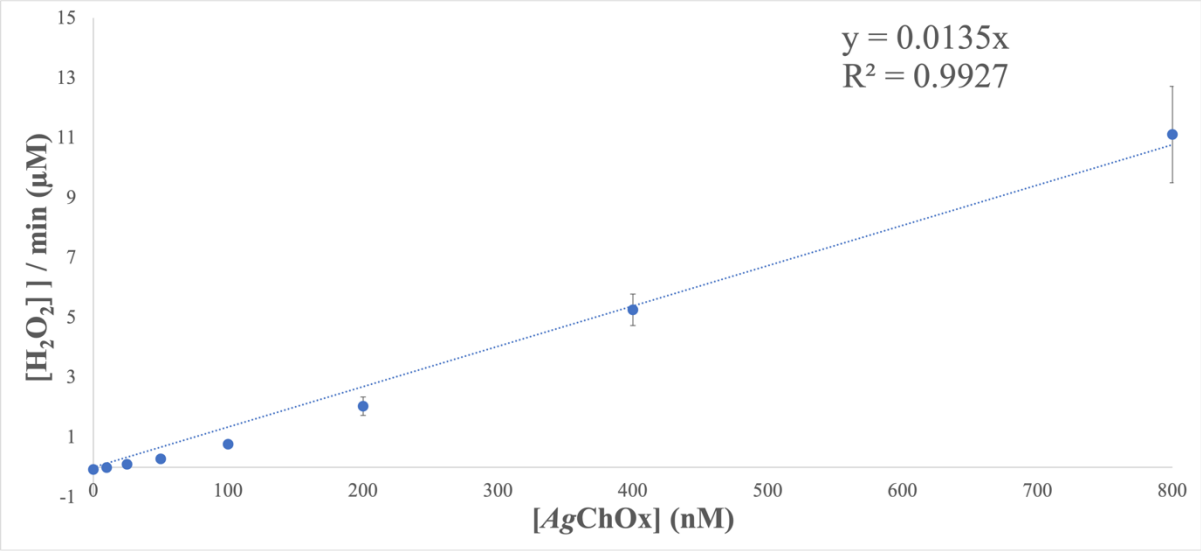

Figure 4.3 ***Oxidase activity of AgChOx by Amplex ™ Red assay****. Total hydrogen peroxide produced per minute (y-axis) by concentration of choline oxidase in nM (x-axis). The reaction included different concentrations of AgChOx from 0 to 800 nM, 1 mM choline chloride, 1 µM Amplex ™ Red reagent, 5 U/mL HRP in 50 mM sodium phosphate pH 7. The data are the average of three replicates performed three separate days with a daily fresh enzyme stock from freeze-dried enzyme. The standard deviations are presented as error bars (n=3).*

The results of the averages of three replicates(y-axis) where n=3 are plotted against the concentration of *Ag*ChOx in nM(x-axis) (Figure 4.3). The assay gave the slope of y=0.0135x as a linear regression model with the R^2 value of 0.9927. Qualitatively the standard deviation increases with the concentration of *Ag*ChOx.

4.3 Time-course assays on β-chitin

4.3.1 Initial time-course experiments

Individual time-course assays for both *Sm*ChiA and *Sm*AA10A were performed on β-chitin to check for activity and ensure that a baseline of activity is established prior to monitoring the enzymes together.

The activity of the LPMO *Sm*AA10A on β-chitin was examined by a time-course experiment as described in 3.6, with 1 µM enzyme, and 10 mg/mL β-chitin in the reaction and initiated with 1 mM ascorbic acid. Sample aliquots were terminated by filtration and incubated with 1

μM *Sm*CHB overnight to produce chitobionic acid that was quantified by HPLC as in 3.7, Rezex RFQ-fast acid H+ column at 85 °C with 1 mL/min flow rate monitoring product by UV A-194. Chitobionic acid product was quantified using an in-house generated standard of chitobionic acid ranging from 25-1600 μM in Chromeleon (Figure 8.2A in appendix) and the product formation over time is shown in Figure 4.4A indicating that the enzyme was active and successfully purified.

Time course assay of *Sm*ChiA activity on β-chitin and the combination of both enzymes *Sm*AA10A and *Sm*ChiA used the setup described in 3.6. The reaction mixture contained 10 mg/mL β-chitin, and 1 μM *Sm*ChiA with or without 1 μM *Sm*AA10A and 1 mM Ascorbic acid, Sample aliquots were terminated in 50 mM sulfuric acid and filtered prior to analysis by HPLC as in 3.7, Rezex RFQ-fast acid H+ column at 85 °C with 1 mL/min flow rate monitoring product by UV A-194, and are shown in Figure 4.4B. To investigate the main products obtained during the reaction with both enzymes present, samples were analyzed and quantified for GlcNAc, chitobiose and chitobionic acid, shown in Figure 4.4C using standard (25-1600 μM in appendix Figure 8.2).

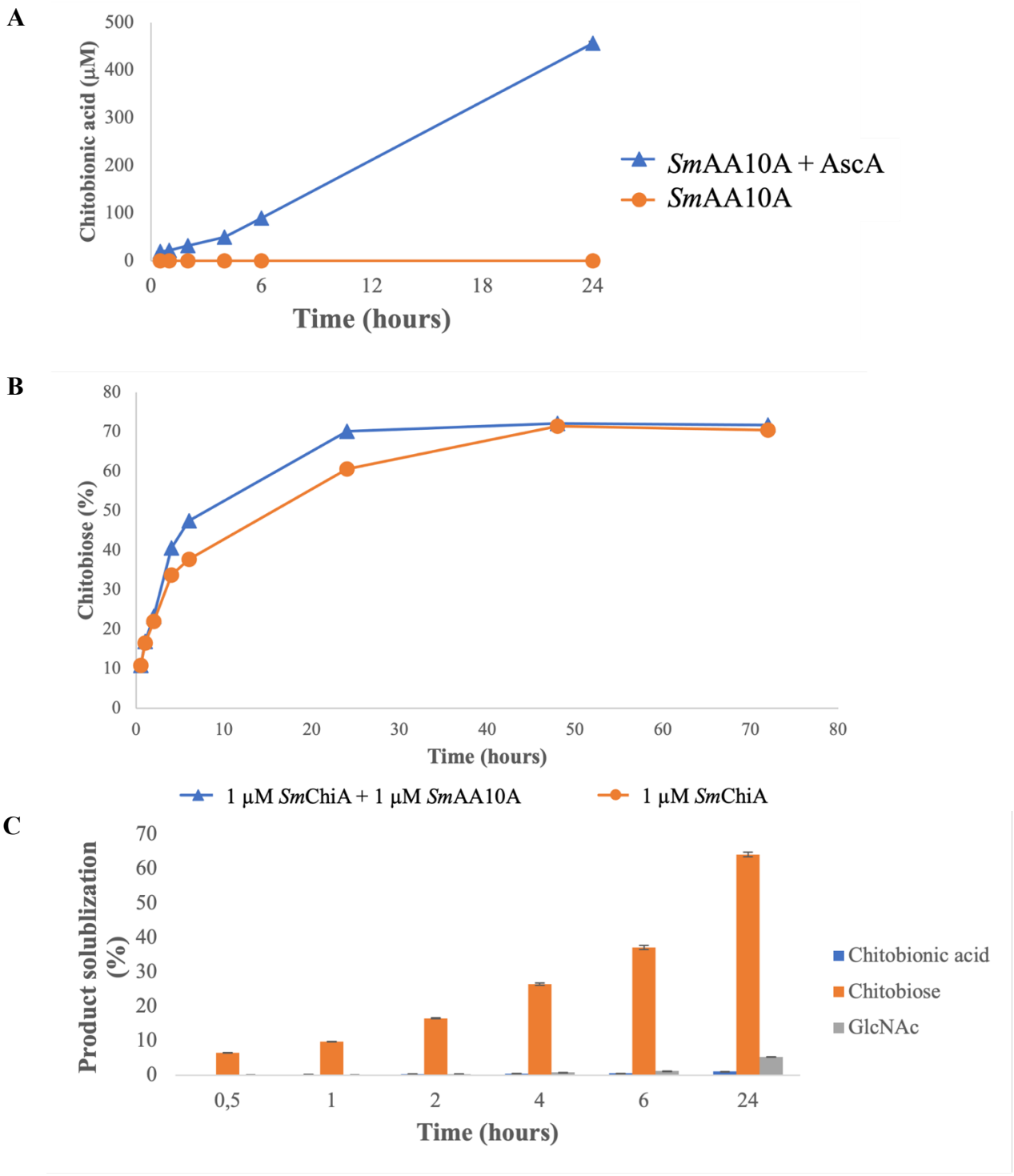

Figure 4.4 ***Initial time-course experiments of chitin solubilization.*** *Reactions were performed with 10 mg/mL β-chitin in 50 mM sodium phosphate pH 7.0.* ***(A)*** *assay of 1 µM SmAA10A with (blue triangles) and (orange circles) without 1 mM ascorbic acid.* ***(B)*** *Reactions with 1 µM SmChiA with (blue triangles) or without (orange circles) 1 µM smAA10A and 1 mM ascorbic acid.* ***(C)*** *reactions with 1 µM SmChiA, 1 µM SmAA10A and 1 mM Ascorbic acid quantified for GlcNAc (grey), chitobiose(orange) and chitobionic acid(blue) in percent of theoretical maximum. All panels show standard deviations as error bars of n=3.*

The reaction that examined the LPMO activity, as 1 µM *Sm*AA10A with or without ascorbic acid (Figure 4.4A) show a clear indication of oxidized product with ascorbic acid, 457 ± 3.5 µM chitobionic acid after 24 hours, and no formation of product without reductant. The 72-hour assay with 1 µM *Sm*ChiA reaction (Figure 4.4B) with (blue triangles) or without (orange dots) 1 µM *Sm*AA10A (and 1 mM ascorbic acid) analyzed for chitobiose both reached a maximum yield of 70 % chitin solubilization, however, the reaction with *Sm*AA10A reached approximately 70 % after 24 hours, while the reaction without LPMO reached 70 % after 48 hours. The largest difference in product solubilization in these reactions was at approximately 10 %, with 47.4 ± 0.04 % vs. 37.7 ± 0.17 % at 6 hours, and 70.1 ± 0.01 % vs. 60.6 ± 0.07 % at 24 hours, for the reaction of *Sm*ChiA + *Sm*AA10A and the reaction for only *Sm*ChiA, respectively.

Figure 4.4C displays the reaction with 1 µM of both *Sm*ChiA and *Sm*AA10A with 1 mM ascorbic acid, and the product solubilization in percent shows that chitobiose is the main product with a relative percentage of 90 % of the measured products, as GlcNAc yielded 5 % and chitobionic acid yielded 1 % after 24 hours. The product profile for the reaction with 1 µM *Sm*ChiA + 1 µM *Sm*AA10A (without 1 mM ascorbic acid) gave a similar profile, just with lower yields for every product. Therefore, in further analysis, only the chitobiose product will be quantified.

4.3.2 Pretreatment of β-chitin with *Sm*AA10A

To increase the rate of chitin solubilization different strategies were investigated, where the first of them was pretreatment. Herein, pretreatment experiments are defined as samples that have been pretreated with *Sm*AA10A and ascorbic acid for 24 hours prior to the addition of *Sm*ChiA. The reaction mixture contained 10 mg/mL β-chitin and *Sm*AA10A (1 or 0.1 µM) before a short pre-incubation to facilitate LPMO-substrate binding before pretreatment was initiated by the addition of ascorbic acid (1 or 0.1 mM) as in 3.6. The *Sm*ChiA reaction was initiated precisely 24 hours after the preincubation started by the addition of *Sm*ChiA (1 µM, 100, 50, or 10 nM) and sample aliquots were terminated in 50 mM sulfuric acid before storage at -20 °C upon HPLC analysis as in 3.7, Rezex RFQ-fast acid H+ column at 85 °C

with 1 mL/min flow rate monitoring product by UV A-194. Chitobiose product was quantified using an in-house generated standard of chitobiose raging from 25-3000 µM (see appendix Figure 8.2B for chitobiose standard curve example).

The different experiments had the goal of finding the ratio/conditions that results in the largest effect of pretreatment of the substrate with *Sm*AA10A. The first pretreatment experiments where both enzymes had concentrations at 1 µM are not shown as there was no difference between the pretreated vs. the non-pretreated sample, therefore the concentration of *Sm*ChiA was scaled down to 100 nM, as shown in Figure 4.5A. The initial effect (60 minutes) on 100 nM *Sm*ChiA activity after pretreatment with 1 µM *Sm*AA10A (1 mM ascorbic acid), indicated that the LPMO aids the chitinase in substrate solubilization. The same reaction was investigated for 24 hours (24 hours pretreatment by 1 µM *Sm*AA10A followed 24 hours reaction with 100 nM *Sm*ChiA) and chitobiose solubilization was quantified as previously described. Due to the non-stagnant results shown in Figure 4.5B, the enzyme concentration ratio was decreased by a factor of 10, in an attempt to reduce *Sm*ChiA´s activity, i.e., creating a larger difference between control and samples. As shown in Figure 4.5C this was unsuccessful, therefore, a pretreatment experiment was investigated at a set concentration of 1 µM *Sm*AA10A (so that the synergy effect is not limited by LPMO content), with different concentrations of *Sm*ChiA (10, 50 and 100 nM) shown in Figure 4.5D.

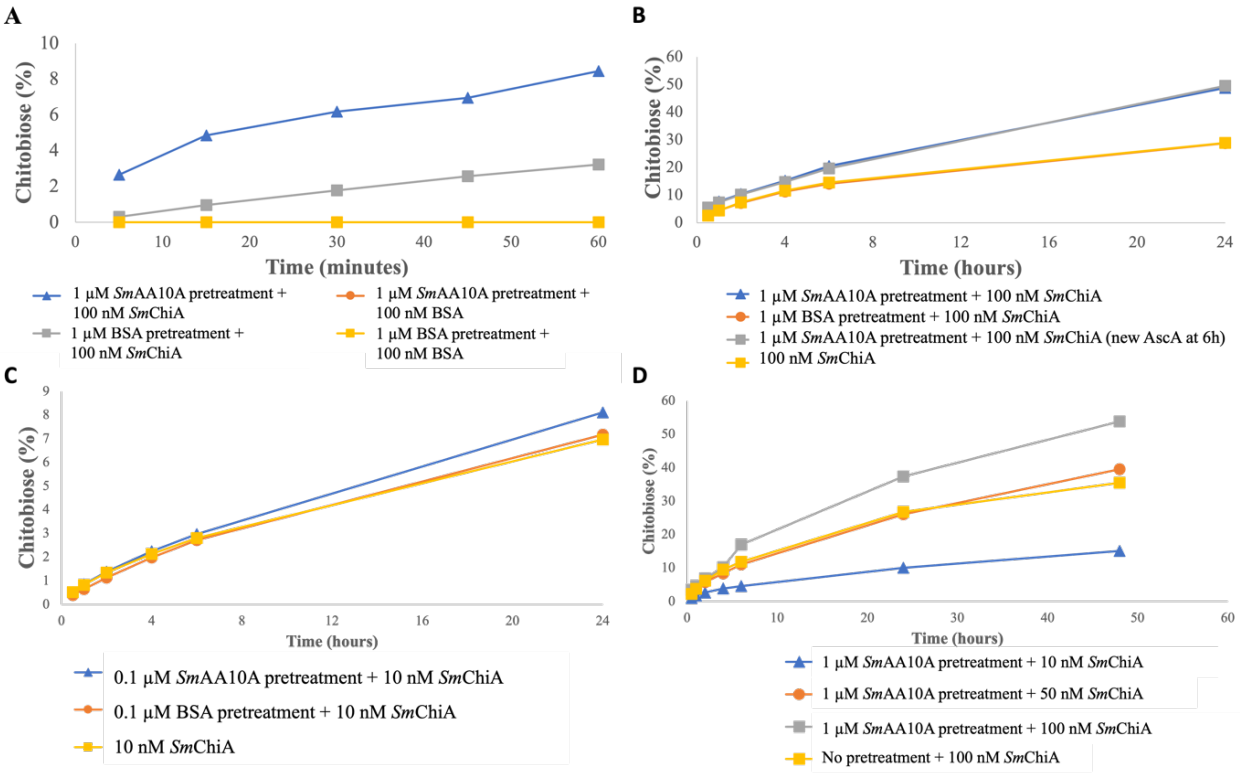

Figure 4.5 ***Pretreatment time-course assays.*** *Pretreatments assays with 10 mg/mL were prepared in 50 mM sodium phosphate pH 7.0.* ***(A)*** *Pretreatment experiment with 1 µM SmAA10A, 1 mM Ascorbic acid, and 100 nM SmChiA samples were taken for 60 minutes.* ***(B)*** *Pretreatment experiment with 1 µM SmAA10A, 1 mM Ascorbic acid, and 100 nM SmChiA with samples analyzed for 24 hours.* ***(C)*** *Pretreatment with 0.1 µM SmAA10A, 0.1 mM Ascorbic acid, and 10 nM SmChiA with a control of 1 µM SmAA10A.* ***(D)*** *Pretreatment experiment with 1 µM SmAA10A and 1 mM Ascorbic acid, with different concentrations of SmChiA (10, 50, and 100 nM). Standard deviations are error bars of n=3.*

There is an initial effect of pretreatment of 10 mg/mL β-chitin for the first 60 minutes where the samples that were pretreated with 1 µM *Sm*AA10A yielded approximately 5 % more than samples that were pretreated with 1 µM BSA, seen in Figure 4.5A. The control experiment replacing 100 nM *Sm*ChiA with 100 nM BSA gave no chitobiose product. When expanding this experiment to 24 hours of reaction with 100 nM *Sm*ChiA (Figure 4.5B), it yielded similar results, and worth noting that a set of triplicates were added fresh 1 mM Ascorbic acid 6 hours after the addition of *Sm*ChiA (grey data) yielded the same results as the samples with no addition of fresh Ascorbic acid (blue data). After 24 hours the samples with 1 µM *Sm*AA10A (blue and gray in Figure 4.5B), yielded approximately 50 % chitobiose solubilization from 10 mg/mL β-chitin, and the difference between pretreated with 1 µM *Sm*AA10A (blue and gray)

and 1 μM BSA (orange and yellow) was at approximately 20 % chitobiose yield in favor to the *Sm*AA10A pretreatment.

Further the pretreatment experiment with a 10-fold decrease in enzyme concentration (for both *Sm*AA10A and *Sm*ChiA compared to the previous pretreatment experiment) to investigate how lower concentrations influence the effect of pretreatment, and if the reduced *Sm*ChiA concentration results in a lower activity rate earlier giving a larger difference in final chitobiose yield. The results of the 1/10 scale experiment are shown in Figure 4.5C, and compared to the experiment in Figure 4.5B by observing yield similar qualitative results of the slopes and difference in solubilized chitobiose at a lower scale with the highest yield at approximately 9 %.

The final pretreatment experiment, seen in Figure 4.5D, tested a fixed concentration of LPMO, to ensure that LPMO concentration does not limit the possible pretreatment boost, with different concentrations of the chitinase; 1μM *Sm*AA10A and 1 mM ascorbic acid, for pretreatment with 10 mg/mL β-chitin in 50 mM sodium phosphate pH 7.0. The chitinase *Sm*ChiA was added with a final concentration of 10, 50 and 100 nM and was added after 24 hours of pretreatment. Samples were analyzed throughout 48 hours, giving a total reaction time of 72 hours. The results after the total reaction time were 15.1 ± 0.02 %, 39.6 ± 0.02 % and 53.8 ± 0.10 %, for the concentrations in increasing order (10, 50 and 100 nM respectively). The chitobiose yield rate has yet not stagnated fully at 48 hours of *Sm*ChiA treatment. For the first 4 hours of the *Sm*ChiA reaction, 50 and 100 nM *Sm*ChiA give similar chitobiose yields, but at 6 hours and further, 100 nM *Sm*ChiA resulted in a higher yield. The rate of the 50 nM *Sm*ChiA pretreated reaction compares to the 100 nM *Sm*ChiA non-pretreated control.

4.3.3 Pretreatment vs. synergy

Pretreatment in this thesis is defined as pretreating the β-chitin substrate with *Sm*AA10A (and ascorbic acid) for 24 hours prior to the addition of *Sm*ChiA, that initiates the chitobiose solubilization that was quantified by HPLC. The effect of pretreatment was compared to a setup where *Sm*ChiA was added directly after *Sm*AA10A, indicating that the substrate wasn't

pretreated with LPMO, defined as synergy experiments further in this thesis. For all further experiments, a *Sm*AA10A concentration of 1 µM was established so that the effect of synergy or pretreatment would not be limited by the amount of LPMO.

Reactions were pretreated with 1 µM *Sm*AA10A for 24 hours and were compared to synergy samples from the time 100 nM *Sm*ChiA was added to the reactions. This means that in the pretreatment reactions, the total reaction time including pretreatment was 72 hours, while the synergy reactions had a total time of 48 hours. All reactions included 10 mg/mL β-chitin in 50 mM sodium phosphate pH 7.0. *Sm*AA10A (1 µM) was always preincubated to facilitate substrate binding before reduction by the addition of 1 mM Ascorbic acid (for pretreatments 24 hours prior to *Sm*ChiA was added) before the reactions were initiated by 100 nM *Sm*ChiA. Sample aliquots were terminated by 50 mM sulfuric acid and filtered before storage at 20 °C upon analysis by HPLC as in 3.7, Rezex RFQ-fast acid H+ column at 85 °C with 1 mL/min flow rate monitoring product by UV A-194. Chitobiose product was quantified using an in-house generated standard of chitobiose ranging from 25-3000 µM in Chromeleon (see appendix Figure 8.2B for chitobiose standard curve example).

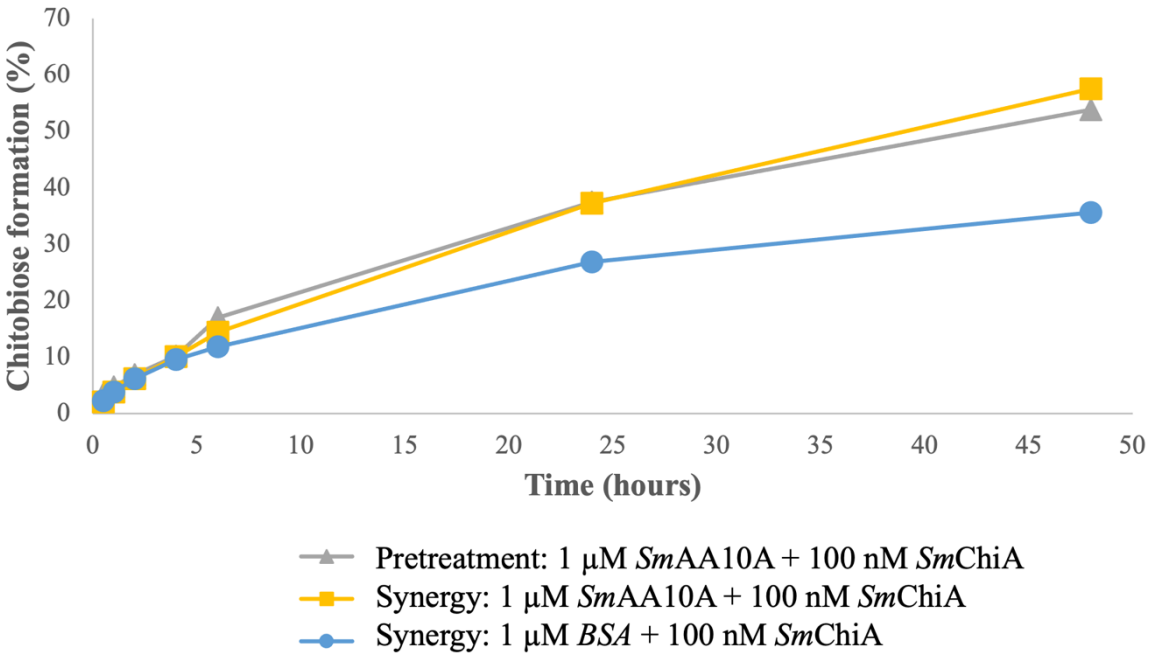

Figure 4.6 ***Pretreatment vs. synergy time course assay.*** *Experiments with 1 µM SmAA10A, 1 mM ascorbic acid, and 100 nM SmChiA were prepared with 10 mg/mL β-chitin in 50 mM sodium phosphate pH 7.0 for pretreatment and synergy experiments (marked in figure). Time in hours was based on when SmChiA was added, and the estimated chitobiose is displayed as percent of theoretical maximum yield and standard deviations are error bars of n=3.*

Pretreatment and synergy experiments yield similar chitobiose solubilizing from when *Sm*ChiA was initiated, shown in Figure 4.6 where both had the same enzyme concentrations, with the only difference being if 1 µM *Sm*AA10A (and 1 mM ascorbic acid) was used to pretreat the β-chitin substrate for 24 hours or just added directly prior to 100 nM *Sm*ChiA. The chitobiose solubilization over the course of 48 hours with *Sm*ChiA reaction is shown in Figure 4.6, and notably does not display clear differences as the yield in percent at 48 hours was 53.9 ± 0.10 % and 57.5 ± 0.33 %, for pretreatment (Figure 4.6 grey) and synergy (Figure 4.6 yellow) respectively. That corresponds to an approximate difference of 4 % that is only 7% relative to the highest obtained yield in this experiment. The synergy control with BSA replacing *Sm*AA10A had a yield of 42.5 ± 0.07 % after 48 hours resulting in a difference of over 10 % yield reduction when *Sm*AA10A wasn't added, with the synergy effect evident first after 6 hours.

4.3.4 Synergy

Since the observed difference between synergy and pretreatment was so small, and in favor of synergy it would increase efficiency and time consumption to pursue synergy further, rather than optimize the pretreatment reaction. As mentioned earlier, synergy experiments in this thesis are defined as the addition of *Sm*ChiA directly after *Sm*AA10A, indicating no pretreatment of the substrate.

4.3.4.1 Effect of substrate concentration

The effect the LPMO activity has on the chitinase activity was investigated at different β-chitin substrate concentrations. Reactions with 10 (Figure 4.7A), 2.5 (Figure 4.7B) and 0.45 (Figure 4.7C) mg/mL β-chitin were tested with or without 1 µM *Sm*AA10A (and 1 mM Ascorbic acid) in the presence of varying *Sm*ChiA concentrations (100, 50 and 10 nM) was prepared in 50 mM sodium phosphate pH 7.0. Sample aliquots were terminated by 50 mM sulfuric acid, filtered and stored at -20 °C upon analysis by HPLC, as in 3.7, Rezex RFQ-fast acid H+ column at 85 °C with 1 mL/min flow rate monitoring product by UV A-194. Chitobiose product was quantified using an in-house generated standard of chitobiose raging from 25-3000 µM in Chromeleon (see appendix Figure 8.2B for chitobiose standard curve example).

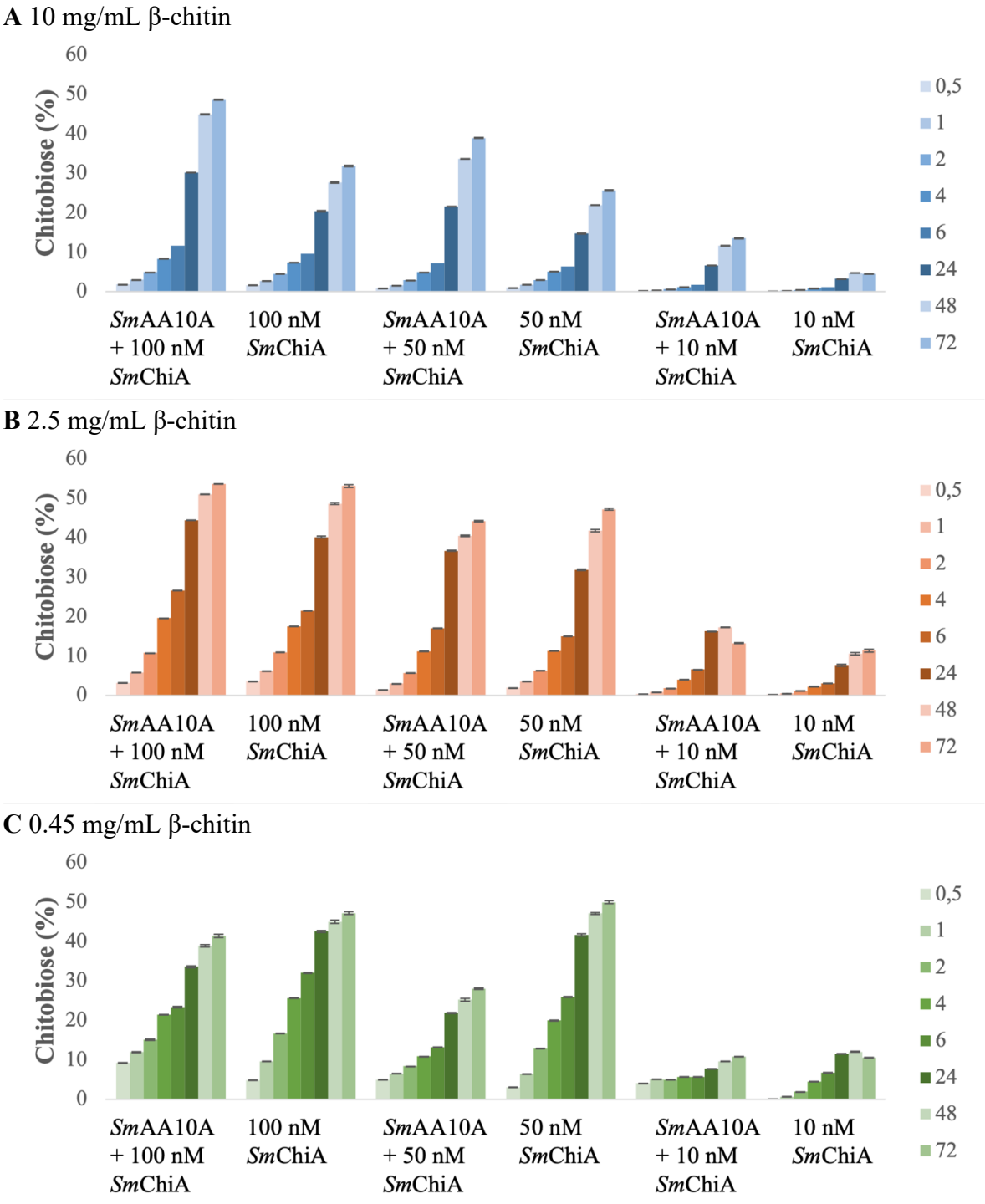

Figure 4.7 ***Effect of different substrate concentrations on synergy time-course assays with*** **Sm*ChiA and SmAA10A.*** *Time course experiment with different concentrations of β-chitin (10, 2.5 and 0.45 mg/mL) at different concentrations of SmChiA(10, 50 and 100 nM) in 50 mM sodium phosphate pH 7 over 72 hours. The chitobiose yield in percent (y-axis) relative to time in hours (bars). Along the x-axis is the different concentrations of SmChiA at 10, 50 or 100 nM with or without 1 µM SmAA10A and 1 mM ascorbic acid. **(A)** Substrate concentration at 10 mg/mL β-chitin, **(B)** substrate concentration at 2.5 mg/mL β-chitin, **(C)** substrate concentration at 0.45 mg/mL β-chitin. Standard deviations are shown as error bars of n=3.*

The results of the time-course assay with different substrate concentrations gave a clear indication that higher substrate concentrations resulted in an increased effect of *Sm*AA10A. As visualized in Figure 4.7A for 10 mg/mL, 100 nM *Sm*ChiA and 50 nM *Sm*ChiA, both with 1 µM *Sm*AA10A have higher chitobiose solubilization at 10 mg/mL β-chitin than the reactions with only *Sm*ChiA, where the highest chitobiose yield was obtained by 100 nM *Sm*ChiA+ 1 µM *Sm*AA10A at just below 50 %. Overall, for 10 mg/mL there is a dose-response associated with *Sm*ChiA concentration as well as a synergy effect that results in synergy reactions yielding better than their respective with only *Sm*ChiA. Interestingly the synergy effect for 1 µM *Sm*AA10A + 50 nM *Sm*ChiA giving a higher chitobiose yield than 100 nM *Sm*ChiA without the LPMO.

When reducing substrate concentrations to 2.5 mg/mL, Figure 4.7B, a chitobiose yield of just above 50 % is achieved by all reactions with 50 nM and higher *Sm*ChiA and the effect of *Sm*AA10A is lower as the difference between reaction with both enzymes and with only *Sm*ChiA is decreased. For 10 nM *Sm*ChiA (with and without 1 µM *Sm*AA10A), the chitobiose yield is substantially lower with a yield of 10-20 %.

The results for the lowest substrate concentration of 0-45 mg/mL β-chitin, displayed in Figure 4.7C, the production yield of chitobiose is more randomly distributed between the reactions with 100 and 50 nM *Sm*ChiA that reach a chitobiose yield of approximately 50 %. It seems to be a trend that the samples with *Sm*AA10A have a lower chitobiose yield, as represented by the yields of 100 and 50 nM *Sm*ChiA + *Sm*AA10A, compared to the reactions with only *Sm*ChiA. Again the 10 nM *Sm*ChiA reactions (with and without *Sm*AA10A) have a significantly lower yield in the 10 % range.

(See Figure 8.3 in the appendix for line chart representation of the data)

4.3.4.2 Peroxygenase experiments with *Ag*ChOx

An attempt to increase the synergy effect was made by increasing the LPMO catalytic rate under LPMO peroxygenase conditions, that successively increase chitobiose yield by the chitinase. Previous experiments in this thesis can be defined as so-called monooxygenase conditions since the reaction did not have an external supply of H_2O_2, and *Sm*AA10A´s activity was then dependent on its ability to convert O_2 to H_2O_2 (oxidase activity). Synergy time course experiments under peroxygenase conditions were performed by the addition of choline and *Ag*ChOx, that oxidize choline producing glycine-betaine and H_2O_2. This to boost the LPMO and GH interplay to improves chitobiose solubilization. The activity rate of an LPMO has been shown to increase significantly when H_2O_2 is supplied (see introduction 1.6.2). Still, care must be taken as external addition of H_2O_2 can increase the inactivation of the enzyme, as discussed in 1.6.3 in the introduction.

The reaction mixture consisted of 10 mg/mL β-chitin, 50 mM sodium phosphate pH 7.0, 1 µM *Sm*AA10A, 1 mM ascorbic acid, *Sm*ChiA of concentrations 10, 50 and 100 nM, 1 mM choline chloride and *Ag*ChOx concentration ranging from 0-800 nM. Control samples were reactions with only *Sm*ChiA added to the reaction mixture. Samples were analyzed on HPLC Rezex RFQ-fast acid H+ column at 85 °C with 1 mL/min monitored by UV A-194 for chitobiose solubilization. The chitobiose product was quantified using an in-house generated chitobiose standard in Chromeleon (see appendix Figure 8.2B for chitobiose standard curve example).

The synergy time-course assay is presented as a heat map of chitobiose solubilization in µM at 24 hours. Figure 4.8 include the results of only *Sm*ChiA (with no *Sm*AA10A and *Ag*ChOx) enzyme reaction, and gradually add boosters consisting of 1 µM SmAA10A (1 mM Ascorbic acid) and AgChOx of increasing concentrations. The intensity of the color corresponds to a value of chitobiose formation in µM displayed in the legend at det bottom of the figure.

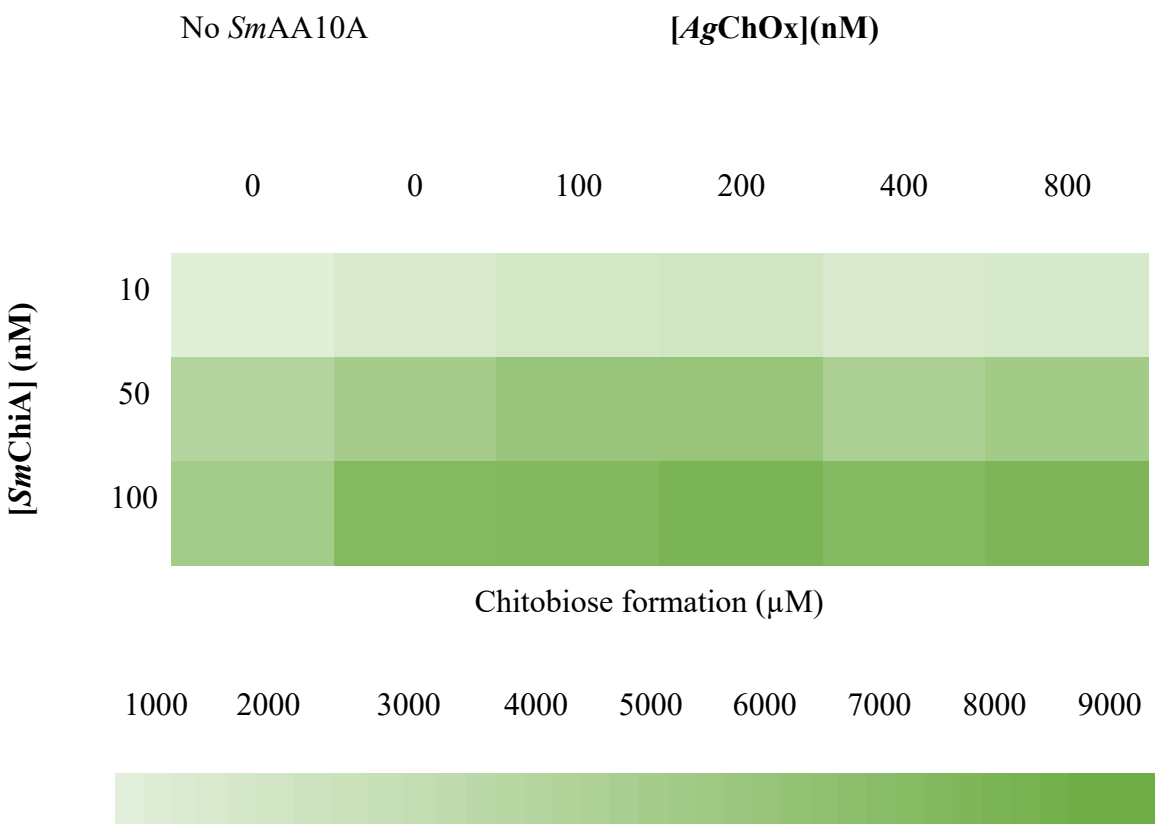

Figure 4.8 ***Heat map of synergy time-course assays with AgChOx.*** *Estimated concentrations of chitobiose in µM after 24 hours of reactions with β-chitin, with or without 1 µM SmAA10A, 1 mM ascorbic acid, and different concentrations of SmChiA (10, 50 and 100 nM) and AgChOx (0 – 800 nM) in 50 mM sodium phosphate pH 7.0. The legend (below) explains the color intensity of the blocks in the heat map.*

The overall trend of the heat map is that the yield gets higher towards the bottom right, apart from 400 nM *Ag*ChOx that have lower chitobiose product than 200 nM *Ag*ChOx. The highest values of chitobiose solubilization are the reactions with 100 nM *Sm*ChiA, 1 µM *Sm*AA10A and 200 or 800 nM *Ag*ChOx, where both have an estimated chitobiose formation over 8000 µM. All the reactions show a dose-response based on *Sm*ChiA concentration, as the only variable for each column in the heat map is the *Sm*ChiA concentration and the value increases towards the higher concentrations. The *Ag*ChOx response is dependent on concentration up to 200 nM, further the boost effect at 400 and 800 nM is lower and unstable.

A final synergy experiment with *Ag*ChOx as an H_2O_2 *in situ* producer was performed in order to see if the same effects can be obtained at a higher concentration of *Sm*ChiA. A 72-hour time course to see if the overall total yield of chitobiose can be higher under peroxygenase conditions for a reaction with 10 mg/mL β-chitin with 1 µM *Sm*ChiA, 1 µM *Sm*AA10A, 1

mM Ascorbic acid, and 200 nM *Ag*ChOx in 50 mM sodium phosphate. Reactions were prepared in 2 mL tubes in a Thermomixer C at 37 °C agitated at 850 rpm. Samples aliquots were terminated in 50 mM sulfuric acid and filtered before storage at -20°C upon HPLC analysis with Rezex RFQ-fast acid H+ column at 85 °C and 1 mL/min 5 mM sulfuric acid. Isocratic elution was monitored by UV A-194, where samples and standard were analyzed in Chromeleon (examples of chitobiose standard curve in appendix Figure 8.2B).

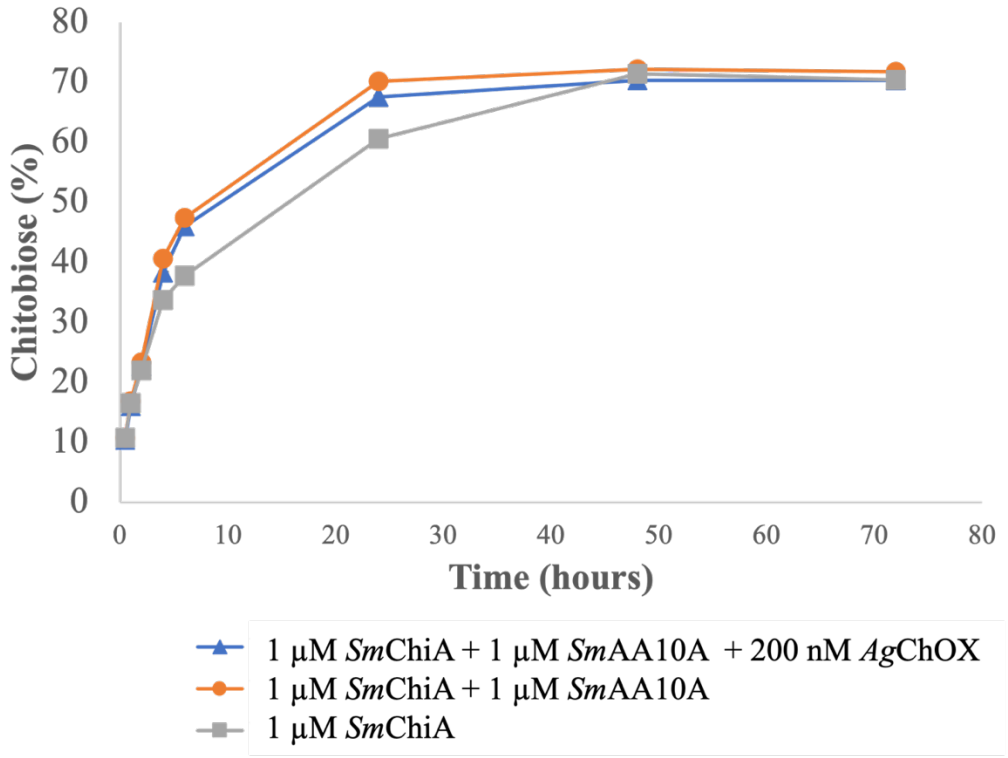

Figure 4.9 ***High concentration of SmChiA in a synergy time-course assay.*** *Experiment on 10 mg/mL β-chitin in 50 mM sodium phosphate pH 7.0 at 1 µM SmChiA, 1 µM SmAA10A with 1 mM Ascorbic acid and 200 nM AgChOx. Standard deviations are shown as error bars of n=3.*

Reactions with 1µM *Sm*ChiA reach a chitobiose yield of 70 %, however, at different rates dependent on *Sm*AA10A content. The reaction with 1 µM *Sm*ChiA will reach 70 % within 48 hours, while the reactions with 1 µM *Sm*AA10 (+ 1 mM Ascorbic acid) present will reach a 70 % chitobiose yield within 24 hours. Furthermore, the same result applies for the 1 µM *Sm*ChiA + *Sm*AA10A + 200 nM *Ag*ChOx, that yields the slightly highest chitobiose percent visualized in Figure 4.9.

4.4 SmChiA into P. pastoris

4.4.1 Cloning of *Sm*ChiA into *P. pastoris*

The bacterial chitinase, *Sm*ChiA, was cloned into the yeast strain *P. pastoris* BSYBG11 to investigate increase in enzyme yield and simplify purification, as the protein will be secreted into the extracellular matrix. *P. pastoris* is one of the most used host systems for fungal LPMO expression, and it holds great potential in hosting an entire chitinolytic cocktail.

The gene for *chiA* (without native signal peptide) was cloned into the pBSYP$_{acw14}$Z-OST1 by Gibson Assembly® before the plasmid was transformed into One shot ® Top10 *E. coli*. Colonies were screened by colony PCR after growing on LB-zeocin agar plates. The colony PCR, shown should give gene fragments of approximately 1500 bp by PCR amplifications using primers designed and ordered by Dr. Kelsi Hall. The screened colonies of One Shot ® Top10 *E. coli Sm*ChiA, are shown in Figure 4.10A and colonies with prominent bands with an approximate size of 1500 bp are colonies 2, 3, 4, 7, 9, and 12. Colonies marked with 2 and 3 (later named (E-2 and E-3) were inoculated in 5 mL LB-zeocin for glycerol stock preparation, and plasmid isolation for retransformation and sequence verification. Plasmid from the E-3 was sequence verified by sequencing by Eurofins and alignment in SnapGene (results not shown).

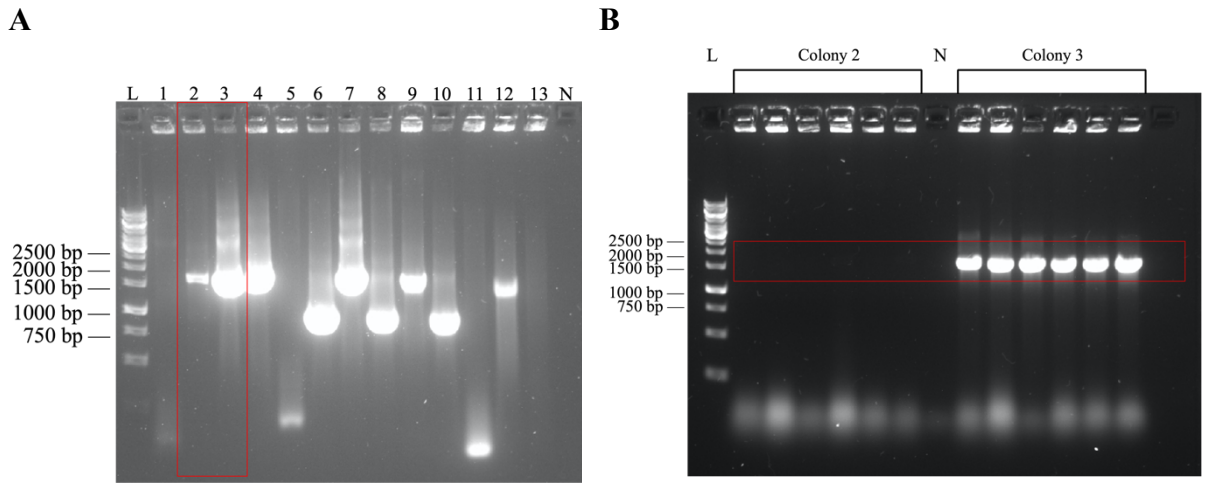

Figure 4.10 ***DNA agarose gel electrophoresis of colony PCR screen.*** *(A) E. coli TOP10 colonies named 1-13, the negative control (N) and ladder (L) GeneRuler 1 kb labeled with 2500 bp to 750 bp. Glycerol stocks were prepared from the red-marked colonies. (B) Colony PCR after transformation into P. pastoris. Colony 2 and colony 3 refer to the plasmids from E. coli TOP10 colony 2 (E-2) and 3 (E-3) in (A). The ladder (L) GeneRuler 1 kb, negative control (N) is an empty P. pastoris strain.*

Both the plasmid from E-2 and E-3 were linearized by the incubation with the restriction enzyme SwaI and transformed into electrocompetent *P. pastoris BSYBG11.* The transformants were plated individually and analyzed by colony PCR along an empty *P. pastoris* strain. The gel in Figure 4.10B shows the DNA fragments produced by transformants in the *P. pastoris* colony PCR. Colonies from the E-2(colony 2) plasmid had no band showing, but all analyzed colonies with the E-3 (colony 3) plasmid included the correctly sized gene fragment of 1500 bp.

The integration of the plasmid into the genome of *P. pastoris* can give a difference in protein expression dependent on the location of the integration. This effect will result in different protein yields of the transformants in a methanol-chloroform protein precipitation test of the colonies after inoculation in 5 mL YPD media (3.1.7), visualized by a more prominent band in a SDS-page of the transformants (3.1.8).

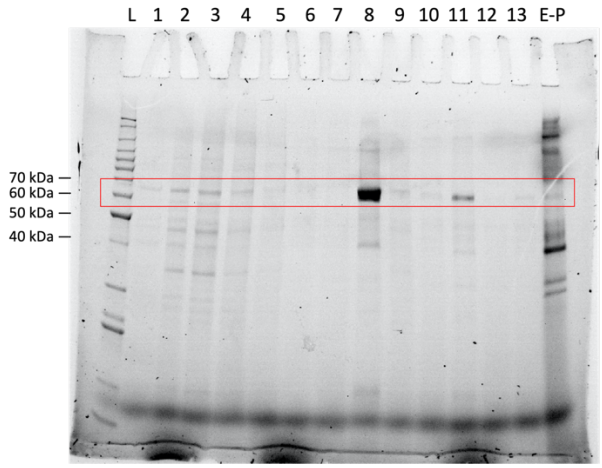

Figure 4.11 ***Protein precipitation of P. pastoris transformants including the SmChiA gene.*** *The protein ladder (L) is marked with sizes ranging from 40-70 kDa and 60-70 kDa is marked in red. The negative control is an empty P. pastoris strain (E-P).*

The result of the protein precipitation is shown in Figure 4.11 alongside a non-transformed P. *pastoris* culture. Proteins with the size of approximately 60 kDa corresponding to *Sm*ChiA was marked in red. While the majority only have faint bands in this test, glycerol stocks were made of positive hits. In contrast colony 8 in the gel visualized a more prominent band and it is assumed that it produces more protein, resulting in the use of that glycerol stock for medium-scale cultivation.

4.4.2 Purification of *Sm*ChiA from *P. pastoris*

The chitinase, *Sm*ChiA, was cloned and transformed into *P. pastoris* in 3.1. The glycerol stock of the highest-yielding transformant from the protein precipitation test (Figure 4.11) was grown on YPD-agar plates (100 µg/mL zeocin) and colonies were used for inoculation of 500 mL YPD media as in 3.2.1. The supernatant of the culture was separated from the cells by centrifugation and concentrated using Vivaflow 10 MWCO filter cassette described in 3.2.1. *Sm*ChiA was separated from the concentrated supernatant by HIC as in 3.3.2 HiTrap Phenyl HP 5 mL column, as shown in Figure 4.12A, and collected fractions were analyzed for protein content using SDS-page shown in Figure 4.12B (3.1.8).

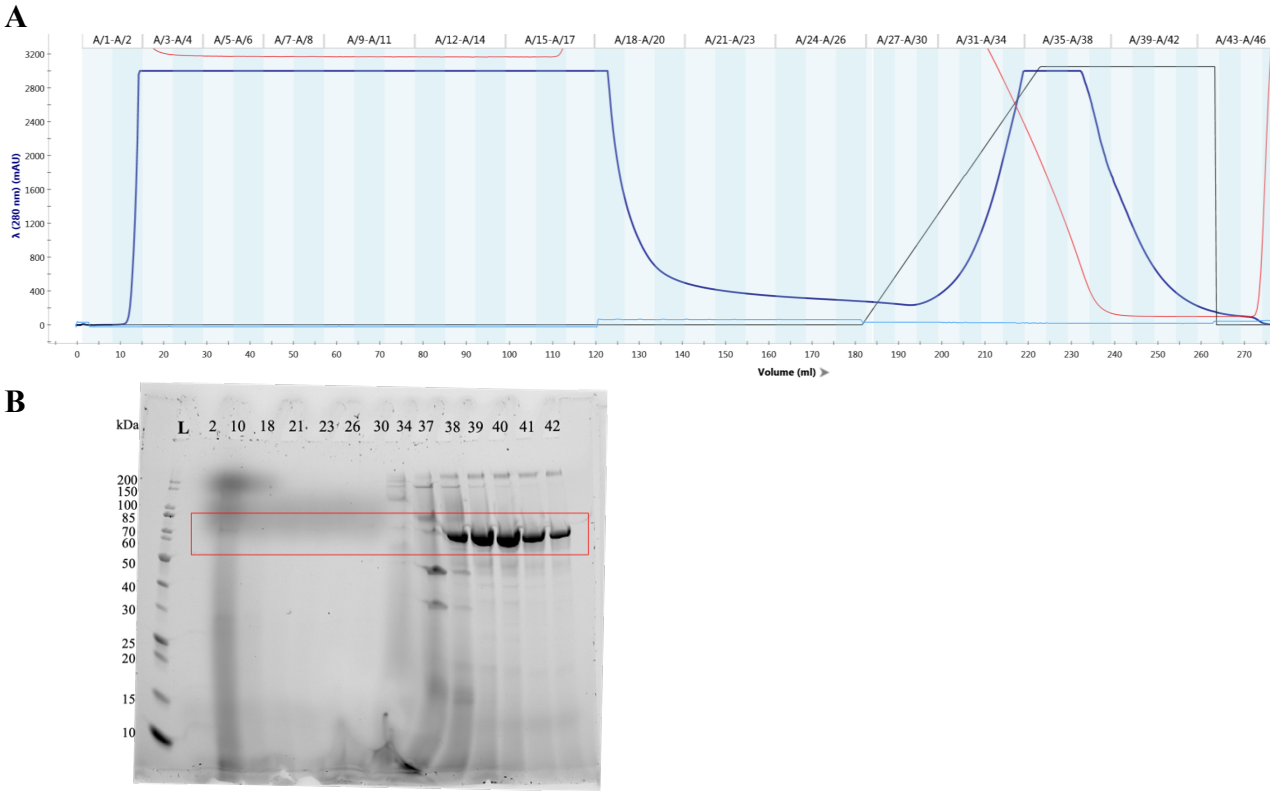

Figure 4.12 ***HIC-purification of SmChiA****.* ***(A)*** *HIC chromatogram, y-axis shows the UV-signal in mAU, and the x-axis is the volume in mL. The blue line is the UV signal, the red line is conductivity, and the black line is % of HIC buffer B (50 mM Bis-Tris pH 6.5) compared to HIC buffer A (50 mM Bis-Tris pH 6.5 + 2 M ammonium sulfate).* ***(B)*** *SDS-page analysis of HIC fractions. The protein ladder (L) is marked with the kDa size. Protein size corresponding to 60-70 kDa is marked with a red box.*

The purification of *Sm*ChiA with HIC presented the chromatogram in Figure 4.12A where the blue line showing UV A-280 trace, indicating the elution of protein by distinct peaks in the UV trace. The collected fractions from the separation by HIC were visualized in the SDS-

page gel in Figure 4.12B, where protein with the size corresponding to the approximately 60 kDa *Sm*ChiA was marked in red. Fractions 38-42 corresponded to the peak eluting after applying a gradient with reduced salt content and correspond to *Sm*ChiA in size. Fractions from 38 to 42 were concentrated to 1 mL using Amicon Ultra-15 centrifugal filter units with a 30 kDa cutoff, prior to purifying the protein using SEC.

Further *Sm*ChiA was purified by SEC, as described in 3.3.3, will separate the protein sample by size of proteins as the small proteins will interact more with the column material. The isocratic elution with the HiLoad 16/160 Superdex 75 ng 120 mL column, is presented in Figure 4.13A, and the collected fractions were analyzed by SDS-page in Figure 4.13B. Finally, in Figure 4.13C, the purity of the protein solution was analyzed by SDS-page.

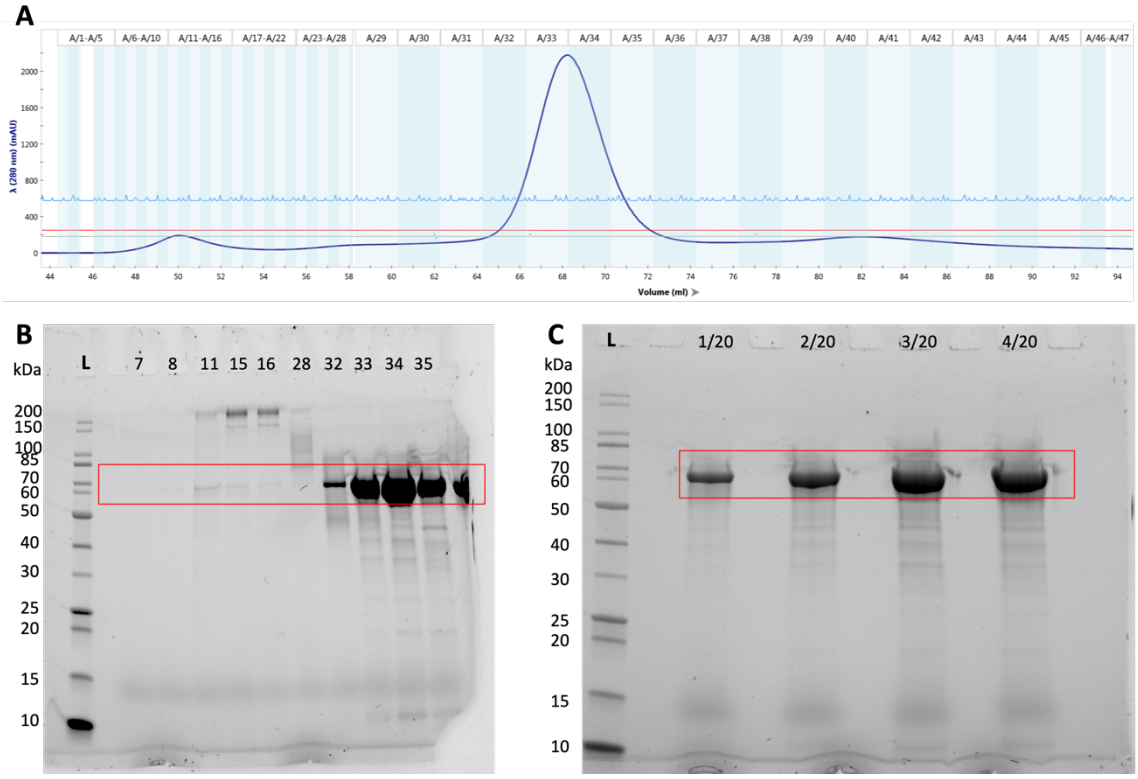

Figure 4.13 ***Size exclusion chromatography of SmChiA produced in P. pastoris****. **(A)** show the chromatogram, the y-axis shows the UV-signal in mAU, and the x-axis is the volume in mL. The blue line is the UV-signal and, the red line is conductivity. **(B)** SEC fractions analyzed on SDS-page. The protein ladder (L) marked with the kDa size. **(C)** shows SDS-page analysis of purity. Dilutions of the final protein stock from 1/20 to 4/20. Image Lab report of that gel was used for purity. The same protein ladder (L) was used in both gels.*

The SEC chromatogram showed a peak eluting after approximately 60 mL in the chromatogram in Figure 4.13A, with a UV A-280 signal of 2000 mAU, indicating a large

amount of protein. Collected fractions were analyzed on SDS-page (3.1.8), and the fractions from the peak showed protein with the size of 60 kDa in Figure 4.13B, indicating successful separation. Fractions 32- 35 were concentrated by Amicon Ultra-15 centrifugal filter units with a 30 kDa cutoff to approximately 1 mL before the purity of the protein sample was estimated by analyzing dilutions on an SDS-page gel in Figure 4.13C, resulting in 95 % purity in Image Lab. The concentration of the protein sample was estimated by analyzing triplicate on Nanodrop A-280, giving 140 µM and a yield of 9 mg per 500 mL culture.

4.4.3 Activity assays of *Sm*ChiA produced in *P. pastoris* vs *E. coli*

The *P. pastoris* produced enzyme may not have the same activity as previously analyzed *Sm*ChiA produced by *E. coli*. Therefore, two different enzymatic assays were performed to examine the activity, the first on a synthetic substrate that emits a fluorescent group that can be measured when cleaved, and the second being a time-course assay on degradation of β-chitin analyzed by HPLC.

4.4.3.1 Specific enzymatic activity of *Sm*ChiA

*Sm*ChiA is active on the 4-MU analog to chitin 4-MU-$(GlcNAc)_2$, and this substrate can be used to estimate enzyme activity by measuring the fluorescence of the 4-MU unit as it is cleaved of chitobiose. This method was used to check if there was a difference in specific enzyme activity between the *P. pastoris* or *E. coli* produced *Sm*ChiA. The reaction mixture of 1.9 nM of *Sm*ChiA (produced either in *P. pastoris* or *E. coli*), 69 µM 4-MU-$(GlcNAc)_2$, 0.1 mg/mL BSA in 0.2 M citrate phosphate buffer pH 6. Reactions were stopped after 10 minutes, and the fluorescence was measured and compared to a standard of 100 µM 4-MU. The specific enzyme activity was estimated using Equation 4.1.

Equation 4.1

$$\frac{(avg) \times (0.2 \times 10^{-12} mol)}{10\ min} / volume(mL) / concentration(mg/mL)$$

Equation 4.1 shows the calculation for specific enzyme activity where the average (avg) of the measurement, 0.2 pmol equals the value of each measured unit in mol of the 4-MU standard, volume (mL) refers to the calculated volume taken from the original stock and concentration (mg/ml) refers to the concentration of corresponding enzyme stock.

Table 4.1. Table of comparison of specific enzyme activity between SmChiA produced in P. pastoris and E. coli. The calculation of specific enzyme activity was performed using Equation 4.1. The blank value was removed from the measurement.

***Sm*ChiA produced in:**	**Measurement: average ± standard deviation (n=3)**	**Specific enzyme activity (µmol min^{-1} mg^{-1})**
P. pastoris	130 ± 40	2.2
E. coli	140 ± 20	2.4

The specific enzyme activity of *Sm*ChiA was estimated to be 2.2 and 2.4 µmol min^{-1} mg^{-1}, for *P. pastoris* and *E. coli* produced enzyme, respectively. There is no significant difference between the enzyme produced by *E. coli* or *P. pastoris* due to the overlapping of averages and deviations in the measurements.

4.4.3.2 Time-course experiment of *Sm*ChiA produced by *P. pastoris* relative to *E. coli*

The relative activity of *Sm*ChiA produced in *P. pastoris* was compared to the activity of *E. coli* produced enzyme on β-chitin, to evaluate the activity on chitin substrate. The time-course experiment was performed as described in 3.6, with 2 mg/mL β-chitin in 50 mM sodium phosphate pH 6.4 at 37 °C and 859 rpm in a Thermomixer C. The reactions were initiated by adding 1 µM *Sm*ChiA, and aliquoted samples were terminated in 50 mM sulfuric acid and filtered before analysis by HPLC Rezex RFQ-fast acid H+ column at 85 °C with 1 mL/min flow rate monitoring product by UV A-194. The most prominent product of the processive *Sm*ChiA is the dimer chitobiose, and the result of the analysis for chitobiose was compared to a in-house generated standard of chitobiose (as the example shown in Appendix Figure 8.2). Finally, the results of the *P. pastoris* produced enzyme was compared relatively in percentage to the *E. coli* produced enzyme.

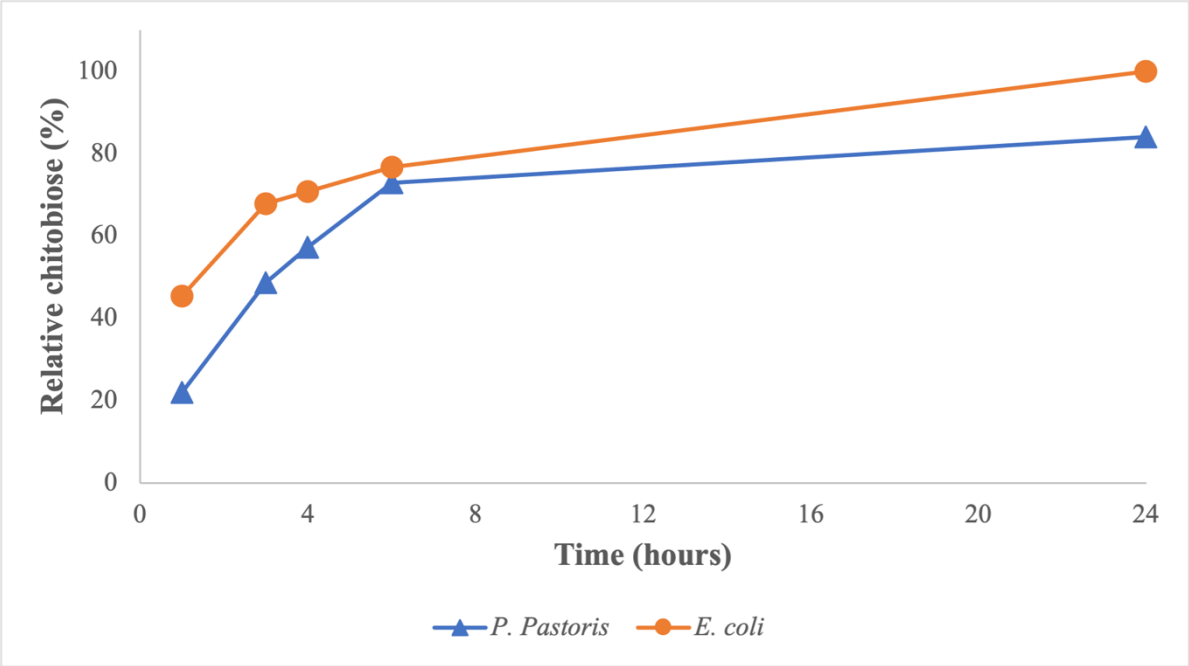

Figure 4.14 ***Time-course experiment of SmChiA produced in P. pastoris vs. E. coli****. Production of relative chitobiose yield in percent of the maximum chitobiose product in this experiment by 1 µM SmChiA produced in E. coli, on the y-axis and time in hours on the x-axis. Standard deviations are included as error bars of n=3.*

The results were calculated in percent of the chitobiose product yield for *E. coli Sm*ChiA at 24 hours (Figure 4.14), and in comparison, the *P. pastoris* produces *Sm*ChiA gave 85 % product yield. There is a significant difference between *Sm*ChiA produced in *P. pastoris vs E. coli* due to low standard deviations, giving no overlap of the results. Furthermore, *E. coli* produced *Sm*ChiA had a higher product yield the first hour, different from the *P. pastoris* produced *Sm*ChiA that had a higher incline for the first 6 hours but stagnated more between 6 and 24 hours.

5 Discussion

The imposing threat of climate change, increased dependency on oil and waste production from a continuously increasing population have set the focus on a greener bioeconomy, where the use of Nature's renewable resources has recently spiked interest. Upcycling and utilizing resources that previously were considered waste holds immense potential and contributes to reaching the SDGs developed by the UN (United Nations, 2015). Enzymatic degradation of biomass proposes a greener method for utilizing materials such as chitin that is estimated to produce 1 billion tons each year (Nelson & Cox, 2017), including seafood shell waste that is estimated to be 6-8 million tons annually (FAO, 2014). Great progress in enzymatic degradation of biomass has been made, however, industrial-size degradation of chitin still utilizes chemical extraction methods that require great energy and strong chemicals (Younes & Rinaudo, 2015), enzymatic degradation is still limited to laboratory studies but shows great promise (Chakravarty & Edwards, 2022; Gooday et al., 1990; Inokuma et al., 2013; Johansen, 2016; Reese et al., 1950; Rinaudo, 2006; Younes & Rinaudo, 2015; Zhu et al., 2016). The use of industrial cocktails is well known from the degradation of cellulose-rich biomass (Wood & Garcia-Campayo, 1990), and the use of several enzymes in synergy has greatly increased the efficiency of biomass valorization, although, there are still advances to be made concerning the chitin yield obtained by enzymatic methods, as there is only reported a few incidents of industrial applicable methods that gives the same yield as chemical extraction (Vazquez et al., 2017).

Chitinolytic enzymes in synergy enhance the degradation of the recalcitrant polysaccharide of chitin. The enzymatic system for chitin degradation in *S. marcescens* includes three GH18 chitinases, a GH20 chitobiase, and an AA10 LPMO that has complimentary activity on degrading crystalline or oligomers of chitin (Vaaje-Kolstad et al., 2013). The main contributor in this cocktail is *Sm*ChiA, which will processively degrade chitin from the reduced end of the chitin chain to yield chitobiose (Mekasha et al., 2017). For highly crystalline chitin *Sm*AA10A has proved to efficiently create oxidative cleaving of glycosidic bonds, creating accessible ends for *Sm*ChiA and therefore increasing *Sm*ChiA activity (Hamre et al., 2019) The use of several enzymes in synergy has been of interest in other work, however, recent

work done on LPMOs presenting limiting reaction conditions (Bissaro et al., 2017; Kuusk et al., 2018; Wang et al., 2020) warrant revisiting work on LPMO aided chitinase activity.

This thesis investigated how enzymatic degradation of β-chitin by *Sm*ChiA gains a synergistic effect with *Sm*AA10A concerning different enzyme concentrations, pretreatment of the substrate with *Sm*AA10A, substrate concentration and if peroxygenase conditions for the LPMO increase synergy effect. In addition to the enzymatic assays, *Sm*ChiA was cloned into the industrial-relevant expression system of *P. pastoris* to investigate the activity of *P. pastoris* produced *Sm*ChiA against the widely used laboratory expression system of *E. coli* (Balamurugan et al., 2007).

Both the LPMO and the Chitinase A of *S. marcescens* have activity towards β-chitin (Figure 4.4A for *Sm*AA10A and Figure 4.4B for *Sm*ChiA), however, they produce different products. The LPMO, with an endo-acting cleavage of glycosidic bonds on the crystalline substrate will create cuts of different ranging lengths (Vaaje-Kolstad et al., 2010). Whilst the processive GH18 *Sm*ChiA will primarily produce chitobiose from the crystalline substrate (Brurberg et al., 1994; Horn et al., 2006b; Hult et al., 2005), however, *Sm*ChiA will also degrade the oligomers released by SmAA10A. The product profile from both enzymes in combination is therefore a mixture of both oxidized dimer (chitobionic acid), monomer (GlcNAc), and dimer (chitobiose). The control experiments of product formation by 1 µM enzyme show that the native dimer is the by far most prominent product (Figure 4.4C) and therefore, allowing a simplified product quantification by only quantifying the native dimer, chitobiose. The main reason for this could be the high processive mechanism of *Sm*ChiA, and the addition of *Sm*AA10A supports *Sm*ChiA with chain ends that are easily accessible resulting in easier processive action. Hamre et al. (2019) discussed that the addition of LPMO to chitin degradation relieves the need for chitinases to act processive, due to the amount of chain ends accessible increased accessible substrate. Therefore, the strength of the hydrophobic interactions between enzyme and the substrate limits the catalytic speed. On the other hand, the basis of *Sm*ChiA´s high catalytic activity is due to the strength of the hydrophobic stacking interactions between substrate and enzyme (Horn et al., 2006a; Uchiyama et al., 2001).

Due to the synergistic effect that previously has been displayed between *Sm*ChiA and *Sm*AA10A (Hamre et al., 2019), a baseline of the synergy effect on chitobiose solubilization was investigated for 1 µM of the enzymes (Figure 4.4B). Both the synergy reactions (*Sm*ChiA + *Sm*AA10A) and the reaction with only *Sm*ChiA resulted interestingly in the same total yield, although at different speeds revealing the synergistic effect as the synergy experiment solubilized 70 % chitobiose faster, with the largest difference in yield at 10 % at 24 hours. As a result of the similar yield, it can be discussed if the *Sm*ChiA concentration was too high, as the synergy effect only resulted in a faster degradation activity. Furthermore, that *Sm*ChiA's ability to degrade β-chitin already is excellent. That could be explained by the morphology of β-chitin (Figure 1.1B) with the parallel alignment of the chitin chains resulting in a more flexible chitin structure due to a lower order of hydrogen-bond network, compared to α-chitin. Indicating, that the amount of accessible chain ends is sufficient for good *Sm*ChiA activity or possibly explained by the "cleft" topology it can implement endo-activity.

An attempt was made to improve the synergy effect on chitobiose yield by adapting a pretreatment method on the β-chitin substrate. Previously both mechanical and enzymatic pretreatment have been explored for chitin substrates resulting in higher chitinase efficiency (Nakagawa et al., 2013; Zhu et al., 2016), and Hamre et al. explored synergy effects where the substrate was treated with *Sm*AA10A prior to the addition of the chitinase (Hamre et al., 2015a; Hamre et al., 2019). Therefore, an enzymatic pretreatment method for 24 hours with *Sm*AA10A was pursued to investigate if the LPMO could create more accessible chain ends that provide *Sm*ChiA with more binding sites and therefore a boost in activity.

The first experiments investigating the effect of pretreatment at 1 µM enzyme concentrations gave no difference between the pretreated and non-pretreated samples (data not shown). As discussed earlier, *Sm*ChiA concentration may be too high to gain an effect. Therefore, the following experiments reduced the concentrations of *Sm*ChiA with the hope of observing a larger effect of pretreatment, i.e., the stagnation for the control reaction without pretreatment, resulting in a higher yield for pretreated reactions. An initial boost was observed for the first 60 minutes of the reaction with 100 nM *Sm*ChiA (Figure 4.5A), with a difference in chitobiose yield of approximately 5 %. The same boost was observed for 24 hours, but in the 24-hour perspective the boost seemed smaller, especially for the first 6 hours (Figure 4.5B). The minimal differences observed could be explained by how efficient *Sm*ChiA is to utilize

chitin as a substrate (as discussed above) especially in the initial 6 hours, as there are plenty of available chain ends and 100 nM *Sm*ChiA did not stagnate in these conditions.

To investigate if decreasing in total enzyme amount would show a pronounced effect on the pretreatment of the substrate, the enzyme concentrations (both *Sm*ChiA and *Sm*AA10A) were decreased by a factor of 10. Surprisingly, 1/10 reduced enzyme ratios yielded a similar-looking trend (Figure 4.5C), indicating that reducing both enzymes correspond to the reduction of the boost and yield, still resulting in reactions that have yet to stagnate at 48 hours, and an indication that a limiting factor of the boost could be due to a reduction in the *Sm*AA10A concentration. Subsequently, the pretreatment effect was investigated for a longer period at a fixed concentration of 1µM *Sm*AA10A with variating *Sm*ChiA concentrations (Figure 4.5D). As suggested by the *Sm*ChiA concentrations at 100, 50 and 10 nM, a corresponding dose-response should be observed if the yield is only dependent on *Sm*ChiA, but on the contrary as the 50 nM and 10 nM (*Sm*ChiA) pretreatment reactions resulted in higher yields than 50 % and 10 % of 100 nM yield, respectively. Indicating that for a set concentration of the LPMO, the synergy effect was inversely proportional to chitinase concentration, thus the highest boost effect was for the 10 nM *Sm*ChiA reaction. Furthermore, the boost effect for pretreated substrate with 50 nM *Sm*ChiA yielded an almost identical curve compared to a non-pretreated control with 100 nM *Sm*ChiA, indicating that at these concentrations *Sm*ChiA is working better when the substrate is pretreated, and therefore at these concentrations, there is a synergy effect. With the depletion of accessible substrate a plateau is expected as the recalcitrancy of the crystalline is more evident, as shown by the 1 µM *Sm*ChiA reaction (Figure 4.4). Also, it's expected that the processive actions of the chitinase should decrease (Hamre et al., 2014), resulting in lower activity towards stagnation, furthermore, that was not observed at these conditions with a total reaction time of 72 hours. This could indicate that at these concentrations, the reaction needs more time or the concentrations may be too small to reach the point where stagnation of *Sm*ChiA becomes evident.

Since the pretreatment results have yet to plateau after 48 hours of *Sm*ChiA (+24 hours of pretreatment) (Figure 4.5D), the efficiency of pretreatment can be questioned, especially if the goal is industrial application where time is costly. Resulting in experiments performed where *Sm*ChiA was added directly after *Sm*AA10A, thus saving 24 hours and non-pretreatment that

were called synergy experiments. The comparison between pretreatment and synergy experiments gives almost identical yields and rates, highlighting that pretreatment with *Sm*AA10A on this β-chitin substrate is negligible and the little effect it may give corresponds to non-pretreatment synergy in the long run, as seen in Figure 4.6. As previously mentioned, the similarity of synergy and pretreatment experiments could be explained by *Sm*ChiA access to chain ends in the beginning of the reaction and that the synergy effect becomes evident after the initial 6 hours, as the recalcitrant characteristic emerges.

Due to the fact that the synergy experiments didn't stagnate at 72 hours, the synergy effect was investigated at different substrate concentrations, both to identify if substrate concentration affects synergy and to evaluate the preceded stagnation of the degradation rate. Three different concentrations of β-chitin were selected based on Vaaje-Kolstad et al., that revealed a synergy effect between *Sm*AA10A and *Sm*ChiC at 0.45 mg/mL β-chitin (Vaaje-Kolstad et al., 2010), and previous substrate concentrations at 10 mg/mL corresponds to the standard reaction conditions set by Bissaro et al. that was used on LPMO reactions considered as substrate saturating (Bissaro et al., 2017), the final concentration of 2.5 mg/mL was determined as a middle concentration between 0.45 and 10 mg/mL.

Firstly, the substrate concentration at 10 mg/mL results in synergy effects (Figure 4.7A), explained by both sufficient substrate binding by the LPMO that prevents inactivation by auto-oxidation (Bissaro et al., 2017; Kuusk et al., 2018), and sufficient substrate to observe the catalytic activity of *Sm*ChiA prior to the decrease of reaction rate due to recalcitrancy (Hamre et al., 2014), and therefore observe synergy effect. It is worth noting that the accuracy of the product quantification after the reaction past 24 hours is reduced due to evaporation of the solvent, and therefore overestimation of the yield was likely.

As the substrate concentration was decreased to 2.5 mg/mL β-chitin, the synergy effect faded as all reactions of 50 nM *Sm*ChiA and over approximately reached the same yield of 50 % chitobiose (Figure 4.7B). Thus, the substrate concentration resulted in a dependence on *Sm*ChiA to obtain a high yield, where a lower concentration, 50 nM, was just as efficient as 100 nM. In contrast, low *Sm*ChiA concentration (10 nM) yielded a small synergy effect. Interestingly, 2.5 mg/mL β-chitin displays the same issues as the initial experiments in this thesis, with 1 µM concentrations of both *Sm*ChiA and *Sm*AA10A with 10 mg/mL β-chitin in

Figure 4.4. This indicates that the enzyme amounts were too large compared to the substrate amount. Therefore, a high concentration of substrate is beneficial to view a synergy effect, in contrast to low β-chitin concentrations that may as well have a lower GH concentration (i.e., 50 nM *Sm*ChiA yield similar to 100 nM *Sm*ChiA) and no LPMO. When comparing substrate concentration (in mg/mL) to enzyme concentration of *Sm*ChiA (in nM) a ratio can be determined to be at least 20:1 for all experiments with a minimal synergy effect, while the experiments with observed synergy have ratios of 10:1 or lower. For this reason, the results displayed in Figure 4.4B and Figure 4.7B can be explained by a high ratio between high GH concentration compared to substrate concentration.

Furthermore, the opposite of a synergy effect was observed for 0.45 mg/mL β-chitin in Figure 4.7C, where the highest yielding reactions was those of only 100 and 50 nM *Sm*ChiA, indicating that at low substrate concentrations, *Sm*AA10A may inhibit in some way the reaction of *Sm*ChiA. It is relevant to associate low substrate concentrations with LPMO inactivation as unbound LPMO increases the risk of inactivation by auto-oxidation when being reduced unbound to substrate (Forsberg et al., 2019; Kuusk et al., 2019; Stepnov et al., 2021). The product yield of *Sm*ChiA may have been reduced by the inactivation of *Sm*AA10A followed by an accumulation of H_2O_2 or other reactive oxygen species that can influence *Sm*ChiA catalysis (Bissaro et al., 2017; Kuusk et al., 2018). Brurberg et al. (1996) showed that the presence of metal ions in a mM scale this did not affect enzymatic activity of *Sm*ChiA, therefore the release of copper from inactivated *Sm*AA10A can be neglected.

As the true co-substrate in LPMO catalytic mechanism is speculated to be H_2O_2, previously investigated synergy experiments need to be revisited under peroxygenase conditions to assess the true interplay between *Sm*AA10A and *Sm*ChiA (Bissaro et al., 2017; Kuusk et al., 2018; Wang et al., 2018). The reported k_{cat} of *Sm*AA10A in peroxygenase conditions is reported to be orders of magnitude higher than in monooxygenase conditions (Kuusk et al., 2019), resulting in the interest of peroxygenase condition on the synergy effect. As suggested by Bissaro et al., which used a glucose oxidase for controlled *in situ* H_2O_2 production to fuel the LPMO reaction that yielded similar results for the catalysis of chitin oxidation as reactions with added H_2O_2 (Bissaro et al., 2017). Similarly, in this thesis experiments were performed with *Ag*ChOx that produces H_2O_2 by oxidation of choline to glycine-betaine producing two H_2O_2 per catalysis (Gadda, 2003). Using this approach, peroxygenase conditions were

obtained for *Sm*AA10A that could result in a higher synergy effect compared to the experiments with only *in situ* H_2O_2 production by the LPMO and the auto-oxidation by the reductant. The Amplex ™ Red assay (Kittl et al., 2012) was adjusted to measure oxidase activity of *Ag*ChOx in the presence of choline to produce a total of 1.4 to 11 µM/min of H_2O_2 using 100 and 800 nM respectively (Figure 4.3).

The synergy effect under peroxygenase conditions was investigated by reactions with *Sm*AA10A (0 or 1 µM), *Sm*ChiA(10, 50 and 100 nM) and *Ag*ChOx (0-800 nM) in the presence of choline, and showed a clear dose response effect where higher concentrations of the chitinase and higher concentrations of the choline oxidase yielded a high chitobiose yield when the LPMO was present (heat map in Figure 4.8). The results indicate that there is an additional boost of the synergy effect under peroxygenase conditions, where a higher controlled dose H_2O_2 supply proceeded to not inactivate the LPMO. This means that the synergy effect was enhanced by the peroxygenase conditions, aligning with the documented boost peroxygenase conditions have on LPMOs (Bissaro et al., 2017; Kuusk et al., 2018; Wang et al., 2018; Wang et al., 2020), as seen in the increase of chitobiose yield within a set concentration of *Sm*ChiA, for every increase of *Ag*ChOx up to 200 nM. The dose-response results are inconsistent for the *Ag*ChOx concentrations of 400 nM, where there are lower chitobiose yields across every *Sm*ChiA concentration compared to at 200 nM of added *Ag*ChOx. Furthermore, this could indicate that the high H_2O_2 levels lead to inactivation despite having high substrate concentration (i.e., large amount of chitin still available at 24 hours). Too high H_2O_2 concentration may have led to the accumulation of reactive oxygen species resulting in the gradual inactivation of LPMO. Another inconsistent observation is that the reactions with 800 nM of added *Ag*ChOx yield similar chitobiose yields as the corresponding reactions with 200 nM *Ag*ChOx. Following the argument that the LPMO was inactivated at 400 nM *Ag*ChOx, the chitobiose yield for 800 nM should be even lower. On the contrary, it resembled the one of 200 nM raising speculations of the stability of the *Ag*ChOx, i.e., if fractions of *Ag*ChOx were inactivated, it would produce lower H_2O_2 concentrations.

Finally, peroxygenase conditions were investigated for 1 µM concentrations of both *Sm*AA10A and *Sm*ChiA with a supply of H_2O_2 from 200 nM *Ag*ChOx in the presence of choline, to see if the increased synergy effect by peroxygenase conditions is applicable using a relatively high *Sm*ChiA concentration. The results displayed similar trends as the initial 1

μM synergy experiments of both *Sm*ChiA and *Sm*AA10A (Figure 4.4B), with a minor increased chitobiose yield for the peroxygenase synergy experiment compared to the monooxygenase synergy experiment (Figure 4.9). As explained by the lack of synergy effects obtained with 2.5 mg/mL (synergy at different substrate concentrations), the enzyme ratio compared to the substrate may be too high, minimizing synergy effect. On the other hand, the results of 1 μM reaction of *Sm*ChiA yield 70 % chitobiose while 100 nM *Sm*ChiA only managed approximately 50 % when obtaining the highest synergy effects. A key finding is that it is important to have high β-chitin concentration and a at least 1/10 ratio of *Sm*ChiA vs. *Sm*AA10A to ensure that the LPMO do not limit the synergy effect. Furthermore, to increase product yield using both an LPMO and a GH, it may be relevant to investigate less processive mutants for the GH enzymes, as suggested by Hamre et al. (2019).

The cloning of *Sm*ChiA into *P. pastoris* resulted in a relatively easy production of the enzyme and is beneficial for industrial scale production which is well established for *P. pastoris*. This provides benefits such as post-translational folding and secretion into the extracellular space (Balamurugan et al., 2007). This study will be the first time for cloning a chitinase from *S. marcescens* into *P. pastoris*. A relevant long-term goal is to develop a secreteable chitinolytic cocktail in *P. pastoris*. The cloning resulted in a protein yield and activity that was compared to *E. coli* BL21(DE3) produced enzyme on two different substrates. This demonstrates that *P. pastoris* has an exciting potential as an expression platform for chitinolytic enzymes at an industrial level for the enzymatic conversion of chitin into products of value.

6 Conclusion and future perspectives

The main result from the work presented in this thesis is that the combination of *Sm*ChiA and *Sm*AA10A results in higher degradation of β-chitin compared to by themselves, although dependent on enzyme ratio and substrate concentration. In modern biorefinery setup, enzyme cost is one of the key parameters in the sustainable use of enzymes into products of value. The results demonstrate that *Sm*ChiA alone is an efficient enzyme for chitin degradation, but the potential in the results shows an increase in the chitobiose yield for experiments with high β-chitin concentration, when the concentration of *Sm*ChiA was least a ten-fold lower than *Sm*AA10A, and a steady supplement of the co-substrate H_2O_2. These findings serve as beneficial information in developing the most efficient combination of LPMOs and GHs for the sustainable solubilization of crystalline chitin, which is abundantly produced in Nature.

Future work may further adapt this system with an emphasis on the bioeconomy towards enzyme cost using the knowledge obtained in this work. Moreover, the benefits of adding another GH, e.g., *Sm*CHB, or less processive mutants of *Sm*ChiA (Hamre et al., 2019), in a chitinolytic cocktail to increase the yield of the recalcitrant chitin. In addition, examine the application on a diversity of chitin substrates, including α-chitin, and e.g., natural chitin-protein and mineral complexes.

The long-term goal of demonstrating a sustainable chitinolytic machinery that can convert biomass to products of value. Here, it is vital to recognize and adapt how Nature achieves this, attempt to improve, and then apply such machinery in modern biotechnology. In this regard, it was demonstrated in this work that the bacterial *Sm*ChiA was successfully cloned into the already well-used industrial expression system of *P. pastoris*, with the same chitin degrading ability as when expressed in *E. coli*.

7 References

Agger, J. W., Isaksen, T., Varnai, A., Vidal-Melgosa, S., Willats, W. G., Ludwig, R., Horn, S. J., Eijsink, V. G. & Westereng, B. (2014). Discovery of LPMO activity on hemicelluloses shows the importance of oxidative processes in plant cell wall degradation. *Proc Natl Acad Sci U S A*, 111 (17): 6287-92. doi: 10.1073/pnas.1323629111.

Baeshen, M. N., Thamer A. F. Bouback, Mubarak A. Alzubaidi, Roop S. Bora, Mohammed A. T. Alotaibi, Omar T. O. Alabbas, Sultan M. Alshahrani, Ahmed A. M. Aljohani, Rayan A. A. Munshi, A. A.-H., Mohamed M. M. Ahmed, et al. (2016). Expression and Purification of C-Peptide Containing Insulin Using Pichia pastoris Expression System. *BioMed Research International*: 7.

Balamurugan, V., Reddy, G. R. & Suryanarayana, V. V. S. (2007). Pichia pastoris: A notable heterologous expression system for the production of foreign proteins - Vaccines. *Indian Journal of Biotechnology*, 6: 175-186.

Beckham, G. T., Stahlberg, J., Knott, B. C., Himmel, M. E., Crowley, M. F., Sandgren, M., Sorlie, M. & Payne, C. M. (2014). Towards a molecular-level theory of carbohydrate processivity in glycoside hydrolases. *Curr Opin Biotechnol*, 27: 96-106. doi: 10.1016/j.copbio.2013.12.002.

Bissaro, B., Røhr, Å. K., Müller, G., Chylenski, P., Skaugen, M., Forsberg, Z., Horn, S. J., Vaaje-Kolstad, G. & Eijsink, V. G. H. (2017). Oxidative cleavage of polysaccharides by monocopper enzymes dependent on H2O2. *Nature chemical biology*, 13.

Bissaro, B., Streit, B., Isaksen, I., Eijsink, V. G. H., Beckham, G. T., DuBois, J. L. & Rohr, A. K. (2020). Molecular mechanism of the chitinolytic peroxygenase reaction. *Proc Natl Acad Sci U S A*, 117 (3): 1504-1513. doi: 10.1073/pnas.1904889117.

Brurberg, M. B., Eijsink, V. G. H. & Nes, I. F. (1994). Characterization of a chitinase gene (chiA) from Serratia marcescens BJL200 and one-step purification of the gene product. *FEMS Microbiology letters*, 124.

Brurberg, M. B., Eijsink, V. G. H., Haandrikman, A. J., Venema, G. & Nes, I. F. (1995). Chitinase B from Serratia marcescens BJL200 is exported to the periplasm without processing. *Microbiology(1995), 141, 123-131*.

Brurberg, M. B., Nesl, I. F. & Eijsinkl, V. G. H. (1996). Comparative studies of chitinases A and B from Serratia marcescens. *Microbiology(1996), 142, 1581-1 589*.

Chakravarty, J. & Edwards, T. A. (2022). Innovation from waste with biomass-derived chitin and chitosan as green and sustainable polymer: A review. *Energy Nexus*, 8. doi: 10.1016/j.nexus.2022.100149.

Chen, C., Wang, Z., Zhang, B., Miao, L., Cai, J., Peng, L., Huang, Y., Jiang, J., Huang, Y., Zhang, L., et al. (2017). Nitrogen-rich hard carbon as a highly durable anode for high-power potassium-ion batteries. *Energy Storage Materials*, 8: 161-168. doi: https://doi.org/10.1016/j.ensm.2017.05.010.

Consortium, C. (2018). Ten years of CAZypedia: a living encyclopedia of carbohydrate-active enzymes. *Glycobiology*, 28 (1): 3-8. doi: 10.1093/glycob/cwx089.

Dai, T., Tanaka, M., Huang, Y.-Y. & Hamblin, M. R. (2011). Chitosan preparations for wounds and burns: antimicrobial and wound-healing effects. *Expert Review of Anti-infective Therapy*, 9 (7): 857-879. doi: 10.1586/eri.11.59.

Davies, G. & Henrissat, B. (1995). Structures and mechanisms of glycosyl hydrolases. *Structure*, 3 (9).

Drula, E., Garron, M. L., Dogan, S., Lombard, V., Henrissat, B. & Terrapon, N. (2022). The carbohydrate-active enzyme database: functions and literature. *Nucleic Acids Res*, 50 (D1): D571-D577. doi: 10.1093/nar/gkab1045.

Eijsink, V. G. H., Petrovic, D., Forsberg, Z., Mekasha, S., Rohr, A. K., Varnai, A., Bissaro, B. & Vaaje-Kolstad, G. (2019). On the functional characterization of lytic polysaccharide monooxygenases (LPMOs). *Biotechnol Biofuels*, 12: 58. doi: 10.1186/s13068-019-1392-0.

Expasy. *ProtParam tool*. Available at: https://web.expasy.org/protparam/ (accessed: 11.05.23).

FAO. (2014). *The State of World Fisheries and Aquaculture - Oppertunities and challenges*

Forsberg, Z., Rohr, A. K., Mekasha, S., Andersson, K. K., Eijsink, V. G., Vaaje-Kolstad, G. & Sorlie, M. (2014). Comparative study of two chitin-active and two cellulose-active AA10-type lytic polysaccharide monooxygenases. *Biochemistry*, 53 (10): 1647-56. doi: 10.1021/bi5000433.

Forsberg, Z., Sorlie, M., Petrovic, D., Courtade, G., Aachmann, F. L., Vaaje-Kolstad, G., Bissaro, B., Rohr, A. K. & Eijsink, V. G. (2019). Polysaccharide degradation by lytic polysaccharide monooxygenases. *Curr Opin Struct Biol*, 59: 54-64. doi: 10.1016/j.sbi.2019.02.015.

Frommhagen, M., Sforza, S., Westphal, A. H., Visser, J., Hinz, S. W., Koetsier, M. J., van Berkel, W. J., Gruppen, H. & Kabel, M. A. (2015). Discovery of the combined oxidative cleavage of plant xylan and cellulose by a new fungal polysaccharide monooxygenase. *Biotechnology for biofuels*, 8.

Fuchs, R. L., McPherson, S. A. & Drahos, D. J. (1986). Cloning of a *Serratia marcescens* Gene Encoding Chitinase. *Applied And Environmental Micorbiology* 51: 504-509.

Gadda, G. (2003). Kinetic mechanism of choline oxidase from Arthrobacter globiformis. *Biochim Biophys Acta*, 1646 (1-2): 112-8. doi: 10.1016/s1570-9639(03)00003-7.

Golten, O., Ayuso-Fernandez, I., Hall, K. R., Stepnov, A. A., Sorlie, M., Rohr, A. K. & Eijsink, V. G. H. (2023). Reductants fuel lytic polysaccharide monooxygenase activity in a pH-dependent manner. *FEBS Lett*. doi: 10.1002/1873-3468.14629.

Gooday, G. W., Prosser, J. I., Hillman, K. & Cross, M. G. (1990). The ecology of chitin degradation. *Adv. Microb. Ecol.*, 11: 387-430. doi: 10.1007/978-1-4684-7612-5_10.

Hamre, A. G., Lorentzen, S. B., Valjamae, P. & Sorlie, M. (2014). Enzyme processivity changes with the extent of recalcitrant polysaccharide degradation. *FEBS Lett*, 588 (24): 4620-4. doi: 10.1016/j.febslet.2014.10.034.

Hamre, A. G., Eide, K. B., Wold, H. H. & Sorlie, M. (2015a). Activation of enzymatic chitin degradation by a lytic polysaccharide monooxygenase. *Carbohydr Res*, 407: 166-9. doi: 10.1016/j.carres.2015.02.010.

Hamre, A. G., Jana, S., Holen, M. M., Mathiesen, G., Valjamae, P., Payne, C. M. & Sorlie, M. (2015b). Thermodynamic Relationships with Processivity in Serratia marcescens Family 18 Chitinases. *J Phys Chem B*, 119 (30): 9601-13. doi: 10.1021/acs.jpcb.5b03817.

Hamre, A. G., Stromnes, A. S., Gustavsen, D., Vaaje-Kolstad, G., Eijsink, V. G. H. & Sorlie, M. (2019). Treatment of recalcitrant crystalline polysaccharides with lytic polysaccharide monooxygenase relieves the need for glycoside hydrolase processivity. *Carbohydr Res*, 473: 66-71. doi: 10.1016/j.carres.2019.01.001.

Henrissat, B. (1991). A classification of glycosyl hydrolases based on amino acid sequence similarities. *The Biochemical journal*, 280: 309-316.

Horn, S. J., Sikorski, P., Cederkvist, J. B., Vaaje-Kolstad, G., Sorlie, M., Synstad, B., Vriend, G., Varum, K. M. & Eijsink, V. G. (2006a). Costs and benefits of processivity in enzymatic degradation of recalcitrant polysaccharides. *Proc Natl Acad Sci U S A*, 103 (48): 18089-94. doi: 10.1073/pnas.0608909103.

Horn, S. J., Sorbotten, A., Synstad, B., Sikorski, P., Sorlie, M., Varum, K. M. & Eijsink, V. G. (2006b). Endo/exo mechanism and processivity of family 18 chitinases produced by Serratia marcescens. *FEBS J*, 273 (3): 491-503. doi: 10.1111/j.1742-4658.2005.05079.x.

Horn, S. J., Sørlie, M., Vaaje-Kolstad, G., Norberg, A. L., Synstad, B., Vårum, K. M. & Eijsink, V. G. H. (2009). Comparative studies of chitinases A, B and C fromSerratia marcescens. *Biocatalysis and Biotransformation*, 24 (1-2): 39-53. doi: 10.1080/10242420500518482.

Horn, S. J., Vaaje-Kolstad, G., Westereng, B. & Eijsink, V. G. (2012). Novel enzymes for the degradation of cellulose. *Biotechnology for Biofuels*, 5 (45). doi: https://doi.org/10.1186/1754-6834-5-45.

Hou, J., Aydemir, B. E. & Dumanli, A. G. (2021). Understanding the structural diversity of chitins as a versatile biomaterial. *Philosophical Transactions of the Royal Society A: Mathematical, Physical and Engineering Sciences*, 379 (2206): 20200331. doi: doi:10.1098/rsta.2020.0331.

Hult, E. L., Katouno, F., Uchiyama, T., Watanabe, T. & Sugiyama, J. (2005). Molecular directionality in crystalline beta-chitin: hydrolysis by chitinases A and B from Serratia marcescens 2170. *The Biochemical journal*, 388: 851-856.

Igarashi, K., Uchihashi, T., Koivula, A., Wada, M., Kimura, S., Okamoto, T., Penttilä, M., Ando, T. & Samejima, M. (2011). Traffic jams reduce hydrolytic efficiency of cellulase on

cellulose surface. *Science*, 333 (6047): 1279-1282. doi: https://doi.org/10.1126/science.1208386.

Inokuma, K., Takano, M. & Hoshino, K. (2013). Direct ethanol production from N-acetylglucosamine and chitin substrates by Mucor species. *Biochemical Engineering Journal*, 72: 24-32. doi: 10.1016/j.bej.2012.12.009.

Isaksen, T., Westereng, B., Aachmann, F. L., Agger, J. W., Kracher, D., Kittl, R., Ludwig, R., Haltrich, D., Eijsink, V. G. & Horn, S. J. (2014). A C4-oxidizing lytic polysaccharide monooxygenase cleaving both cellulose and cello-oligosaccharides. *J Biol Chem*, 289 (5): 2632-42. doi: 10.1074/jbc.M113.530196.

Johansen, K. S. (2016). Discovery and industrial applications of lytic polysaccharide mono-oxygenases. *Biochem Soc Trans*, 44 (1): 143-149.

Jones, J. D. G., Grady, K. L., Suslow, T. V. & Bedbrook, J. R. (1986). Isolation and characterization of genes encoding two chitinase enzymes from *Serratia marcescens*. *EMBO*, 5: 467-473.

Karagozlu, M. Z. & Kim, S.-K. (2014). *Advances in Food and Nutrition Research*, vol. 72: Academic Press.

Karbalaei, M., Rezaee, S. A. & Farsiani, H. (2020). Pichia pastoris: A highly successful expression system for optimal synthesis of heterologous proteins. *J Cell Physiol*, 235 (9): 5867-5881. doi: 10.1002/jcp.29583.

Kaur, S. & Dhillon, G. S. (2015). Recent trends in biological extraction of chitin from marine shell wastes: a review. *Critical Reviews in Biotechnology*, 35: 44-61. doi: 10.3109/07388551.2013.798256.

Kawata, M., Azuma, K., Izawa, H., Morimoto, M., Saimoto, H. & Ifuku, S. (2016). Biomineralization of calcium phosphate crystals on chitin nanofiber hydrogel for bone regeneration material. *carbohydrate Polymers*, 136: 964-969. doi: https://doi.org/10.1016/j.carbpol.2015.10.009.

Kaya, M., Mujtaba, M., Ehrlich, H., Salaberria, A. M., Baran, T., Amemiya, C. T., Galli, R., Akyuz, L., Sargin, I. & Labidi, J. (2017). On chemistry of gamma-chitin. *Carbohydr Polym*, 176: 177-186. doi: 10.1016/j.carbpol.2017.08.076.

Kittl, R., Kracher, D., Burgstaller, D., Haltrich, D. & Ludwig, R. (2012). Production of four Neurospora crassa lytic polysaccharide monooxygenases in Pichia pastoris monitored by a fluorimetric assay. *Biotechnology for Biofuels*, 5.

Koshland Jr, D. E. (1953). Stereochemistry and the mechanism of enzymatic reactions. *Bilogical Reviews*, 28: 416-436.

Kuusk, S., Sorlie, M. & Valjamae, P. (2015). The predominant molecular state of bound enzyme determines the strength and type of product inhibition in the hydrolysis of recalcitrant polysaccharides by processive enzymes. *J Biol Chem*, 290 (18): 11678-91. doi: 10.1074/jbc.M114.635631.

Kuusk, S., Bissaro, B., Kuusk, P., Forsberg, Z., Eijsink, V. G. H., Sorlie, M. & Valjamae, P. (2018). Kinetics of H2O2-driven degradation of chitin by a bacterial lytic polysaccharide monooxygenase. *J Biol Chem*, 293 (2): 523-531. doi: 10.1074/jbc.M117.817593.

Kuusk, S., Kont, R., Kuusk, P., Heering, A., Sorlie, M., Bissaro, B., Eijsink, V. G. H. & Valjamae, P. (2019). Kinetic insights into the role of the reductant in H(2)O(2)-driven degradation of chitin by a bacterial lytic polysaccharide monooxygenase. *J Biol Chem*, 294 (5): 1516-1528. doi: 10.1074/jbc.RA118.006196.

Lei, J., Yang, L., Zhan, Y., Wang, Y., Ye, T., Li, Y., Deng, H. & Li, B. (2014). Plasma treated polyethylene terephthalate/polypropylene films assembled with chitosan and various preservatives for antimicrobial food packaging. *Colloids and Surfaces B: Biointerfaces*, 114: 60-66. doi: https://doi.org/10.1016/j.colsurfb.2013.09.052.

Loose, J. S. M., Arntzen, M. O., Bissaro, B., Ludwig, R., Eijsink, V. G. H. & Vaaje-Kolstad, G. (2018). Multipoint Precision Binding of Substrate Protects Lytic Polysaccharide Monooxygenases from Self-Destructive Off-Pathway Processes. *Biochemistry*, 57 (28): 4114-4124. doi: 10.1021/acs.biochem.8b00484.

Mekasha, S., Byman, I. R., Lynch, C., Toupalová, H., Anděra, L., Næs, T., Vaaje-Kolstad, G. & Eijsink, V. G. H. (2017). Development of enzyme cocktails for complete saccharification of chitin using mono-component enzymes from Serratia marcescens. *Process Biochemistry*, 56: 132-138. doi: 10.1016/j.procbio.2017.02.021.

Miller, J. M. (2005). *Chromatography: concepts and contrasts*: John Wiley & Sons, inc.

Monreal, J. & Reese, E. T. (1969). The chitinase of *Serratia marcescens*. *Canadian Journal of Microbiology*.

Nakagawa, Y. S., Eijsink, V. G., Totani, K. & Vaaje-Kolstad, G. (2013). Conversion of alpha-chitin substrates with varying particle size and crystallinity reveals substrate preferences of the chitinases and lytic polysaccharide monooxygenase of Serratia marcescens. *J Agric Food Chem*, 61 (46): 11061-6. doi: 10.1021/jf402743e.

Nelson, D. L. & Cox, M. M. (2017). *Lehninger Principles of Biochemistry*. International Edition 7th ed. Houndsmills. Basingstoke. England,: Macmillan higher Education.

New England Biolabs. *Gibson Assembly® Protocol (E5510)*. Available at: https://international.neb.com/protocols/2012/12/11/gibson-assembly-protocol-e5510 (accessed: 27.2.23).

Papanikolau, Y., Prag, G., Tavlas, G., Vorgias, C., Oppenheim, A. & Petratos, K. (2001). High resolution structural analyses of mutant chitinase A complexes with substrates provide new insight into the mechanism of catalysis. *Biochemistry*, 40: 11338-11343.

Parsiegla, G., Reverbel, C., Tardif, C., Driguez, H. & Haser, R. (2008). Structures of mutants of cellulase Cel48F of Clostridium cellulolyticum in complex with long hemithiocellooligosaccharides give rise to a new view of the substrate pathway during processive action. *J Mol Biol*, 375 (2): 499-510. doi: 10.1016/j.jmb.2007.10.039.

Quinlan, R. J., Sweeney, M. D., Lo Leggio, L., Otten, H., Poulsen, J. C., Johansen, K. S., Krogh, K. B., Jorgensen, C. I., Tovborg, M., Anthonsen, A., et al. (2011). Insights into the oxidative degradation of cellulose by a copper metalloenzyme that exploits biomass components. *Proc Natl Acad Sci U S A*, 108 (37): 15079-84. doi: 10.1073/pnas.1105776108.

Quiocho, F. (1989). Protein-carbohydrate interactions: basic molecular features. *Pure and Applied Chemistry,*, 61 (7): 1293-1306.

Reese, E. T., Siu, R. G. H. & Levinson, H. S. (1950). The biological degredation of soluble cellulose derivates and its relationship to the mechanism of cellulose hydrolysis. *Journal of Bacteriology*, 59 (4): 485-497.

Reynolds, J. A. & Tanford, C. (1970). The Gross Conformation of Protein-Sodium Dodecyl Sulfate Complexes. *Journal of Biological Chemistry*, 245 (19): 5161-5165. doi: 10.1016/s0021-9258(18)62831-5.

Rieder, L., Ebner, K., Glieder, A. & Sorlie, M. (2021a). Novel molecular biological tools for the efficient expression of fungal lytic polysaccharide monooxygenases in Pichia pastoris. *Biotechnol Biofuels*, 14 (1): 122. doi: 10.1186/s13068-021-01971-5.

Rieder, L., Petrovic, D., Valjamae, P., Eijsink, V. G. H. & Sorlie, M. (2021b). Kinetic Characterization of a Putatively Chitin-Active LPMO Reveals a Preference for Soluble Substrates and Absence of Monooxygenase Activity. *ACS Catal*, 11 (18): 11685-11695. doi: 10.1021/acscatal.1c03344.

Rieder, L., Stepnov, A. A., Sorlie, M. & Eijsink, V. G. H. (2021c). Fast and Specific Peroxygenase Reactions Catalyzed by Fungal Mono-Copper Enzymes. *Biochemistry*, 60 (47): 3633-3643. doi: 10.1021/acs.biochem.1c00407.

Rinaudo, M. (2006). Chitin and chitosan: Properties and applications. *Progress in Polymer Science*, 31 (7): 603-632. doi: 10.1016/j.progpolymsci.2006.06.001.

Roberts, G. A. F. (1992). *Chitin Chemistry*. 1st edition ed.: Macmillan Education.

Rye, C. S. & Withers, S. G. (2000). Glycosidase mechanisms. *Current Opinion in Chemical Biology*, 4.

Stepnov, A. A., Forsberg, Z., Sorlie, M., Nguyen, G. S., Wentzel, A., Rohr, A. K. & Eijsink, V. G. H. (2021). Unraveling the roles of the reductant and free copper ions in LPMO kinetics. *Biotechnol Biofuels*, 14 (1): 28. doi: 10.1186/s13068-021-01879-0.

Stepnov, A. A., Eijsink, V. G. H. & Forsberg, Z. (2022). Enhanced in situ H2O2 production explains synergy between an LPMO with a cellulose-binding domain and a single-domain LPMO. *Sci Rep*, 12 (1): 6129. doi: 10.1038/s41598-022-10096-0.

Sundheim, L., Poplanwsky, A. R. & Ellingboe, A. H. (1988). Molecular cloning of two chitinase genes from Serratia

marcescens and their expression in Pseudomonas species. *Physiological and Molecular Plant Pathology*, 33: 483-491.

Sørlie, M., Zakariassen, H., Norberg, A. L. & Eijsink, V. G. H. (2012). Processivity and substrate-binding in family 18 chitinases. *Biocatalysis and Biotransformation*, 30 (3): 353-365. doi: 10.3109/10242422.2012.676282.

Tharanathan, R. N. & Kittur, F. S. (2003). Chitin--the undisputed biomolecule of great potential. *Critical reviews in food science and nutrition*, 43: 61–87.

Toratani, T., Shoji, T., Ikehara, T., Suzuki, K. & Watanabe, T. (2008). The importance of chitobiase and N-acetylglucosamine (GlcNAc) uptake in

N, N'-diacetylchitoblose [(GlcNAC)(2)] utilization by Serratia marcescens 2,170. *Microbiology*, 154: 1326-1332.

Uchiyama, T., Katouno, F., Nikaidou, N., Nonaka, T., Sugiyama, J. & Watanabe, T. (2001). Roles of the exposed aromatic residues in crystalline chitin hydrolysis by chitinase A from Serratia marcescens 2170. *J Biol Chem*, 276 (44): 41343-9. doi: 10.1074/jbc.M103610200.

United Nations. (2015). *The UN Sustainable Development Goals*. https://www.undp.org/sustainable-development-goals (accessed: 3.5.2023).

Vazquez, J. A., Noriega, D., Ramos, P., Valcarcel, J., Novoa-Carballal, R., Pastrana, L., Reis, R. L. & Perez-Martin, R. I. (2017). Optimization of high purity chitin and chitosan production from Illex argentinus pens by a combination of enzymatic and chemical processes. *Carbohydr Polym*, 174: 262-272. doi: 10.1016/j.carbpol.2017.06.070.

Vu, T. T., Quyen, D. T., Dao, T. T. & Nguyen Sle, T. (2012). Cloning, high-level expression, purification, and properties of a novel endo-beta-1,4-mannanase from Bacillus subtilis G1 in Pichia pastoris. *J Microbiol Biotechnol*, 22 (3): 331-8. doi: 10.4014/jmb.1106.06052.

Vyas, N. K. (1991). Atomic features of protein-carbohydrate interactions. *Curr Opin Struct Biol*, 1: 732–740.

Vaaje-Kolstad, G., Houston, D. R., Riemen, A. H., Eijsink, V. G. & van Aalten, D. M. (2005). Crystal structure and binding properties of the Serratia marcescens chitin-binding protein CBP21. *J Biol Chem*, 280 (12): 11313-9. doi: 10.1074/jbc.M407175200.

Vaaje-Kolstad, G., Westereng, B., Horn, S. J., Liu, Z., Zhai, H., Sorlie, M. & Eijsink, V. G. (2010). An oxidative enzyme boosting the enzymatic conversion of recalcitrant polysaccharides. *Science*, 330 (6001): 219-22. doi: 10.1126/science.1192231.

Vaaje-Kolstad, G., Horn, S. J., Sorlie, M. & Eijsink, V. G. (2013). The chitinolytic machinery of Serratia marcescens--a model system for enzymatic degradation of recalcitrant polysaccharides. *FEBS J*, 280 (13): 3028-49. doi: 10.1111/febs.12181.

Vaaje-Kolstad, G., Forsberg, Z., Loose, J. S., Bissaro, B. & Eijsink, V. G. (2017). Structural diversity of lytic polysaccharide monooxygenases. *Curr Opin Struct Biol*, 44: 67-76. doi: 10.1016/j.sbi.2016.12.012.

Wang, B., Johnston, E. M., Li, P., Shaik, S., Davies, G. J., Walton, P. H. & Rovira, C. (2018). QM/MM Studies into the H2O2-Dependent Activity of Lytic Polysaccharide

Monooxygenases: Evidence for the Formation of a Caged Hydroxyl Radical Intermediate. *ACS Catalysis*, 8 (2): 1346-1351. doi: 10.1021/acscatal.7b03888.

Wang, B., Wang, Z., Davies, G. J., Walton, P. H. & Rovira, C. (2020). Activation of O2 and H2O2 by Lytic Polysaccharide Monooxygenases. *ACS Catalysis*, 10 (21): 12760-12769. doi: 10.1021/acscatal.0c02914.

Wood, T. M. & Garcia-Campayo, V. (1990). Enzymology of cellulose degradation. *Biodegredation*, 1: 147-161.

Younes, I. & Rinaudo, M. (2015). Chitin and chitosan preparation from marine sources. Structure, properties and applications. *Mar Drugs*, 13 (3): 1133-74. doi: 10.3390/md13031133.

Zakariassen, H., Aam, B. B., Horn, S. J., Varum, K. M., Sorlie, M. & Eijsink, V. G. (2009). Aromatic residues in the catalytic center of chitinase A from Serratia marcescens affect processivity, enzyme activity, and biomass converting efficiency. *J Biol Chem*, 284 (16): 10610-7. doi: 10.1074/jbc.M900092200.

Zhou, M., Diwu, Z., Panchuck-Voloshina, N. & Haugland, R. P. (1997). A Stable Nonfluorescent Derivative of Resorufin for the Fluorometric Determination of Trace Hydrogen Peroxide: Applications in Detecting the Activity of Phagocyte NADPH Oxidase and Other Oxidases. *Analytical Biochemistry*, 253 (3).

Zhu, W., Wang, D., Liu, T. & Yang, Q. (2016). Production of N-Acetyl-d-glucosamine from Mycelial Waste by a Combination of Bacterial Chitinases and an Insect N-Acetyl-d-glucosaminidase. *J Agric Food Chem*, 64 (35): 6738-44. doi: 10.1021/acs.jafc.6b03713.

8 Appendix

8.1 Oxidative activity of *Ag*ChOx

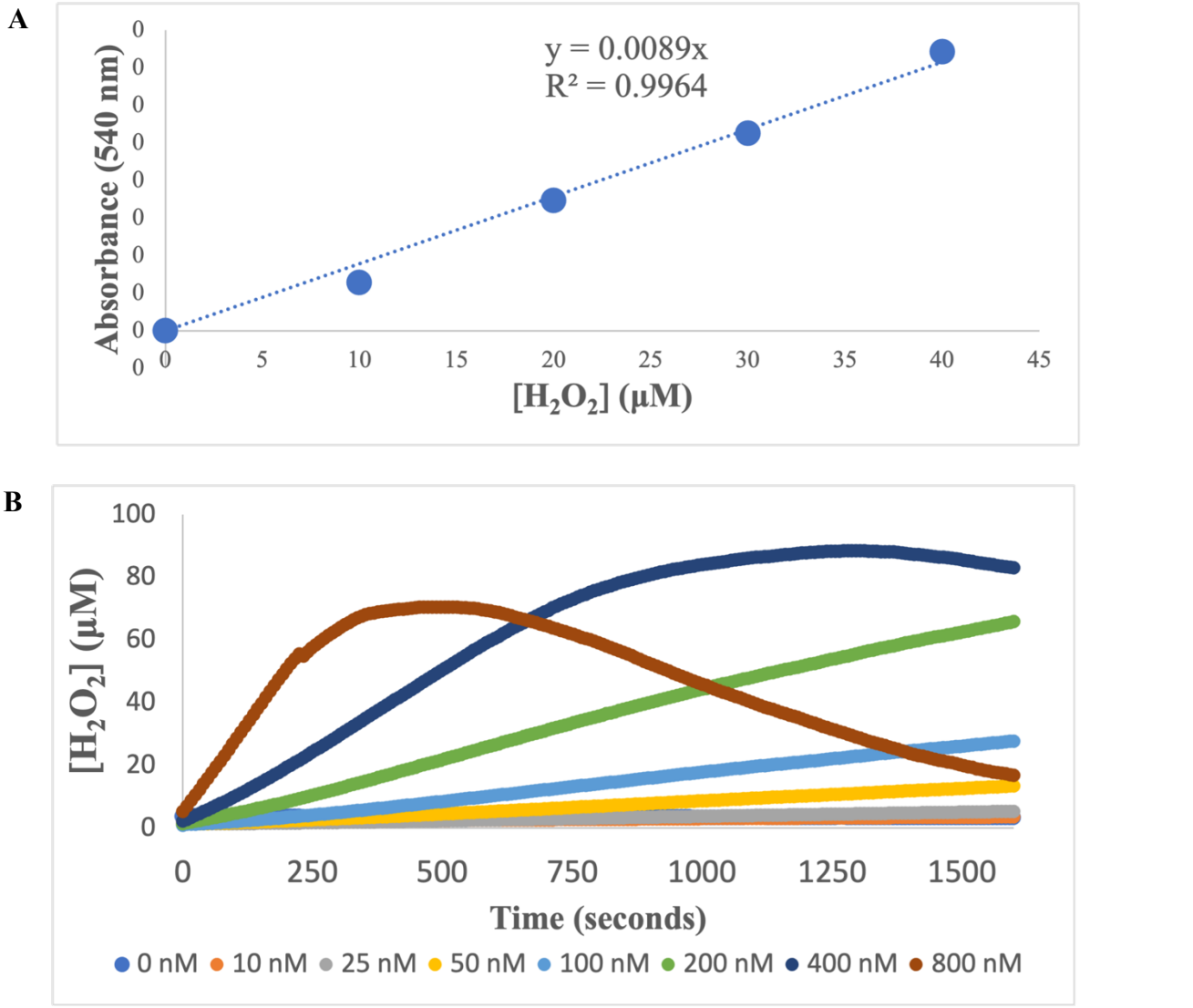

Figure 8.1 Oxidative activity of AgChOx. (A) Standard curve of H_2O_2 for one of the three plates where the H_2O_2 concentration in µM (x-axis) was plotted against the absorption at 540 nm (y-axis) where the blank value was subtracted from the value and the standard deviations are shown as error bars for n=3. (B) Amplex Red assay results of different AgChOx concentration with average data of n=3 were used for visualization of the linear part of the reaction.

8.2 Standard curves for HPLC analysis by rezex fast acid

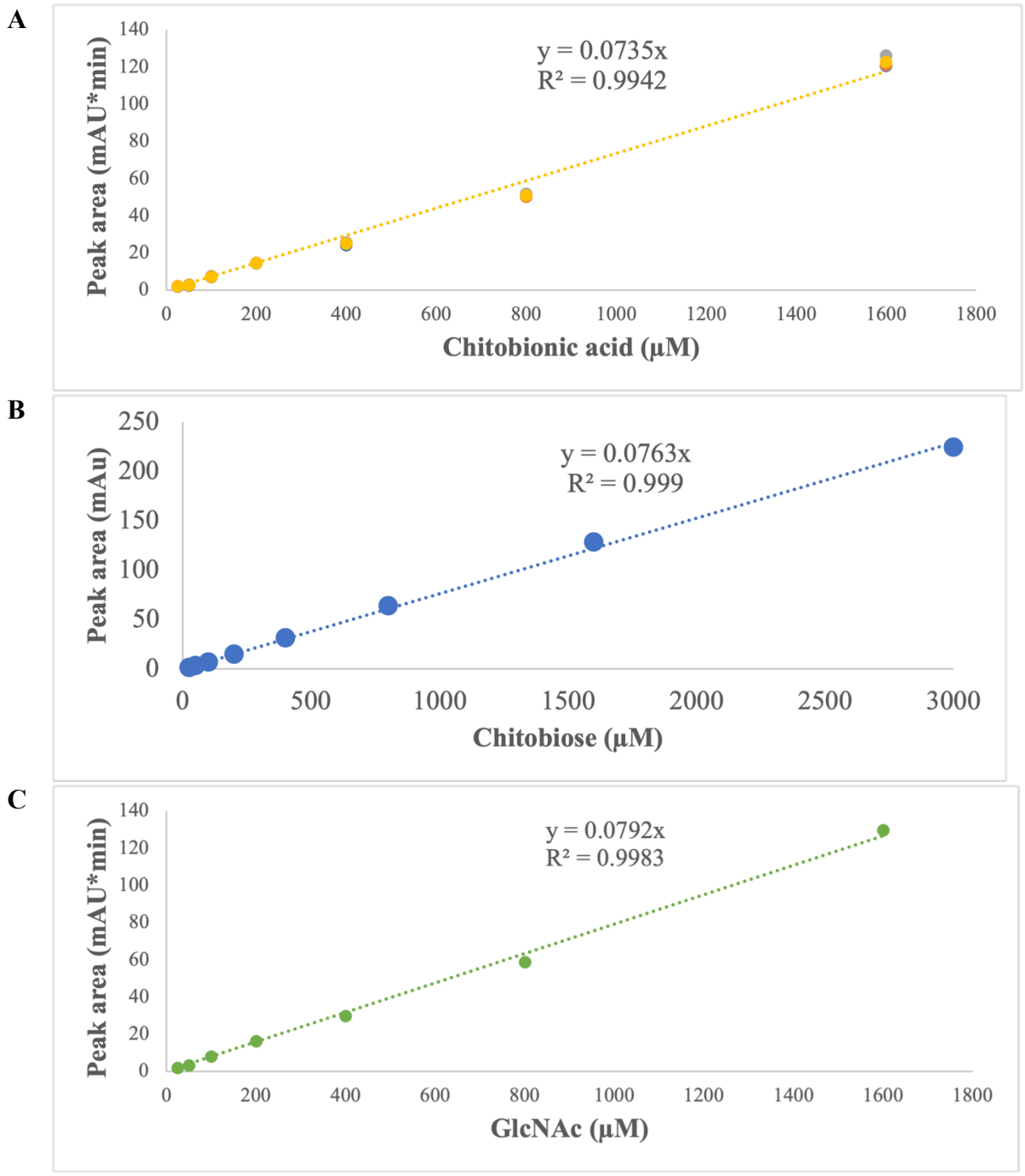

Figure 8.2 Standard curves for HPLC analysis by rezex fast acid. All curves use the integrated peak area (y-axis) plotted against standard concentrations from 25-1600 (3000 for chitobiose) where (A) oxidized dimers, (B) chitobiose, and (C) GlcNAc. Standard deviations are shown as error bars for n=3.

8.3 Effect of substrate concentration

A 10 mg/mL β-chitin

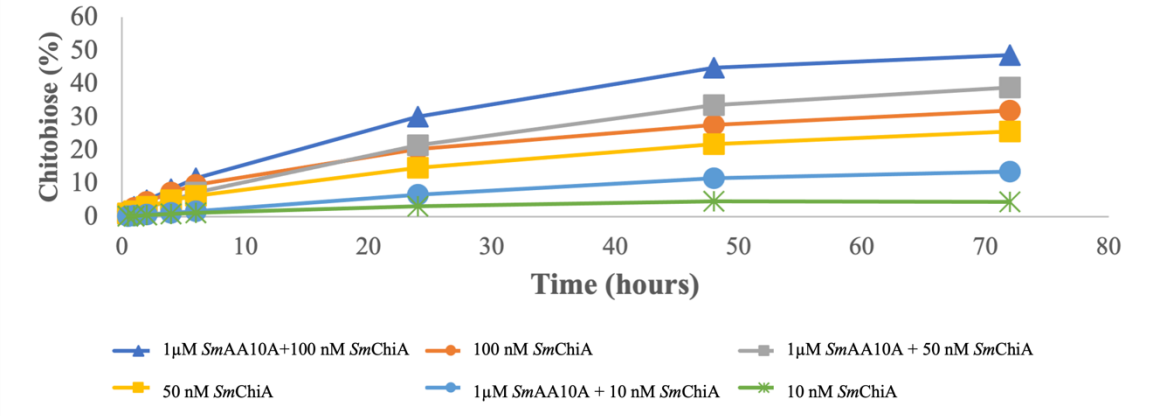

B 2.5 mg/mL β-chitin

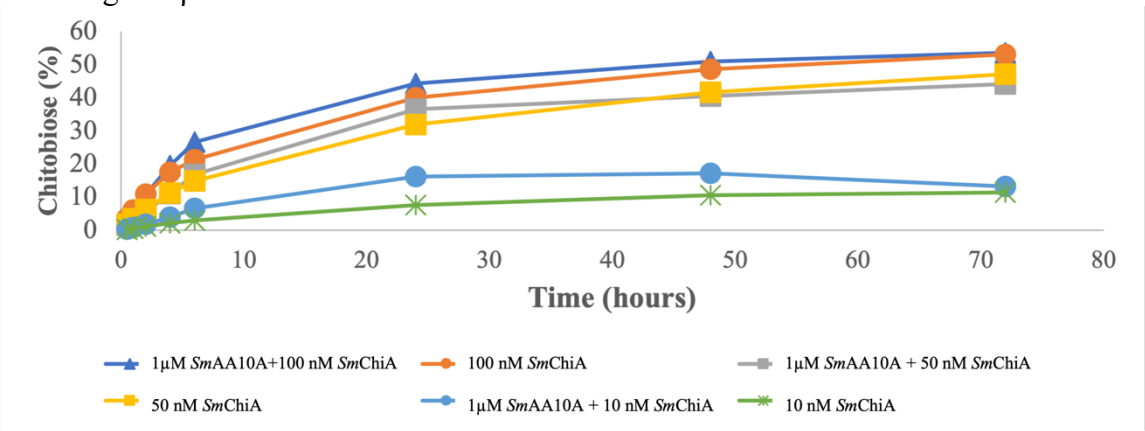

C 0.45 mg/mL β-chitin

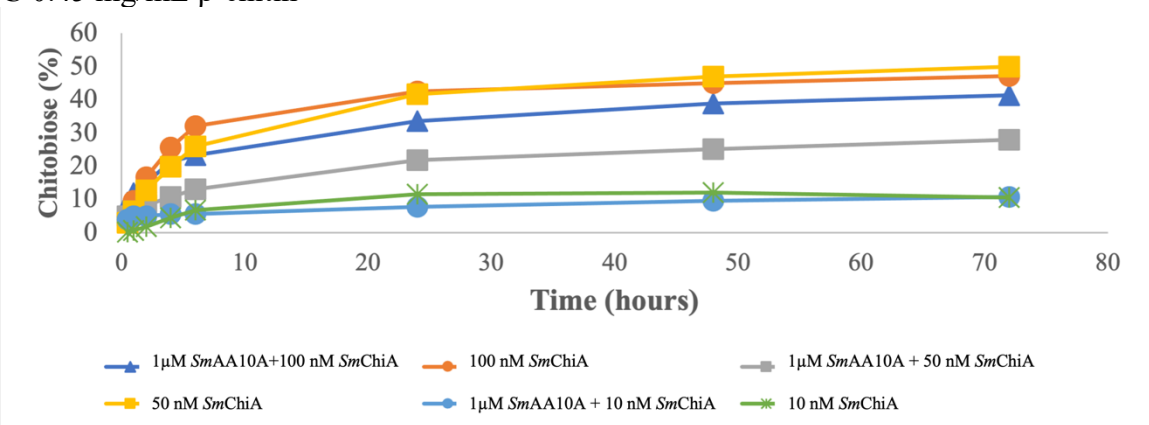

Figure 8.3 Effect of substrate concentration in synergy with SmChiA and SmAA10A. Time course experiment at different concentrations of β-chitin (10, 2.5 and 0.45 mg/mL) at different concentrations of SmChiA(10, 50 and 100 nM) in 50 mM sodium phosphate pH 7 over 72 hours. The y-axis is chitobiose formation in percent of theoretical maximum yield. Along the x-axis is the different concentrations of SmChiA at 10, 50 or 100 nM with or without 1 μM SmAA10A and 1 mM ascorbic acid. ***(A)*** *Substrate concentration at 10 mg/mL β-chitin,* ***(B)*** *substrate concentration at 2.5 mg/mL β-chitin,* ***(C)*** *substrate concentration at 0.45 mg/mL β-chitin. Standard deviations are shown as error bars of n=3.*

Norges miljø- og biovitenskapelige universitet
Noregs miljø- og biovitskapelege universitet
Norwegian University of Life Sciences

Postboks 5003
NO-1432 Ås
Norway